Analysis of synchronization and leadership emergence in human group interaction

Carmela Calabrese

THÈSE POUR OBTENIR LE GRADE DE DOCTEUR DE L'UNIVERSITÉ DE MONTPELLIER

En *Sciences du Mouvement Humain*

École doctorale 463

Unité de recherche EuroMov

En partenariat international avec
Università degli Studi di Napoli "Federico II", Italy

ANALYSE DE LA SYNCHRONISATION ET ÉMERGENCE DU LEADERSHIP AU COURS DE L'INTERACTION HUMAINE DE GROUPE

Présentée par Carmela Calabrese
Le 15 mars 2021

Sous la direction de Prof. Benoit Bardy
et Prof. Mario di Bernardo

Devant le jury composé de

Franck Multon, Professor, University of Rennes 2, France	Président du jury
Maurizio Porfiri, Professor, NYU Tandon School of Engineering, USA	Membre du jury
Benoit Bardy, Professor, University of Montpellier, France	Directeur de Thèse
Mario di Bernardo, Professor, University of Naples- Federico II, Italy	Co-directeur de Thèse

UNIVERSITÉ DE MONTPELLIER

All'instancabile, inevitabile e tormentata ricerca
del perché di ciò che vivo.

Abstract

Perceptual-motor synchronization in small human groups is crucial in many human activities from musical ensembles to sports teams. Unveiling the underlying mechanisms of human coordination has attracted the interest of researchers from diverse disciplines from psychology to complex systems. Several studies in social and nonlinear systems sciences have highlighted the main features characterizing synchronization within human dyads and large crowds, whereas the investigation in human groups with multiple agents ($5-7$ people) remains preliminary, and rarely captured by a consistent mathematical framework. In addition, a theory of leadership emergence in human group motor synchronization is still missing. In this thesis, we study group motor synchronization across different experimental conditions. The goal is to uncover the individual and group features that influence group performance; derive a mathematical model able to describe and unfold the mechanisms underlying group coordination; understand how leaders naturally emerge in a group of people coordinating their motion and guide all the other members towards a desired behaviour; and explore if and how artificial agents interacting with humans promote group coordination and influence leadership emergence. To this aim, we built a flexible experimental setup allowing to implement a group version of the "mirror game", which is considered as a paradigmatic coordination task in human groups. In our setup, participants were asked to perform oscillatory movements and synchronize with the others in the group. We considered different groups of participants, characterized by different kinematic features, and studied how group coordination emerged.

Addressing this challenge plays a crucial role in the case of humans performing some joint task with patients affected by social disorders. Indeed, social psychology suggests that coordination enhances social attachment and we envisage the results of our study can be used for the rehabilitation of patients affected by social disorders, to develop a control-based cognitive architecture that drives virtual agents' (robots or avatars) behaviour to promote patients' participation and leadership, and drive players and patients towards a preferred group behaviour.

This doctoral work was conducted in the context of a Ph.D. *cotutelle* between *Università degli Studi di Napoli Federico II* and *Université de Montpellier*, and was funded by the VINCI program promoted by *Università Italo-Francese/ Université Franco-Italienne* (Scholarship number C3-862).

Acknowledgements

Telling you that this Ph.D. journey has been wonderful and fantastic would be a lie and, as you know, women and men of science look for the truth. I do not want to show the successful side of the research coin.

I fell, I fell so many times that I am still learning how to do it at the best. I realized that infallibility does not belong to the human nature and that it is not absolutely inborn in research world. Science and research wallow in a perpetual doubt and what makes it charming is not the collection of the achievements but the tortuous growth path associated to them. I realized how difficult conducting research is and how challenging being true with yourself is, when competition devours and contaminates the pure pursuit of the reason of things.

I will end this journey feeling that I did not live this experience in full. The COVID outbreak in 2020 crushed all my enthusiasm to run fundamental experiments for this research and swept away all the plans for the culturally rich period abroad. However, I tried to do the best I could. I wish that all the world will be free of this nightmare very soon.

In each project, people are the most important part and make the difference. For this reason, I wish to thank my supervisor professor Mario di Bernardo, who greatly contributed to this work with deep technical comments and accurate revisions, for his fundamental teachings and for making me a better scientist. I am grateful to you for supporting my great passion.

I am thankful to professor Benoit Bardy (University of Montpellier, France) for his guidance in the movement science (a novel research field for me), for his help and hospitality when I arrived for the first time in Montpellier (I will never forget the Raclette party), and for his important support when I was performing some of the experiments discussed in this thesis. Your contribution has been precious.

I would like to express sincere gratitude to professor Pietro De Lellis, first for all the times he helped me when the deepest part of me was in trouble and he donated me a different and positive perspective to go on. I thank him for his attention addressed not only to my mood but also to my research ideas and results, for his valuable collaboration and technical recommendations on many of the topics addressed in this thesis. Thank you for being such a great friend and advisor.

I thank you all for the precious time you spent to review this work.

I am grateful to the people of our SINCRO Lab for the amazing time spent together, especially to my friend Marco Coraggio and the funny Davide Fiore, but also to my desk mates Achille Caldara, and Michele Pugliese. Thanks for all our funny meals!

The greatest thank goes to my parents for their support and confidence in me. A special thank to my great little brother Giuseppe, I have always looked up to you for your passion and I will always be behind you. I love you more than anything in this world. I would also like to thank the person who supports me unconditionally and brings joy in my life: my lovely dog, Bartolomeo Patrizio Maria de' Calabresi or simply Barry (I could not keep him out).

I wish to deeply thank my true Friend, Annalisa. Time goes by and our friendship never fades but evolves. Thank you for being always present in the most important moments of my life. I am also grateful to Alberto, unique of his kind, who is always close to me even if he is far away. Thank you!

A special gratitude to Paola Minieri.

Finally, I dedicate this "season finale" to my precious person, Stefano. I am grateful that you chose to be on my side during this (sometimes hard) journey that united us. Thank you for your attention on me in all the little things, I have always felt warm hugs in your reassuring words. I need to thank you for our funny times and for hardest but constructive moments. You are my safe home and I wish you will always be.

I wish to acknowledge support from the Italian-French University VINCI Program 2017 (Scholarship n. C3-862) that supported this Ph.D. Scholarship.

Résumé etendu en français

Introduction

Comprendre comment et pourquoi les êtres humains se rassemblent et interagissent en groupe pour satisfaire des instincts profonds ou accomplir des tâches collaboratives sont des questions essentielles de recherche dans de multiples disciplines scientifiques telles que les neurosciences [1, 2], la psychologie sociale [3], l'anthropologie [4], l'ingénierie [5–7], l'économie [8], la théorie des jeux [9] ou la science des systèmes complexes [10, 11]. Il est difficile de répondre à ces questions primordiales car la coopération interpersonnelle comporte différents niveaux d'interaction, se produit dans divers contextes sociaux (par exemple, affiliation, agonisme, alimentation) et est réalisée par des personnes très variées ayant de multiples connaissances, compétences, et capacités [12, 13].

Plus précisément, la synchronisation perceptivo-motrice dans les groupes humains est un phénomène courant, crucial pour améliorer la performance dans les ensembles musicaux, les troupes de danseurs ou les sports d'équipe, et peut également être exploitée à des fins de réhabilitation [14–16]. En effet, les sciences cognitives et la psychologie sociale suggèrent que le processus de synchronisation, ou de coordination, contribue à renforcer le lien social et peut être utilisé pour la rééducation des troubles sociaux, par exemple grâce au développement d'architectures cognitives pilotant le comportement d' agents artificiels (par exemple, robots ou avatars) de manière à promouvoir la participation des patients au sein du groupe (par exemple, le projet européen AlterEgo- www.euromov.eu/alterego/).

Dévoiler les mécanismes sous-jacents de la coopération humaine et les principales caractéristiques de la synchronisation sensorimotrice au sein des groupes humains est un problème actuel. Dans la littérature, les recherches sur les interactions de groupe avec un nombre limité de membres ($N = 5 - 7$ personnes), c'est-à-dire au-delà de la coopération dyadique et en deçà des comportements de foule, sont rares, et les résultats sont rarement formalisés par un cadre mathématique. En outre, afin de concevoir, comme évoqué ci-dessus, un agent artificiel capable de réguler la dynamique de groupe, il est nécessaire de comprendre comment émerge le leadership et comment identifier l'individu le plus influent dans le groupe. Dans ce contexte, une théorie de l'émergence du leadership dans la synchronisation motrice de groupe est toujours manquante.

Objectifs de la thèse

La coordination est un trait essentiel dans de nombreuses activités humaines, où les acteurs, par exemple dans une dyade ou dans un groupe, effectuent une tâche commune et communiquent entre eux [17–22]. En effet, la synchronisation humaine est omniprésente, des activités simples de la vie quotidienne telles que les réunions de travail, la danse populaire et les sports d'équipe, ou lorsque nous jouons de la musique dans un ensemble. Différents canaux sensoriels d'interaction, à travers la vision, la proprioception ou l'audition, ainsi que l'établissement d'une identité sociale et d'une connexion mentale entre tous les membres, sont nécessaires pour atteindre une cohésion et un comportement stable dans le groupe [19, 23, 24].

Dévoiler les mécanismes qui encourage les êtres humains à coordonner leurs mouvements, à les adapter afin de les faire correspondre à ceux des autres de manière à atteindre et maintenir un comportement collectif stable, représente un défi clé, à la fois d'un point de vue psychologique et mathématique. La contribution principale de cette thèse, à l'intersection entre la science du mouvement, la théorie du contrôle et les mathématiques appliquées, est l'investigation expérimentale, l'analyse de données et la modélisation de la coordination motrice de groupe et l'émergence du leadership dans les ensembles humains, à partir de travaux récents [25, 26]. Bien que la coordination humaine ait été analysée en détail dans les interactions dyadiques ([27–31]), ou dans de grands groupes d'individus ([22, 32]), plusieurs questions en suspens relatives à la synchronisation humaine demeurent, par exemple:

- comprendre les caractéristiques individuelles et celles du groupe qui influent sur la performance de l'ensemble,
- développer des modèles mathématiques capables de saisir et de déployer les mécanismes sous-jacents à la coordination de groupe,
- découvrir à partir de données si et comment un ou des leader(s) émerge(nt) naturellement pour organiser la synchronisation et guider les autres membres vers le comportement souhaité,
- déterminer si des agents artificiels interagissant avec des groupes d'individus favorisent la coordination de groupe et influencent l'émergence du leadership.

Notre approche

Afin d'aborder ces questions, nous analysons dans cette thèse le comportement humain à travers un paradigme de coordination simple mais efficace, connu sous le nom du jeu en miroir (*mirror game* [33]), dans lequel les participants sont invités à produire un mouvement oscillatoire d'une partie du corps en synchronie avec d'autres individus. Différents groupes et topologies sont considérés, tant en présence qu'en l'absence d'interaction sociale. Dans ce dernier cas, nous utilisons une configuration informatisée qui permet d'effectuer des taches de coordination tout en minimisant diverses formes d'interaction sociale, récemment présentées dans [34]. Nous proposons également un réseau d'oscillateurs hétérogènes couplés avec différentes structures, comme modèle

mathématique capable de rendre compte de la dynamique de la coordination observée expérimentalement. Nous effectuons une analyse minutieuse des données expérimentales pour découvrir l'émergence du leadership dans le groupe, montrant que cette émergence se produit dans un nombre réduit de scénarios. En outre, nous présentons des résultats préliminaires portant sur l'influence d'un joueur virtuel sur la dynamique de groupe, évaluant sa capacité à interagir avec les membres d'un ensemble humain, par exemple pour influencer la synchronisation pour la réhabilitation des personnes socialement déficientes. Relever ce défi est crucial dans les contextes cliniques où, par exemple, des actions de synchronisation en groupe sont menées par et avec des patients souffrant de troubles sociaux. Une meilleure compréhension de la façon dont personnes en bonne santé et patients convergent vers des régimes spécifiques de synchronisation sensorimotrice, et de la façon dont ces régime favorisent la participation, la cohésion et le leadership, est aujourd'hui nécessaire.

Les résultats obtenus dans cette thèse peuvent être instrumentaux dans un certain nombre d'applications. D'abord et avant tout, les résultats que nous présentons peuvent être cruciaux pour le développement d'avatars et d'acteurs virtuels pour la réhabilitation des patients souffrant de troubles sociaux, tels que la schizophrénie [35] ou l'autisme [36]. L'autisme touche environ 1% de la population adulte et entraîne des coûts très élevés pour nos systèmes de santé. Les déficits d'interaction sociale, généralement diagnostiqués lors de conversations, sont les déficits les plus importants et les plus difficiles à réhabiliter pour un patient autiste. Contrairement aux thérapies traditionnelles, le but final de ce projet est le développement d'une nouvelle plateforme logicielle pour la télé-réadaptation de groupe, capable d'aider le personnel médical et de minimiser les distances, le temps et le coût des traitements. Notre approche implique des travaux expérimentaux, ainsi que des techniques de modélisation et de classification dans le contexte de la synchronisation sensorimotrice humaine. Ils impliquent également une analyse fine de la coordination et de l'émergence du leadership au sein d'un groupe de personnes engagées dans une tâche coopérative, et constituent un exemple parfait à étudier grâce aux outils des réseaux complexes.

Notre approche est également pertinente pour la robotique, discipline dans laquelle des modèles mathématiques et des algorithmes de contrôle sont nécessaires pour que les robots coopèrent avec les humains de manière sûre, et dans les situations d'interaction homme-machine, pour réaliser des tâches difficiles, par exemple dans la logistique ou dans des environnements à risque.

Résumé des chapitres et principaux résultats

Les travaux expérimentaux et de modélisation présentés dans ce manuscrit sont le résultat d'un programme de doctorat international basé sur la collaboration entre le *Département d'Ingénierie Electrique et de Technologie de l'Information* de l'Université de Naples Federico II en Italie et le *Centre EuroMov* de l'Université de Montpellier en France (programme bilatéral VINCI).

Nous commençons nos travaux par un aperçu de la littérature existante sur la coordination humaine (Chapitre 2). Nous détaillons l'objectif principal de ce projet et la

pertinence du développement d'exercices de groupe, puis nous passons en revue les études les plus importantes sur la coordination humaine et animale, ainsi que celles portant sur l'émergence du leadership. Ensuite, nous synthétisons les modélisations existantes dans la littérature qui peuvent être utilisées pour décrire la coordination des mouvements dans les ensembles humains, et nous présentons un aperçu synthétique des outils d'analyse de données utilisés pour rendre compte des phénomènes de synchronisation, en mettant l'accent sur ceux qui se sont révélés utiles pour étudier et explorer les processus comportementaux découlant de la coordination au sein du groupe.

Notre contribution personnelle commence par le Chapitre 3, dans lequel nous nous concentrons sur les propriétés caractérisant la coordination interpersonnelle entre plusieurs agents. Plus précisément, nous analysons la continuité de l'interaction malgré une perte transitoire de contact perceptif. Nous étudions la dynamique de cette continuité, dans deux expériences utilisant la version de groupe du *mirror game* [33] où les participants sont invités à synchroniser leurs mouvements dans l'espace et dans le temps. Nous analysons les caractéristiques qui peuvent influer sur la qualité de la coordination au sein du groupe dans deux scénarios complémentaires manipulant la similarité entre les participants, la similarité cinématique (l'homogénéité de la fréquence des mouvements) et l'expertise (par la comparaison entre participants novices et danseurs). Nous montrons que la coordination de groupe peut être maintenue après une interruption du contact perceptif pendant environ 7s, et que la similarité améliore la performance de synchronisation. Nous proposons et comparons trois modèles mathématiques (c'est-à-dire des réseaux d'oscillateurs de phase non linéairement couplés) pour capturer les observations et clarifier la double origine de cet effet de mémoire, individuelle et sociale. Ces résultats offrent un nouvel éclairage sur les raisons pour lesquelles nous continuons à nous synchroniser malgré une perte de couplage sensoriel; ils ont été publiés dans [37].

Notre contribution se poursuit dans le Chapitre 4 par un raffinement des modèles de synchronisation. Nous focalisons ici particulièrement notre attention sur les raisons conduisant les participants engagés dans une tâche commune de synchronisation à réduire leur fréquence d'oscillation. Nous proposons trois modifications alternatives du modèle traditionnel de Kuramoto pour expliquer nos observations expérimentales, fondées sur trois principales hypothèses neuroscientifiques différentes. Tout d'abord, nos résultats de modélisation montrent des valeurs de retard qui se situent dans la fourchette généralement démontrée dans la littérature en sciences du mouvement [171, 226]. Nous montrons ensuite qu'un modèle tenant compte des retards neuronaux dans le traitement de l'information est le plus performant pour saisir le ralentissement observé expérimentalement.

Dans le Chapitre 5, nous nous concentrons sur le problème épineux de l'émergence du leadership et de ses effets au sein du groupe. Nous constatons que l'émergence du leadership favorise effectivement la coordination et est donc un phénomène naturel qui se produit dans les groupes même lorsqu'il n'est pas établi a priori. Fait intéressant, avec l'utilisation combinée de deux indicateurs - le leadership de *phase* et le leadership *d'influence* - nous montrons l'existence de trois principaux scénarios dans lesquels le leadership émerge : leadership de phase, leadership d'influence, et leadership mixte. De façon cruciale, ces trois scénarios peuvent être immédiatement liés à des scénarios naturels dans le règne animal, confirmant que l'émergence du leadership est un phénomène

organisateur naturel lorsque la coordination est le but du groupe. Ces observations s'avèrent indépendantes de la présence d'une interaction perceptivo-motrice physique entre les participants. En effet, les résultats sont confirmés par des expériences utilisant une configuration informatique empêchant les participants d'interagir directement et laissant les volontaires percevoir seulement le mouvement des autres participants à travers un écran d'ordinateur portable. Les résultats présentés dans ce chapitre sont soumis pour publication.

Enfin, le Chapitre 6 est consacré à une étude préliminaire portant sur l'influence d'un joueur virtuel, interagissant au sein d'un ensemble humain, sur les niveaux de synchronisation de groupe ainsi que sur l'émergence de leadership. Nous montrons que des agents artificiels ayant des caractéristiques cinématiques spécifiques, reliées de façon appropriée à un sous-ensemble de participants de l'ensemble, sont capables d'influencer la dynamique de coordination des deux groupes. Ces résultats encourageants constituent la base de l'élaboration d'une stratégie de contrôle que les joueurs virtuels peuvent utiliser pour améliorer la coordination entre les humains d'un groupe, affecter le leadership au sein de l'ensemble, ou même détourner le comportement de l'ensemble des régimes synchrones indésirables. À cet égard, des agents artificiels pourraient être effectivement utilisés pour offrir des méthodes thérapeutiques complémentaires pour réhabiliter les personnes socialement handicapées.

Un résumé de nos résultats et une discussion de leurs implications, complétées par des orientations pour les travaux futurs, sont présentées dans le Chapitre 7. Enfin, deux annexes présentent des travaux connexes effectués au cours de la thèse. Dans l'annexe A, la définition d'une signature de groupe est présentée. Elle représente un outil d'analyse potentiel peu coûteux et non invasif permettant d'évaluer les déficiences sociales, identifier le type de tâche collective et explorer l'influence du groupe sur la plasticité individuelle. L'annexe B présente les résultats des travaux corrélés sur la modélisation de la propagation de la COVID-19 en Italie.

Applications possibles et travaux futurs

L'utilisation adaptée d'agents artificiels représente une nouvelle méthode pour étudier la coordination des mouvements humains au sein des groupes, explorer certains principes importants de la psychologie sociale, et tester de multiples hypothèses dans le monde réel et dans le monde numérique. La disponibilité d'un modèle mathématique de coordination au sein du groupe est d'une importance cruciale pour mettre en œuvre des avatars interagissant avec d'autres partenaires à des fins de réadaptation dans l'interaction avec des personnes socialement déficiences (par exemple, patients souffrant de schizophrénie ou du syndrome autistique).

Une description mathématique de la coordination au sein du groupe, comme celle proposée dans les Chapitres 3 et 4, est fondamentale non seulement pour faire la lumière sur les mécanismes sous-jacents de coopération et de synchronisation, mais aussi afin de prévoir le niveau de performance atteint en fonction de structures d'interconnexion ou de comportements intrinsèques individuels, et permettant un meilleur développement d'entités artificielles. Dans ce dernier scénario, puisque les leaders sont ceux qui

influencent le plus le mouvement des autres agents, il est raisonnable de les mettre en contact avec un joueur virtuel afin de promouvoir un comportement désiré sur le groupe humain engagé dans un exercice de réadaptation.

En ce qui concerne les travaux futurs possibles, concernant la modélisation, les extensions possibles et les améliorations des travaux présentés dans cette étude incluent la possibilité de combiner les paramètres adaptatifs et personnalisés du comportement individuel, ainsi que des quantités variant dans le temps en fonction du niveau de coordination en temps réel avec les autres partenaires. Une telle extension peut permettre aux joueurs virtuels de faire correspondre encore plus étroitement leurs comportements à ceux des personnes réelles. Il existe une pléthore de caractéristiques différentes qui influencent les comportements collectifs et qui méritent d'être étudiées plus en profondeur, permettant de contraster les stratégies de modélisation proposées dans une variété de situations, où les paramètres perceptifs et topologiques sont manipulés afin de mieux caractériser leur contribution respective et leur effets interactionnels.

De plus, l'étude analytique de l'émergence du leadership au sein du groupe présentée dans le Chapitre 5 peut être appliquée à des mouvements différents et certainement plus complexes. Les situations ordinaires, comme l'aviron, les réunions de travail quotidiennes ou l'exécution d'ensembles musicaux, sont beaucoup plus riches que les simples tâches oscillatoires exécutées ici, tant du côté de l'action que du côté de la perception, par la contribution multiple de nos modalités sensorielles aux fonctions de coupage identifiées. La façon dont des configurations multiples et co-existantes, pour chaque sens et dans l'interaction entre eux, modulent nos comportements collaboratifs, dans ces situations et dans d'autres, reste largement inconnue et constitue un axe de recherche prometteur pour les études futures.

En dépit de leur caractère préliminaire, nos résultats expérimentaux présentés dans le Chapitre 6 sur le leadership de phase et d'influence dans le jeu en miroir peuvent fournir des conseils sur la façon de sélectionner les participants à la modulation par un agent artificiel, afin d'obtenir un comportement souhaité, par exemple lors de procédures d'évacuation à large échelle, ou lors de la sélection des membres d'équipage dans une course d'aviron d'équipe. Un problème qui reste à étudier est l'émergence du leadership avec un agent virtuel dans des configurations expérimentales plus systématiques pour confirmer nos résultats.

Enfin, les stratégies de leadership que nous avons soulignées pourraient être utilisées pour planifier le mouvement d'un ou de plusieurs agents artificiels afin d'améliorer la performance des groupes humains-robots. Cette approche pourrait être pertinente, par exemple pour aider à la conception de partenaires artificiels innovants pour des applications industrielles, où un compromis optimal entre l'autonomie des robots et l'intervention humaine est nécessaire pour maximiser la production d'une manière sûre [247], ou pour la recherche et le sauvetage dans des zones dangereuses non accessibles aux êtres humains [248].

Liste des publications

Les résultats de cette thèse ont fait l'objet de plusieurs publications énumérées ci-dessous:

- Bardy B. G.*, **Calabrese C.***, De Lellis P., Bourgeaud S., Colomer C., Pla S., di Bernardo M. (2020).*Moving in unison after perceptual interruption.* Scientific Reports, 10(1), 1-13;

- **Calabrese C.**, De Lellis P., Bardy B. G., di Bernardo M. *Capturing human slowing down during group interaction: modified Kuramoto models*, en préparation;

- **Calabrese C.**, Lombardi M., Bollt E., De Lellis P., Bardy B. G., di Bernardo M. (2020). *Self-emerging leadership patterns facilitate the onset of coordinated motion in human groups*, soumis pour publication;

- Della Rossa F.*, Salzano D.*, Di Meglio A.*, De Lellis F.*, Coraggio M., **Calabrese C.**, Guarino A., Cardona-Rivera R., De Lellis P., Liuzza D., Lo Iudice F., Russo G., di Bernardo M. (2020). A network model of Italy shows that intermittent regional strategies can alleviate the COVID-19 epidemic. *Nature communications*, 11(1), 1-9.

* Ces auteurs ont également contribué à ce travail.

Contents

List of Figures

List of Tables

1 Introduction

Man is by nature a *social animal*- claimed Aristotle in his book "Politics".

Understanding how and why human beings gather and interact in groups to accomplish and satisfy deep instincts and primary needs are key research questions across different scientific disciplines such as neuroscience [1, 2], social psychology [3], anthropology [4] engineering [5–7], economics [8], game theory [9] and complex systems science [10, 11]. Answering these paramount questions is challenging as interpersonal cooperation involves different levels of interactions, it occurs across diverse social contexts (e.g., affiliation, agonistic, feeding) and relates to different types of individuals with various knowledge, skills, and abilities [12, 13].

Specifically, perceptual-motor synchronization in human groups is a common phenomenon which is crucial to enhance performance in musical ensembles, dancers' crews, or team sports and can also be exploited for rehabilitative purposes [14–16]. Indeed, social psychology suggests that coordination enhances social attachment and can then be used for rehabilitation of social disorders, to develop control-based cognitive architectures, that drive virtual agents' (robots or avatars) behaviour to promote patients' participation and lead players and patients towards preferred group behaviour (e.g., www.euromov.eu/alterego/).

Unveiling the underlying mechanisms of human cooperation and the main features characterizing motor coordination within human groups is a challenging open problem. In the literature, the investigations on group interactions with a finite number of members ($N = 5 - 7$ people)- differently from dyadic cooperation and crowds- is much less studied and the results are rarely formalized through a mathematical framework. In addition, in order to design an artificial agent with the ability to regulate the group dynamics, it is necessary to know how leadership emerges among humans and how to identify the most influential individual in the ensemble, to better diffuse the control action of the artificial agent and gain the leadership role. However, a theory of leadership emergence in human group motor synchronization is still missing.

1.1 Human group synchronization

Coordination is an essential trait in many human activities, where people, for instance in a dyad, or in a group, perform a joint task and communicate with each other [17–22]. Indeed, human synchronization is pervasive, from simple daily life activities such as work meetings, to popular dancing and playing team sports, or when playing music in an ensemble (see Figure 1.1). Different channels of perceptual interaction, through vision, proprioception or hearing, as well as the establishment of social identity and mental connectedness among all members, are necessary to reach a cohesiveness and stable behaviour in the group [19, 23, 24].

Figure 1.1: **Examples of human group coordination.** Four familiar human cooperation situations in various contexts: (a) an ordinary organization during everyday work meetings; (b) often present in sports, for instance in team rowing; (c) popular dances in cultural contexts or among children at play (round dance); (d) musical ensembles performing a concert. The image in panel (b) comes from *unsplash.com*, all the others from *pixabay.com*.

Unveiling the mechanisms that drive people to coordinate, adjust their movements to match those of the others, reach and maintain a stable coordinated behaviour represents a key challenge, both from a psychological and a mathematical point of view.

The main contribution of this thesis, at the intersection between movement science, control theory and applied mathematics, is the experimental investigation, data analysis and modeling of group motor coordination and leadership emergence in human ensembles, starting from the work presented earlier in the literature [25, 26].

Although human coordination has been analysed in details in dyadic interactions ([27–31]), or in large groups of individuals ([22, 32]), several open questions in human synhronization remain. For example,

- understand how individual and group features that affect the performance of the

ensemble,
- mathematical models able to capture and unfold the mechanisms underlying group coordination,
- uncover from data if and how leaders naturally emerge to organise the synchronisation onset and guide all other members towards a desired behaviour,
- investigate if artificial agents interacting with groups of individuals in a human-like fashion promote group coordination and influence leadership emergence.

Addressing this challenge is crucial in clinical contexts where, for instance, joint actions are performed by and with patients suffering from social disorders. As research in social psychology has suggested that coordination enhances social attachment. A better understanding of how healthy individuals, and/or patients, converge to specific sensorimotor synchronization patterns, and how these patterns promote participation, cohesion and leadership is required.

In order to tackle these challenging questions, in this Thesis we analyse human behaviour through a simple yet effective coordination paradigm, known as the *mirror game* [33], where participants are asked to produce an oscillatory movement in synchrony with other individuals. Different groups and topologies are considered, in the presence as well as in the absence of social interaction. In this latter case, we use a computer-based set-up that makes it possible to perform coordination tasks while minimising various forms of social interaction, recently presented in [34]. We also propose a network of coupled heterogeneous oscillators with different structures as a mathematical model capable of capturing the dynamics of human group coordination observed experimentally. We carry out a careful analysis of the experimental data to detect and uncover leadership emergence in the group, showing that such emergence mostly occurs in three different scenarios. In addition, we present preliminary results on the influence of a virtual player on group dynamics, evaluating its ability to interact with members of a human ensemble, for instance to influence synchronisation for rehabilitation of socially challenged people.

The results presented in this Thesis can be instrumental in a number of different applications. First and foremost, the results we presented can be crucial in developing avatars and virtual players for the rehabilitation of patients suffering from social disorders, such as schizophrenia [35] or autism [36].

Autism affects about 1% of the adult population with very high associated costs. Deficits in social interaction, typically diagnosed during conversations, are the most significant and the most difficult deficits to rehabilitate for an autistic patient. Differently from traditional therapies, the final goal of this project is the development of a new software platform for group tele-rehabilitation able to assist medical staff and minimize distances, time and costs. The proposed approach involves experimental work, as well as modelling and classification techniques in the context of human sensorimotor synchronization.

Investigations of the emergence of movement coordination and leadership within a group of people engaged in a cooperative task represents a perfect example to be studied through complex networks.

Our approach is also relevant for robotics, where mathematical models and control algorithms are needed for robots to cooperate with humans in a safe manner, and in

human-machine interaction to perform challenging tasks, for example in logistics or in risky environments (see Figure 1.2).

(a) (b)

Figure 1.2: **Examples of Human-Robot cooperation.** Panel (a) shows Robonaut, a humanoid robotic torso, developped by the NASA laboratory and designed to assist ISS crew during extravehicular activities[1] whereas in panel (b) a woman cooperates with the robot Baker that helps moving and orienting parts from the assembly line[2].

1.2 Thesis structure and outline

The research presented in this manuscript is the result of an international joint doctorate program based on the collaboration between the Department of Electrical Engineering and Information Technology of the University of Naples Federico II in Italy and the EuroMov Centre at the University of Montpellier in France.

This Thesis is organised as follows.

We start with an overview of the existing literature on human coordination in Chapter 2. Firstly, we detail the main goal of this project and the relevance of the development of group exergames, and we review some of the most significant studies on animal and human interpersonal coordination, as well as on leadership emergence. Secondly, we provide an overview of the modelling results from the existing literature that can be used to describe movement coordination in human ensembles, and we present a synthetic overview of the state of the art of the data analysis tools that allow to capture behavioural observations.

Humans interact in groups through various perception and action channels. We begin our investigation of human coordination, analysing the continuity of interaction despite a transient loss of perceptual contact in Chapter 3. Here, we study the dynamics of this continuity, in two experiments employing the group version of the mirror game [33] where participants are asked to synchronize their movements in space and in time. We analyse the features that can influence the quality of group coordination in two different scenarios when either participants' similarity (i.e., homogeneity in movement frequency) is manipulated or participan's expertise is varied (i.e., through comparisons between novice individuals and dancers). We show that group coordination can be maintained

[1] *Image credit*: www.datamanager.it/news/robanaut-il-chirurgo-spaziale-della-nasa-53970.html
[2] *Image credit*: Rethink Robotics

after perceptual contact has been lost for about 7s, and that agent similarity in the group modulate synchronization performance. We propose and compare three mathematical models (i.e., networks of nonlinearly coupled phase oscillators) to capture the observations and to clarify the double origin of this memory effect, of individual and social nature. These results shed new light into why humans continue to move in unison after perceptual interruption and were published in [37].

Our study of human coordination continues in Chapter 4 where we propose three alternative modifications of the traditional Kuramoto model to explain our experimental observations. In particular, we propose three alternative extensions of the original model presented in [38], grounded into three main alternative neuroscientific hypotheses, to explain some of the observed group effects, such as the slowing down of the oscillation frequency during synchronization.

In Chapter 5 we shed light on the self-emerging strategies that drive human group coordination, investigating the emergence of leadership in a group of people performing a joint motor task. The contribution of this study is represented by the quantitative identification and definition of leadership patterns, by means of the proposed combination of two metrics, phase leadership and degree of influence. Our data analysis shows that coordination in human groups is driven by, and enhanced through one of three possible leadership emerging patterns. We confirm our finding by repeating the experiments with two different set-ups, with and without direct visual interaction between the participants, using a computer-based set-up preventing participants to perceptually interact directly. The results presented in this Chapter were recently submitted for pubblication.

In Chapter 6, we discuss preliminary findings on leadership emergence obtained experimentally in a human ensemble interacting without and with a virtual agent. This work starts to unveil the influence an artificial avatar can have on group coordination dynamics and can, therefore, represent the basis for the development of a control strategy that virtual players can use to enhance coordination among humans in a group, assign leadership in the ensemble, or even steer the behaviour of the ensemble away from unwanted synchronous regimes.

A summary of our results and discussion of their implications, complemented by directions for future work, are drawn in Chapter 7. Finally, two appendices contain other worked carried out during the PhD. In Appendix A the definition of a group signature is given that represent a low-cost and non-invasive potential analysis tool for several diseases and that can help to distinguish ensembles, to identify the kind of collective task and to explore group influence on individual plasticity. Appendix B presents the results of correlated work on modeling the spread of COVID-19 in Italy.

1.3 List of publications

The results in this Thesis were the subject of several publications as listed below:

- Bardy B. G.*, **Calabrese C.***, De Lellis P., Bourgeaud S., Colomer C., Pla S., di Bernardo M. (2020).*Moving in unison after perceptual interruption.* Scientific Reports, 10(1), 1-13 (Chapter 3);

- **Calabrese C.**, De Lellis P., Bardy B. G., di Bernardo M. *Capturing human slowing down during group interaction: modified Kuramoto models*, In preparation (Chapter 4);

- **Calabrese C.**, Lombardi M., Bollt E., De Lellis P., Bardy B. G., di Bernardo M. (2020). *Self-emerging leadership patterns facilitate the onset of coordinated motion in human groups.* Submitted for pubblication (Chapter 5);

- Della Rossa F.*, Salzano D.*, Di Meglio A.*, De Lellis F.*, Coraggio M., **Calabrese C.**, Guarino A., Cardona-Rivera R., De Lellis P., Liuzza D., Lo Iudice F., Russo G., di Bernardo M. (2020). A network model of Italy shows that intermittent regional strategies can alleviate the COVID-19 epidemic. *Nature communications*, 11(1), 1-9 (Appendix B).

* These authors equally contributed to this work.

2 State of the art on human coordination

In this Chapter, we review previous investigations in the literature on the study of collective behaviour and interpersonal synchronization, especially in the case of movement coordination, in animal and human kingdom (see Section 2.1), and continue with a review of leadership across several scientific fields (Section 2.2). We focus on the principles governing group synchronization, highlighting the missing points that we try to address in this doctoral work. In particular, we show that while most studies are focused on the emergence of leadership, little is still known on how this phenomenon occurs within groups of human players, and how to quantitatively describe this emergent process. In Section 2.3 we highlight the different modelling approaches that have been used to reproduce and simulate experimental observations on group interactions, complemented by an overview of the analytic tools useful to unfold mechanisms about animal group coordination that we later exploit (see Section 2.4). Then, we give a synthetic description of an exergame and its fundamental properties for rehabilitative purposes (Section 2.5). We highlight the importance of the deployment of such platforms for autism rehabilitation, and present existing cognitive architectures. A summary of the Chapter is presented in Section 2.6.

2.1 Multi-agent group synchronization

Understanding how multiple agents synchronize their behaviours and which individual or group features facilitate the collective coordination has been studied in several areas of Science and Technology. A large part of the literature has looked at human cooperation as a result of evolution. In fact, collective behaviours emerge in different species [39, 40] such as birds [41], fish [42] or insects [43], and researchers have analysed the advantages that promote the development of group formation. It is postulated that animal grouping yields several benefits for the group members including reduced individual predation risk, joint resource defence, cooperation and information transfer for a more efficient regulation of food foraging and shared vigilance [44–47]. In particular, recent studies have shown that cooperation fosters the information flow among the agents and contribute to group decision making. For example, in animal group traveling (e.g., in pigeon homing [48] or

fish schooling [42]), integration of navigational decisions by group members is crucial, where individuals continuously solve conflicts between personal directional preferences and group interests. Alexander [49] claimed that groups form because all individuals experience the benefits of living together. Therefore, the crucial evolutionary transition in the animal world is represented by the shift from an originally solitary lifestyle to a group or tribal one [50], and there is an important difference between humans and other animals that is worth to highlight. As all animals, humans were collaborative foragers and interdependent individuals but, as soon as new skills and motivations scaled up to group life, regulation with norms and institutions was necessary. In this way, cooperation became an emergent property based not on altruistic helping but on mutualist collaboration where the unique capability of humans to coordinate and communicate about their decisions has represented the key-point to form joint goals and cooperate [51].

In what follows, we present a survey of studies from the literature that have explored group dynamics occurring in the animal world, with a particular emphasis on human contexts.

2.1.1 Examples in the animal world

Social animals that forage or travel in groups afford a multitude of group decisions involving coordination of activities and travel directions' choice, by **self organizing interaction patterns** among group members [52]. This collective behaviour cannot be fully understood in terms of the dynamics of any individual agent but it is important to take into account group wide effects such as how social information is integrated, **positive feedback** or response thresholds, that are repeatedly observed in very different animal societies [53] (see Figure 2.1). In many cases, few individuals have relevant information, such as knowledge about the location of a food source or of a migration route [39]. Therefore, achieving collective group action may not be accomplished by simple rules alone but requires averaging preferences (democracy), or following choices of specific leaders (despotism) [54].

(a) (b)

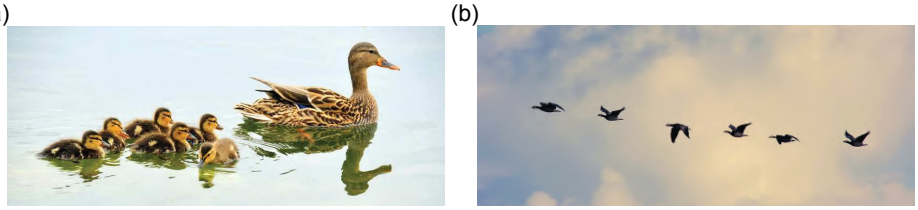

Figure 2.1: **Examples of animal group interaction.** In panel (a), a typical example of group synchronization in the animal kingdom- the very early stage of life is characterized by learning "filial imprinting", during which a young animal surrounds and coordinates with its parent as a result of exposure to it. Panel (b) represents a stunning example of animal collective behaviour, during migration stage, where all birds follow who knows the route without missing any element, creating wonderful single shapes in the sky. The images come from *pixabay.com*.

Individual attributes represent the primary elements that influence the group dynamics including temperamental and personality traits, such as boldness [42, 55]. It has been shown that, in pairs of sticklebacks, bolder individuals displayed greater initiative in movement and were less responsive to their partners, whereas shyer individuals displayed less initiative but followed their partners more faithfully; they also elicited greater leading tendencies in their bold partners. These results demonstrate that not only group dynamics is influenced by personal characteristics but also that these traits are reinforced by **positive social feedbacks** among the agents. In fact, positive feedbacks allow the emergence of collective behaviour, amplifying events through reinforcement [53]. As imitation behaviour continues, the number of partners performing an activity explodes exponentially and this allows information to spread quickly through a group.

Also the way information flows among agents is crucial for the coordination of multi-agents systems. For example, in [56], researchers observed that during birds' migrations, although a large variety of path shapes are displayed, the paths of the bats within a pair are qualitatively similar. Orange et al. showed that **directional information transfer** exists within the bat pairs and that higher information transfer flows from the bat flying in front to the bat flying in the rear. This study highlights how **relative spatial positioning** plays an important role during navigation. Similar analyses have been carried in other animal groups such as insect [57], where coordinated group behaviors emerge from agents' choices of the interacting partner.

Next, we discuss the case of human group coordination.

2.1.2 Examples in the human world

The daily situations where examples of human synchronization arise, such as team rowing, everyday working meetings, or musical ensemble performance, are varied and generally too complex, both on the action side and on the perception side, to reveal basic processes of coordination. For this reason, researchers have begun to investigate interpersonal coordination in simpler contexts (see Figure 2.2). Scientists in Complexity have primarily looked at dyadic interactions ([17–20, 27–31]) where just two individuals interact with each other, or at the case of crowds with a large number of agents ([21, 22, 32]). There are fewer studies in the literature on group interactions containing a small number ($N > 2$) of agents, such as [32, 58], and, in addition, they do not always focus on motor synchronization between human participants.

In addition, analytical and modelling aspects are often missing. What makes these studies challenging is the fact that researchers often have little control over the participants' characteristics and strategies that affect their interactive behavior, such as the social influence due to visual and auditory coupling. One promising approach, as a preliminary step toward investigating motor synchronization among individuals, is to study cooperation of participants through platforms that simulate the potential behavior of a human partner in the task [20, 27, 34]. This approach makes it possible to control and vary systematically the simulated partner's characteristics, so that there is a limited set of parameters that needs to be inferred from the data.

Some key observations from the existing literature are reported below.

Figure 2.2: **Three paradigmatic examples of human group interaction.** Panel (a) represents a dyadic interaction between mother and daughter, typical of child development[1]. Panel (b) shows a larger group coordination task, common to several team sports[2]. Panel (c) portrays a crowd over the famous Millennium bridge, well-known for its movements caused by a positive feedback phenomenon between the synchronized natural sway motion of people walking and the small oscillations in the structure[3].

The study of interpersonal coordination- both intentional and unintentional- occurring between two people when sitting side-by-side in rocking chairs [31], revealed that the stability of a visual interpersonal coupling is **mediated by attention** and **the degree to which an individual is able to detect information** about a co-actor's movements. Indeed, social interaction implictly requires a **give-and-take** dynamic. In fact, the investigation on the effects of social skills or physical variables on the degree of dyadic coordination [28] has suggested that having partners with high social competences does not guarantee high levels of synchrony. On the contrary, a more successful coordination was achieved in this study when partners had **complementary social competences**. Pairs of high social expertise partners showed higher fluctuations in the relative phase lag than in the other combinations, reflecting the inability of this kind of pair to cooperate and, on the contrary, witnessing the emergence of competition.

Therefore, partner adaptivity plays a fundamental role during intepersonal synchronization. In the literature there are many studies about human sensorimotor synchronization, where people are asked to coordinate actions or movements with computer-controlled event sequences ([20, 27]). The main goal of these works is to study **adaptivity and compensation** abilities of the participants. In particular, in [20] authors used computer platforms that are able to modulate adaptively the timing of a tone's sequence to the auditory pattern of human participants, as a human partner might do. Experiments run in different scenarios by varying error correction parameters over a wide range, revealed that as long as human participants face with a cooperative partner, they mantain their **synchronization strategies**. On the other hand, when faced with an uncooperative partner, humans are forced to adapt and to switch to a guiding role and keep the correct tempo, by increasing, for instance, the gain of their phase correction.

[3] *Image credit*: www.standupcomedyclinic.com/5-reasons-to-use-imitation-and-emulation-to-learn-stand-up-comedy/

[4] *Image credit*: www.theglobeandmail.com/sports/olympics/a-day-at-the-pool-with-canadas-womens-synchro-swim-team/article4224993/

[5] *Image credit*: www.chroniclelive.co.uk/news/history/gallery/queen-opens-millennium-bridge-between-12995658

Sensorimotor synchronization among members becomes more crucial when considering performances of musical ensembles. Temporal coordination among performers is very challenging due to the mixture of global tempo-variations and the highly variable local fluctuations given by personal expressive interpretations and by the noise in the sensorimotor system. Wing et al. [59] showed that the stability of an ensemble's cohesiveness is directly related to the ability of performers to adjust to each other's tempo in a multitude of ways so as to **compensate** any asynchronies.

Information flows across the agents are influenced by the communication structure implemented among them. This topic is particularly important for navigational tasks. Following previous studies about consensus decision making in animal and human groups on the move [39, 60], Dyer et al. [32] focused on the importance of uninformed individuals in reaching consensus in walking groups and on the effect of spatial positioning of informed individuals on the speed and accuracy with which they guide uninformed group members to a target. They found that the **spatial position** of informed individuals affected both the speed and the accuracy with which they guided the uninformed group to the target. They found that having one informed individual starting in the centre and one starting on the periphery of the group was the most effective way to guide the group quickly and accurately to a destination. Similar conclusions were achieved in [25] where Alderisio et al. found that the interaction patterns influenced synchronisation dynamics over time differently across topologies.

In summary, among the results that have been presented in the Literature on human group coordination we highlighted the importance of key points such as the adaptivity behaviours or the influence of information flowing among the group members. However, only a limited analysis has been carried out with respect to the effects that the individual dynamics of group members and the structure of interactions within the group might have on their coordination performance. To address these crucial challenges, in this Thesis we will extend a paradigmatic coordination task (i.e., the mirror game [33]) to a group dimension and shed light on how the sudden loss of visual feedback and the pattern of visual interactions among the people in the group affect their coordination levels. In addition, we will investigate how their individual attributes influence that of the ensemble, and how participants choose to adapt their personal kinematic features in order to meet the synchronization goal. Furthermore, we will derive, where possible, mathematical models able to capture, describe and unfold the mechanisms underlying human group coordination in this context.

2.2 Leadership across different research fields

Leadership emergence is one of the most interesting and important questions in human behaviour. We have already highlighted how the knowledge of leadership emergence is central for the design of artificial avatars that need to gain the leading role to steer the group dynamics towards a preferred behaviour. For this reason, in this section, an overview on the different approaches of leadership definitions found in diverse research fields is provided.

First, given the complexity of human group interaction, we may wonder if leadership in a group of cooperating agents is a necessity at all. Research has demonstrated that leadership is an emergent solution to specific social group coordination challenges, such as group migration, intra-group peacekeeping and inter-group competition [61], where individuals take actions that depend on the simultaneous actions of the others, with the leader mediating and solving social dilemmas, thus promoting cooperation among agents [62]. In the animal domain, researchers have analysed the behaviour of individuals while foraging or during a group migration [39, 63–66]. They found that information about a possible target to reach spreads quite easily within groups even when group members do not know which individuals have that information. In particular, it was found that a small proportion of informed individuals is necessary, but also sufficient, to guide the group, and, therefore, to take collective decisions. Interestingly, **dominance failed to be associated with leadership**. Instead, the level of exploration may be a stronger predictor of leadership that works as a positive feedback reinforcing individual behaviour. In particular, evidence of several changes in guiding the group dynamics, has been found indicating that leadership is not an absolute quality [64, 65] but rather corresponds to situations where individuals dynamically adapt their responses to one another. In addition, the presence of both bold and shy individuals within a group, and therefore variability in agents' response, result in more flexible behaviour at the population level [64]. These aspects were also detected in studies on the emergence of collective behaviour in human groups, e.g. [67].

Several definitions of human leadership have been proposed [54, 68, 69] focusing, however, mostly on *isolated* variables that describe only few of the aspects that characterize a **leader**. Indeed, Winston et al. [70] identified over 90 variables corresponding to leadership, from being an active person, creating connections, being determinate to define directions, exerting power, etc. These definitions may comprise the whole set of leadership qualities but, it is easy to imagine that formulating an integrative definition encompassing all of them is an ambitious goal [68].

Leadership is often defined in terms of the people who are in charge of organizations and their units [69]. By definition, such people are leaders. However, those who rise to the top of large organizations are distinguished by hard work, intelligence, critical thinking skills, intuition, ambition, both persuasive rhetoric and interpersonal communication, and political skills, they seek personal growth and increase in mental, physical, and spiritual states [70]. In this way, a leader can be thought as the person who selects and influences others, and guides them to enthusiastically expend spiritual and physical energy to achieve group goals [69]. In addition, the existing literature on leadership in human groups

postulates the existence of different levels or types of leaders [71, 72], and of personal attributes that could promote the selection of a leader [70, 73]. In this sense, personality allows leadership to emerge and to effectively influence teams and organizations- good leadership promotes group performances, bad leadership degrades the quality of life for everyone within a team. From this point of view, personality accounts for leadership: **who we are is how we lead** [72]. Nonetheless, a large part of the literature today **rejects a person-centric and hierarchical approach** to the study of leadership, where supervisors are leaders, subordinates are followers, and leader–follower identities are static [74]. According to the contrasting point of view, partners co-build their identities through a series of bidirectional leading–following interactions over time [61, 75–77]. Many studies agree that leadership is a **collective phenomenon**, and that a more social and dynamic conception of leading–following processes in groups is needed- individuals are involved in repeated leading–following interactions, and through these, **they co-construct identities as leaders and followers**. Over time, through repeated interactions, these leader–follower relationships emerge to form group-level leadership structures that range from centralized to shared patterns of leading and following, that can evolve to enable groups to adapt in dynamic environments [74]. This adaptivity is supported by a collective process of **learning** that changes reputation relationships among the agents and impacts the structure of the group [78]. During human interactions, agents build their own preferred attachments over time and adjust then to a varying environment [75, 79]. Understanding how people use information available from the behavior of partners is, therefore, important for understanding not only individual decisions but also patterns of change and variation during human interactions [20].

Leadership in moving groups becomes crucial in musical contexts (see Fig. 2.3(a)) where non-verbal interaction needs to efficiently transfer information among people through sensorimotor communication while performers have to afford complex visuo-spatial integrative brain processes [80, 81]. In these cases, communication flows through qualitatively different channels linked to kinematic features, reflecting real-time interpersonal information sharing, modulating the formal roles of the involved partners (e.g., conductor to musicians and musician to musician interactions), influencing the level of synchronization and, therefore, the quality of the execution. In these scenarios, visual information complements auditory information, facilitates interpersonal information flow and improves coordination among co-actors, with followers leveraging visual information to predict the leader's actions.

Besides musical performances, in the majority of studies [32, 82–85], leadership was induced by introducing informational asymmetries among participants, with only a subset of the group having knowledge of the goal of the joint action, for instance preferred direction or final destination. These research studies focused on scenarios in which communication among the agents is limited to the mutual observation of their movements, thus lessening the impact of individual personality traits on leadership. It was found that minorities can successfully lead a majority through immediacy and consistency of the first move. On the contrary, the amount of uninformed individuals in a group can influence the time to reach the goal and the likelihood of group splitting. One of the main results that emerged [32, 83, 85] is that having more than one leader, possibly of two

different types [32] - one informed individual starting in a core position and steering the uninformed individuals towards the target, and one unconstrained on the periphery of the group - is often the most effective way of guiding the group quickly and accurately towards the goal (see Fig. 2.3(b)). Within complex networks theory, these roles have been formalized in the concept of the so- called power and knowledge leaders [86].

Investigation and detection of leader-follower patterns in human ensembles is also a problem of great importance in the context of rehabilitation robotics, where a virtual agent (avatar or robot) is added to the group interaction (see Fig. 2.3(c)). The virtual agent might be required to specifically act as a leader or follower in order to help patients recover from their social disabilities For this reason, the necessity of a quantitative analysis of leadership to design virtual agent and to enable the validation of alternative theories becomes apparent [87].

Figure 2.3: **Leadership in different human contexts.** Panel (a) represents a famous italian orchestra director, Riccardo Muti, conducting a concert[4]. In panel (b), we represented a typical scenario where the cooperation of different and multiple actors is needed[5]. It happens in evacuation contexts where the group in trouble is guided by a leader driving to the exit, and by several security agents making sure people go in the right direction and that any member is not missed. Leader-follower dynamics are crucial to design robots deployed in rehabilitative session dedicated to motor impaired patients[6](panel (c)).

Several leadership theoretic models have thus been presented above [76, 88]. However, they mainly provide qualitative descriptions and, in general, propose regression analyses where perceived leadership identity is treated as dependent variable and cognitive ability, extraversion, self-efficacy or other psychological traits represent predictive factors. For this purpose, in this thesis we investigate the emergence of leadership in human ensembles performing a paradigmatic joint motor task, that is, a multi-player version of the mirror game, where participants are involved in a simple hand movement coordination task when connected over different interaction patterns. We address the problem of quantitative analysis of leadership emergence, proposing the combined use of two metrics, the first based on the relative phase between the partners, and the latter index based on causation entropy (see Section 5.2.2, in Chapter 5). We investigate leadership both in the presence and in the absence of direct visual and social interaction, so as to separate the effects of

[6] *Image credit*:classicalmusicart.wordpress.com/2008/04/29/biografia-del-maestro-riccardo-muti-direttore-dorchestra-e-artista/

[7] *Image credit*:www.ilmessaggero.it/rieti/rieti_scuola_sicurezza-1013118.html

[8] *Image credit*:daywebchronicle.com/2019/11/28/rehabilitation-healthcare-assistive-robot-market-future-scope-2019-2025-opportunities-trends-dynamics-and-growth-factors-hondamotor-hansen-gait-tronics/

individual behaviours from those of complex human social interactions (e.g., hierarchy levels, shared affinities, friendship). Our goal is to unveil whether, when no designated roles are assigned, a leader spontaneously emerges in the group, how such emergence depends on the structure of the interconnections among the team members, and whether it is affected by the presence of social interaction between them. In addition, in this Thesis we also present some preliminary results of our investigation on the influence artificial avatars can have on the leadership emergence process (see Chapter 6).

2.3 Modelling human coordination in literature

Different mathematical models were developed to investigate, describe and understand the main aspects of human interpersonal coordination observed experimentally. They rely on various mathematical tools such as game theory, optimal control, nonlinear dynamics or stochastic behaviour to derive the partners' motor behavior and capture adaptation during group interaction.

One of the final goals of this Thesis is the extension of existing mathematical models used in the context of human group motor synchronization to capture the experimental observations we collected in different experimental setups. Depending on task involved and the captured dynamics, different modelling approaches can be followed. Below, we describe the main modelling avenues adopted in the Literature.

Oscillators models: HKB model and network of Kuramoto oscillators. Coordinated rhythmic behaviour are observed at many levels of biological organization, from populations of molecules to communities of organisms. Systems of coupled oscillators represent a suitable approach for studying these emergent behaviours. Main research investigation focused primarly on the synchronization of simple rhythmic movements [31, 89]. Human interaction partners tend to synchronize their movements during purely rhythmic actions such as walking or clapping, to show approval after a music performance. One of the systems achieving a great deal of success in describing human dyadic coordination is the Haken-Kelso-Bunz model, also known as the HKB model, originally introduced in [89] to account for the transition from phase to anti-phase synchronisation in bimanual coordination experiments. The HKB model can show a large variety of coordination patterns [90] and, for this reason, is potentially able to capture several human coordination observations beyond bimanual synchronisation, such as the coordination between different limbs [29], between two people [31, 91], and perception and action also the coordination between human and virtual partners [92].

The HKB model is suitable to describe dyadic scenarios but it cannot capture as is, the dynamics of larger human ensembles where the number of agents is greater then two. During multi-player interactions, agents self-organize and the emergent behaviour becomes the result of the distributed functional organization of the group, communicating through different sensory channels (e.g., vision, feel, sound) [18]. In these cases, the emergent group dynamics can be described through a network modelling framework where individuals are represented by nodes and the edges model the social links (see Figure 2.4).

A network extension of the HKB model was presented in [93] but can be in general difficult to parametrize from real data.

1. **Agents** (Nodes)

$\dot{x}_i = f_i(x_i,) + g_i(x_i)u_i, \quad i = 1, \ldots, N$

where $x_i \in \mathrm{R}^n$ and $u_i \in \mathrm{R}^n$

2. **Coupling model**

$u_i = \sigma \sum_{j=1}^{N} a_{ij}(h(x_j) - h(x_i))$

3. **Network structure** (Graph)

$\mathcal{G} = \{\mathcal{N}, E\}$

where $\mathcal{N} = \{1, \ldots, N\}$ and $E \subset \mathcal{N} \times \mathcal{N}$

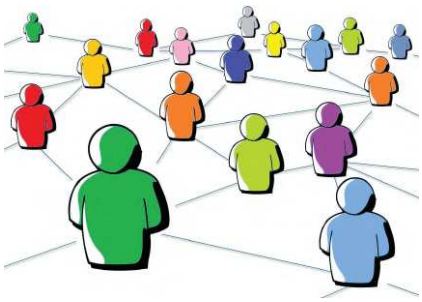

Figure 2.4: **Modelling networks.** The key ingredients to model complex networks of dynamical systems are: 1- a model of the dynamics of each agent; 2- the communication protocol (interaction model) among agents; 3- the structure of the interconnections between agents.

The network of oscillators modelled by Kuramoto [38] is another classic model used to describe the emergent rythmic behaviour in an ensemble, looking only at the phase (macro-description). It has been shown to be powerful in capturing degree of synchronization relevant to any activity requiring the coordination of several people, as in music, sport or at work. For instance, in [25, 94] researchers used Kuramoto oscillators to investigate how coordination emerges in human ensembles. Networks of coupled heterogeneous oscillators with different structures captured well the coordination levels shown by the groups during joint action experiments. This modelling framework also helped researchers to observe new peculiarities of the rhythmic applause [22]. This versatile model has also been augmented with two opposite driving forces to model the attitude of each agent to be part of the group [95]. This approach allows new insights on why synchronization suddenly occurs, and on why synchronization is observed for a specific clapping period. This mathematical framework represents the starting point for our modelling approach to capture our experimental observations (see Chapters 3 and 4).

From synchronization to metastability- multi-layer and mean field models. We have shown above how the dynamics of animal societies emerging from interactions among individuals can be described through a network framework where individuals are represented by nodes and the edges model the social links. However, sometimes standard network modelling approaches cannot be sufficient to capture the heterogeneities that typically characterize human cooperation. In fact, a monolayer approach that try to squeeze all the interactions in one layer can lead to superficial and misleading inferences about the social structure. For this reason, given the complex nature of human communication and the simultaneous presence of several factors that influence group interactions, multilevel modelling frameworks are often necessary to capture the emergent dynamics. The development of multilayer network analysis offers a new promising approach for studying social behavior in animals, the role of social structure in transmitting information [96] and infection [97], and many other features. However, social systems have multiple facets, as they include social interactions that occur at both different times and locations, and traditional network analyses have typically ignored such crucial interdependencies when studying multirelational systems. A multilayer network combines multiple networks, called *layers*, into a unique mathematical object. The analysis of such networks can uncover ways in which different layers interact and impact one another [12].

There are two main types of multilayer networks- multiplex and interconnected networks [98]. Multiplex networks are characterized by edges between layers that connect nodes representing the same entity across different layers. Each layer includes the same individuals, but not all individuals need to be involved in all types of interactions. Analysing these networks enables the examination of individuals' roles in a society by simultaneously considering multiple modes of interaction. Interconnected networks are used to model connections between different subsystems, connecting different types of nodes to each other.

These modelling approaches showed their effectiveness in the analysis of animal movement patterns, in contrast with aggregating individual movements approaches that considerably reduce information on influences among group members, and potentially mislead interpretation of movement patterns [99]. Multiplex representations of interactions among the members of a group have been successfully used in studying the role of individuals and interaction patterns in monkeys' social structures [100] but also in developing attention model over surrounding agents to predict trajectories of members in a human group, with applications, for instance, in robotics, to plan the robot's behaviour navigating through human crowds [101].

When the number of agents involved in group interaction becomes higher, scientists are interested in describing the overall group behaviour, discarding the uninformative particle details. Mean-field approaches are very useful in these cases. They are common in neuroscience where the analysis and reproduction of each single neuron activity is unconceivable and often unuseful. Top-down approaches derive behavioral patterns from neural fields [102]. Whereas synchronization (usually inphase) naturally arises in Kuramoto-like models, it is viewed here as only one regime of brain coordination dynamics. Metastable regime which arises when the system exhibits an integrative tendency, i.e. a tendency to synchronize, together with a tendency for the components

to maintain their autonomy. Metastability is the way the brain constantly creates and destroys neural assemblies. It consists of a more subtle dwell and escape dynamics in which the brain is never stable but merely expresses the joint tendency for neural areas to synchronize together and to oscillate independently. This dynamical behavior is more complex than phase locking. The two main issues are to first determine if a system is metastable and then to quantify its properties to assess the kind of coordination dynamics that exists between the parts. Among the models of neural ensembles [103–105], neural masses consists in replacing the probability density distributions over the state-space by their mass-center which provides a single number that represents the average activity of the population. These mathematical approaches, essential for neuroscience modelling, have been applied also to human crowds dynamics in [106–108] when the number of agents becomes sufficiently large.

To summarize, we presented the most important mathematical framework developed to capture human behaviour dynamics in different conditions: dyads, large ensemble and crowds. We highlighted the variety and complementarity of several models proposed in literature, able to capture diverse group patterns observed in the human repertoire. However, models for group dynamics have not been explored enough in different human contexts. We will present how we tried to contribute to this research area in Chapters 3 and 4. First, we present below data analysis tools that will be used in the rest of the Thesis.

2.4 Data analysis tools

In this last section, we provide an overview of useful tools for data analysis to unfold the mechanisms promoting group cohesiveness and leadership emergence during interpersonal synchronization tasks (see Table 2.1).

It is possible to group and identify the tools in five main categories:

- temporal and frequency relations;
- synchronization indices;
- causal relations among agents;
- individual characterization;
- machine learning for pattern recognition and data reduction.

In the following, we briefly revise each category with specific examples of data analysis tools.

Describing temporal and frequency relations. Since not all features fostering synchronization in a dynamic system are necessarily known a priori, the behavior of these hidden variables can be evaluated via their interaction with, or their influence on, known variables. For this reason, the easiest way in data analysis is to analyse the temporal evolution of signals by extracting relative position or velocity errors, and then extract correlations between them [31, 109, 110]. In these studies, authors used **relative phase**, **linear cross-correlation**- used to measure the strength of the relation and the time delay between pairs of time series-, **cross-recurrence quantification**- a non-linear version of cross-correlation- and **cross-spectral** analysis- which determines the relationship between two time series at each component frequency or lagged cross-correlation that gives an estimate of the symmetry between different time-series. At the local level, linear cross-correlation can be used to measure the strength of the relation and the time delay between pairs of time series. Differently, a non-linear, two-dimensional cross-recurrence analysis can be used to quantify the time-correlated activity between pairs of time series for each dyad in a group [110, 111]. The neighborliness of points within some tolerance can indicate recurrent points in the two time series. These points represent states in one time series that closely correspond to previous, current or future states in the other time series, and can illustrate behavioral patterns of coordination in the observed system. The recurrent points are identified and represented in a cross-recurrence plot, from which a suite of measures can be computed to quantify these patterns, such as the cross-max line that provides a measure of the longest coupling time interval of two participants during a given trial.

Orthogonal to time domain methods, frequency domain techniques have been used to describe how the periodic variations in a time series may be accounted for by cyclic components at different frequencies through the Fast Fourier Transform (FFT) [112]. Quantitative evaluation of spontaneous synchrony is provided by the FFT power spectrum overlap (PSO) between the movements of two participants involved in a coordination action (for instance, [113]). PSO measures the percentage of movement frequencies common to both partners in a pair, by computing the area of intersection between each participant's normalized spectral plots. It represents an indicator of the strength of the frequency entrainment between the two participants. In addition, it is possible to compute the peak frequency (i.e., the maximum of the FFT power spectrum) and cross-spectral analysis- it computes bidirectional weighted coherence- to describe the shared rhythmic variation between a pair of time series.

Quantifying group synchronization. The limit of the temporal and frequency approaches mentioned above is that they work on pairs of signals and are not informative about group performance. For this reason, Richardson et al. in [114] developed a method to quantify phase synchronization in a network of Kuramoto's oscillators. Through this approach, it is possible to compute the order parameter- the degree of phase synchronization among agents-, the degree of synchrony of each agent with respect to the group and within dyads, and the degree of the frequency synchronization of the group. Often scientists want to analyse the global degree of synchronization in contexts where infomation comes from signals of different nature, as it is the case in neuroscience. When dealing with these

situations, events could be defined differently in each time series, since their common cause might manifest itself differently in each series. In this case, event synchronization measures may help. They cannot distinguish between different forms of lockings [115], but they can tell which of two time series leads the other and can show rapid changes of synchronization patterns. This analysis can be useful to detect causality and predictability relations among group members during human synchronization [116].

Detecting causal relations among agents. Evaluation of a participant's behavior predictability is important to verify whether intrinsic variability of their behavior is altered by experimental manipulation or, in particular, by specific individual features such as leadership. Correlational tools are inappropriate for detecting causal communication and influence between a set of agents exhibiting nonlinear behavior during coordinated motion. In cooperative joint action tasks, leaders tend to make their movements more consistent over time to help their partner build a predictive model of other's action [117]. An increase in the predictability of a partner A translates into a smaller uncertainty when partner B needs to predict future signals coming from A to plan the most appropriate action. Such variability can be detected in different ways. It is possible to evaluate the level of predictability of a participant's behavior using the goodness of the fit of the linear autoregressive model computed on the motion profile, or using standard deviation, useful to evaluate the stability of a particular response to perturbations. In experiments however, it is often not possible to compare the perturbed response with the undisturbed trajectory exactly, due to the variability in repeated movements. Alternatively, one can infer stability from observing the deviation of the set of consecutive trajectories in repeated trials. The size of the set of deviations is affected by the amount of motor variability and the magnitude of unpredictable disturbances along the motion as well as by the stability properties of the overall system. The deviation grows with the duration of the observation when the system is unstable, and remains bounded if the system is stable. In this case, an index borrowed from chaos theory, called the Lyapunov exponent, can be useful to capture the stability of dynamic interactions [118].

The problem of defining causality in complex systems is non-trivial. The analysis of predictability of ongoing interactions between different parts of a network system is fundamental to identify causal relations among cooperating agents. The pioneering approach is represented by the Wiener–Granger method [119] that does not require any direct intervention in the system. It relies on the estimation of causal statistical influences between simultaneously recorded time series, based on the statistical predictability of one time series that derives from knowledge of one or more other time series. Unfortunately, the linear autoregressive nature of the models of stochastic processes at the core of this method weakens the effectiveness of this analysis tool to capture complex systems' nonlinearities. However, it is possible to extract nonlinear dependencies among agents in terms of **transfer** and **causation entropy** [56, 57, 75] that measure the reduction in uncertainty of one time series when knowledge of the other time series is gained, by exploiting the notion of entropy.

Causality can be traced also by exploiting the theory of Algorithmic Information [120] that defines what constitutes *a cause* as opposed to randomness in discrete and deterministic

dynamical systems. Formally, the algorithmic complexity- an accepted mathematical measure of intrinsic randomness of an object, independent of probability distributions -is related to a Universal Turing Machine [121]. An object is referred to as random, and consequently *non-causal*, if its algorithmic complexity cannot be generated by any law or rule, only by a copy of itself- simple and predictable outcomes are more likely to be the output of an algorithm. Therefore, the analysis of complexity under perturbations allows to estimate the causal contribution of each system's element. In fact, in a random system, a change would not have a great impact because any part of the system can explain any other part, whereas in a causal generated system some changes will be recognizable. The study of the algorithmic information landscape to identify and rank the elements by their algorithmic contribution, and the changes that they may exert on the original network, moving it towards (negative ranks) or away from randomness (positive), allows to define an information signature.

Characterizing individual motor behaviour. It is clear that in the investigation of interpersonal coordination, behavioral analyses can help to understand the individual role of each group member from the local performance, and extract the particular features that can influence the global interaction, such as leadership. Quantitative methods for the detection of the most influential node are useful tools for decision-making in many real-life social networks.

The analysis of interpersonal and intergroup cooperation in networks is a central topic in the domain of cooperative game theory and one of the fundamental concepts of game theory is the Shapley value [122]. Since coalition building is a natural feature of agents' behavior for leadership emergence in social networks, the Shapley value has a practical importance for real-life applications. It is an index that characterizes the payoffs' distribution among players according to their personal contributions to the overall gain in a cooperative game. Specifically, it reflects the real-world players' interrelations since it counts mutual influence of players measuring the leadership of nodes in all possible coalitions of agents that can be formed within a network [123, 124].

The Shapley value-based centrality metric is not the unique solution to estimate leadership. For large-scale networks, the quantitative assessment of the leadership potential of nodes can be evaluated through the network structural characteristics [125]. Depending on the context of the problem, several conventional centrality metrics, e.g., those based on node degree, closeness, and betweenness, can be considered. Each of these metrics specifies type of leadership and, therefore, their efficiency depends on the application area.

Motor signatures constitute an additional evaluation method to characterize the individual behaviour in movement science. Among the diverse motor signals, micro-movements represent an interesting source to investigate and extract striking observations for researchers [126]. Taken in isolation, small fluctuations in the value of the movement parameters say very little about the individual behavior. Yet, over time, they accumulate evidence of the continuous flow of physical behavior, which can be studied as a stochastic process. It is possible to examine the evolution of the stochastic signatures in real time as well as longitudinally across different sessions. Therefore, micro-movements allow

a useful estimation of the underlying distributions of motor control parameters in a personalized manner and serve to reliably predict different levels of intentionality in the individual's actions. Diverse tools have been proposed to characterize the individual kinematic attributes. Experimental estimation of the probability distributions most likely can describe the unique and individual movement trajectory parameter. It can be done with SPBA [126], a new statistical platform for behavioral analyses that treats the speed-dependent variations from trial to trial as a stochastic process over time, and allows to statistically index the predictability of the estimated probability distribution across different tasks and as a function of different stimuli. A similar approach has been adopted by Slowinsky et al. [79]. They estimated the probability density function of the player's velocity to analyse similarity among participants by using the Earth mover's distance, an established tool in pattern recognition applications. Analyses by means of multidimensional scaling allows to visualize relations between the objects under investigation, reducing dimensionality while preserving as much information as possible. Signatures can be helpful also in studying goal-directed movements such as done in [127] where for each subject, a gamma distribution has been fit to match the personal distribution of peak velocities of individual movements. Here, each subject is represented by two points in the Gamma parameter space- one point representing the goal-directed signature and the other point representing the supplemental signature of variability in the peak velocity.

Pattern recognition and data reduction. In the case of large groups analysis such as crowds, flocks or swarms where a great amount of data is involved, it is often necessary to reduce dimensionality of the problem to reduce the very high computational burden and extract lower-dimensional patterns. In general, collective behaviour can be seen as dynamics on a a low-dimensional manifold on which coordinated group states may be embedded. Recently, a variety of machine learning algorithms have been developed. For this purpose, for example, to evaluate the level of imitative coordination between two participants, principal component analysis (PCA) [128] can be used. PCA is a standard statistical technique generally used to extract a low-dimensional structure from a high-dimensional dataset. In particular, PCA has been used to characterize the degree of covariance across time of different body segments in whole-body movements (e.g. locomotion). Mathematically, the method involves the eigenvalue decomposition of a dataset covariance matrix in order to find the principal directions in high-dimensional space. PCA identifies linear relationships within multi-dimensional datasets and then maps the original data into a newly defined space, with the principal components as its axes. The principal components do not necessarily map directly onto the original dimensions of the actual measurement. The end result is a representation of potentially new, important collective variables that best account for the variance within the observed system.

An alternative nonlinear technique is the isometric mapping algorithm (ISOMAP) that preserves geodesic distances in the raw data set and in the lower-dimensional manifold coordinates it extracts [40].

A recurrence plot is a powerful alternative tool for visualizing and analyzing patterns

of nonlinear dynamical systems when the state space itself is of too high-dimensionality to be visualized [129]. Rather than showing the state variable itself, it shows the relation between states at different points in time, e.g. as a distance matrix, from which one can infer how frequently a system visits different points in the state space. Recurrence plots may not work so well for high-dimensional dynamics involving multiple spatiotemporal scales. In that case, a topological version has been proposed to study metastable patterns [130].

Table 2.1: **Useful data analysis tools to study group interaction during joint action.**

Goal	Data analysis tools	Pros/Cons
Describing temporal and frequency relations	Relative positions, velocity errors, linear and lagged cross-correlation, cross-recurrence quantification, cross-spectral analysis, Fast Fourier Transform (FFT), FFT power spectrum overlap (PSO), peak frequency.	Useful to measure strength of time and frequency relation, and time delay between pairs of time series, to estimate symmetry between different time series, peak frequencies, and bidirectional weighted coherence to describe shared rhythmic variation between two physiological response systems. These methods do not provide any indicator of the quality of a group performance.
Quantifying group synchronization	Order parameter, individual parameter, dyadic synchronization index, frequency synchronization index, event synchronization measures.	Instrumental to quantify degree of phase and frequency synchronization among group agents, cohesiveness of each agent with respect to ensemble and within dyads. They can be used also to detect global degree of synchronization when infomation comes from signals of different nature and rapid changes of synchronization patterns. However, they can be used to analyse only oscillatory dynamics.
Detecting causal relations among agents (leadership)	Linear autoregressive model computed on motion profile, standard deviation, Lyapunov exponent, Wiener–Granger method, transfer and causation entropy, algorithmic complexity.	Helpful to evaluate stability of a particular player from observing the deviation of the set of consecutive trajectories in repeated trials and to estimate causal statistical influences between simultaneously recorded time series data both in linear and in complex systems.
Characterizing individual motor behaviour	Shapley value, centrality metrics (e.g., node degree, closeness, and betweenness), motor signatures, stochastic process, probability distributions of motor control parameters (e.g., individual velocity, peak velocities).	Useful to analyse individual contributions to overall gain in cooperative game and detect central agent role for different problem contexts. Evaluate individual motor signatures and characterize each subject by means of (estimated) individual kinematic attributes in a parameter space to facilitate visualization and behavioural analysis.
Pattern recognition and data reduction	Principal component analysis (PCA), isometric mapping algorithm (ISOMAP), recurrence plot.	Statistical techniques generally used to extract low-dimensional structure from high-dimensional datasets, by identifying linear/nonlinear relationships within multi-dimensional datasets and then map original data into a newly defined low-dimensional space.

In summary, in this section we provided an extensive overview of some useful data analysis tools in social sciences (see Table 2.1, for an overview), from temporal/frequency metrics, instrumental to quantify the strength of relation between pairs of time series, to synchronization indices, useful to measure the level of coordination among several group agents. We presented causality detection metrics that play a crucial role to analyse leadership relations among interacting partners. Then, we provided a collection of methods

for individual behaviour characterization, effective to unfold the influence of personal kinematic features on collective dynamics (and viceversa) and, at the end, we described some data reduction strategies, important to facilitate visualization and manipulation of large datasets.

Providing the mathematical details for each of the introduced tools is not the scope of this survey on human group coordination. Mathematical descriptions for the most important techniques used to analyse group dynamics and leadership emergence in this Thesis will be described later in Chapters 3- 6.

2.5 A possible application: development of exergames for autism

Autism affects about 1% of the adult population with very high associated costs and significant deficits in social interaction. A possible application of the results of this project is the development of a new software platform for tele-rehabilitation able to help medical staff and to minimize distances, time and costs through an approach based on modelling and classification of human motor synchronization.

In individuals diagnosed with autism spectrum disorders (ASD) impairments in executive function [131] and motor skills [132] have been consistently observed. Executive functions refer to cognitive processes used to guide behavior in a changing environment, and include impulse control, working memory, cognitive flexibility, and creativity [133], all skills necessary for social interaction, cognition, and goal-directed activities [134]. At the same time, motor skills are necessary for many types of human activities, such as self-care, writing, or sports [135]. Motor deficits often associated with ASD may include problems in motor planning, coordination, dysrhythmia, and an inability to participate in developmentally appropriate activities, which affect the child's ability to initiate motor activities or switch between motor tasks [132].

Deficits in executive function together with poor motor skills seriously limit participation in many important life activities.

There are different benefits on motor and cognitive abilities from participating in exercise games for children with autism. Evidence in favor of this potential benefit come from studies involving exercise entertainment games, such as sports or dancing games [136, 137] with beneficial effects [138] about motivation to engage in physical activity [137, 139], reducing repetitive behaviors, improving motor skills, and behavior on executive function tasks [136, 139]. For this reason, several computer-based interventions have been proposed to improve the efficacy of rehabilitative procedures.

Progress in telecommunications and information technology during the last decades has promoted and accelerated the growth of telehealth, specifically the development of applications for the delivery of clinical therapies in artificial environments in the context of **telerehabilitation**. In the '80s, the development of first game platforms driven by international game companies, such as Atari or Nintendo, gave birth to a new concept of active video gaming that require bodily movements to play as a form of physical activity. Exergaming has become an emerging trend in fitness, education and health sectors. The

term *exergame* covers its dual nature, as exercise and as games- exergame is more than virtual rehabilitation exercises.

(a) (b)

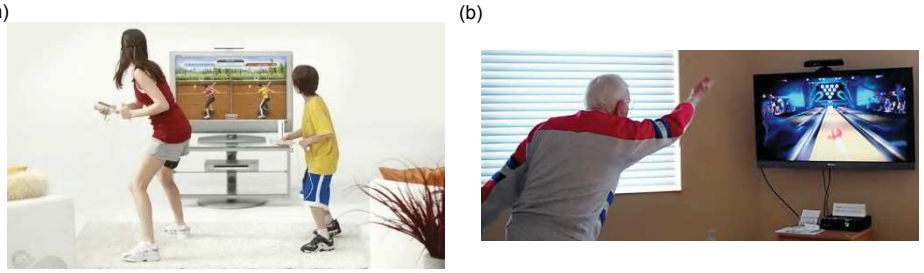

Figure 2.5: **Examples of exergames.** Panel (a) shows a dyadic exergame between two children[7]whereas in panel (b) an old man interacts in a virtual bowling scenario during a training session to improve Parkinson's disease motor symptoms[8]. Children and elderly people both represent the main users for whom exergame applications are addressed.

How to create an effective yet motivating exergame to provide powerful semi-autonomous rehabilitation is a key question. Several requirements need to be taken into account in order to reproduce the activity and the supervision of a human therapist:

- **Therapy efficacy**: exergames should incorporate multiple exercises to cover the whole range of needed movements, appropriate to the therapy;
- **Customization and adaptation**: the therapist needs to configure the parameters of the exercise to customize it for the specific condition of the subject, both off-line and online, to maximize the efficacy of the therapy for different patients. Customization helps in the day-by-day rehabilitation, so that the exercise can be configured to follow the daily progression of the patients and to readjust itself to match the patient's condition transparently during its execution, as a therapist typically does during a rehabilitative session;
- **On-Line monitoring and feedback**: during ordinary rehabilitation sessions, the therapist supervises patient's movements to guarantee a correct and safe execution of the rehabilitation exercise, and advises the patient in case it is not with appropriate feedbacks (verbal, haptic or visual). Clear and immediate feedbacks to the player's actions relate to the concept of quantifiable outcome, which is part of the definition of the game. If the feedback is not immediate, it may be hard to discern which action triggered which feedback, or to correct wrong behavior over time;
- **Motivation**: in traditional rehabilitation environments, therapists also act as motivational guides to the patients: they link with them emotionally, pushing them to perform their exercises and remind them of the final goal [140].

Among the exergaming attempts to motivate autistic patients to exercise, we mention Astrojumper [141], a stereoscopic virtual reality exergame where virtual space-themed

[1]*Image credit*: laurenzai.yolasite.com
[2]*Image credit*: mayo.edu

objects fly toward the patient who must leverage physical movements to avoid collisions. Investigations on children with autism showed that most patients were able to achieve high levels of activity and enjoyment [14]. Another successfull example is represented by the Makoto arena training [139], a light and sound speed-based exergame, used to investigate the response speed, executive function, and motor skills in school-aged ASD children. Significant progress was seen in average reaction speed, working memory and agility. Also social robots (e.g, NAO) may increase motivation by promoting engagement and learning achievement in autistic children with intellectual disability, communication impairments, and low adaptive and social skills (e.g., motor imitation). Results indicate that interacting with a social robot enhance engagement and goal achievement [36, 142].

These encouraging findings suggest that exergames are a promising way to improve autistic people' health and their quality of life. However, the issue of patient motivation is a major topic in rehabilitation, as it is of great importance for patient compliance. Rehabilitation exercises can be quite annoying and demanding. They require slow, monotonous, and often painful movements, performed at high intensity and for long time periods. On the other hand, a great motivation in traditional rehabilitation comes from the social presence of the clinician. In short, the power of simple games alone may not be enough to keep patient motivation high for the duration of the whole therapy.

It is quite hard to emulate the emotional and social capabilities of the therapist but in games, we can find several elements that can help in achieving good motivation, although in a radically different way than in traditional therapy, such as fun, challenge, immersion, curiosity [143], or rewards like verbal approval [144] or virtual achievements.

Special attention should be addressed to the **social dimension** of the play. Indeed, social interaction through game is listed by many authors as a great source of motivation [145, 146]. Traditional rehabilitation is usually performed through single-user exercises tuned to the specific patient's condition and guided by a therapist and, subsequently, the majority of exergames tend to be designed for single players (e.g., the previously cited Astrojumper [14], Makoto Arena [139], NAO [142]). Multi-user exercises are uncommon but exergames could greatly benefit from social play. The specific advantages of using multiplayer games for individuals with autism lie in increasing opportunities for social interactions. In particular, in [147] researchers highlighted the relevance of letting children interact in a multi-players scenarios to encourage pro-social behavior [145, 146] and improvement in learning language skills [148] more likely than single-player games. For example, playing entertainment video games with friends predicts positive friendship qualities for adolescents with ASD [149]. This is because promoting communication between multiple individuals in cooperative games provide safe opportunities to practice communication and social skills within the game, as well as practice with working collaboratively towards achieving their goals. This social aspect is fundamental to promote caregivers or relatives to play alongside the patient, helping with the game while the patient performs the exercise.

However, among the developed rehabilitative platforms very few examples consider a **multiplayer dimension** (e.g., ExerSync platform [150]) and a **model-based approach** is largely missing. The results which will be presented in the rest of this Thesis shed light on several aspects of multi-player coordination tasks and, hence, can be instrumental for the

development of better exergames for rehabilitation of patients affected by social disorders.

2.6 Summary

Coordination is a fundamental aspect of everyday life and exploring cooperation and emergent dynamics in human group contexts is relevant in many areas.

We provided an overview of the main studies on coordination and leadership both in animal and in human groups, and we highlighted the gaps that have not been addressed yet. In particular, current research is not yet fully able to give a unified definition of leadership, to identify a leader in the group, and to understand how to design a virtual therapist that need to guide the group. It is possible to define different types of leaders in terms of what we are interested in, such as a temporal leader [20, 31], structural leader, the person that does not follow the other or the least adaptive agent [86] and multiple types of leaders can coexist and enhance group performance [32, 86].This is possible because the interactions between humans are multidimensional [98] and never static. As often highlighted in this chapter, leadership is a self-organizing process where agents construct their own identities as leaders or followers [74]. This requires an adaptive and, therefore, timevariant attachment between partners allowed by the implicit plasticity in human behaviour. These links are certainly shaped both by the learning of others' behaviour and of the environment, and by the strategy that each agent decides to follow.

Next, we proposed an overview of the models and data analysis tools used in the literature, which were shown to be useful to investigate the synchronization process arising in human groups. Some of the mentioned methods have been used in this study and they will be described in the following chapters.

Finally, we have presented a general overview of the main features that an exergame should satisfy to be effective, and we have higlighted how being part of a group in a rehabilitation program enhances awareness, strategy behaviour, and psychosocial functioning. These aspects impact the ability to synchronize with others and, therefore, to become a socially connected unit in group [151].

In the following chapter, we investigate how coordination in human groups arises and is affected by a possible loss of visual interaction.

3 Moving together during and after visual interaction

Humans and other animals often cooperate in small or large ensembles, for anti-predation, for producing a collective performance, or sometimes just for entertainment. Among all sorts of cooperative behaviours, synchronization in space and/or in time of the members of the group is particularly present in the human repertoire. It is often rooted in perceptuo-motor synergies in which proximal (e.g., postures, breaths) or distal (e.g., gazes, voices, hands, legs) parts of the body are delicately locked, for brief or long periods of time, in frequency and in phase [152, 153]. In these and other examples, moving in unison is either the goal or clearly contributes to it, and results from both (i) personalized characteristics and (ii) the way individuals are coupled together.

Personalized characteristics refer, for instance, to mechanical properties such as body inertia, length of limbs, or location of the centre of mass. A crucial aspect of these personalized characteristics is the degree of similarity between the individuals involved, which facilitates synchronization. The identical mechanical properties of moving limbs, such as their natural oscillation frequencies, increase the level of synchronization by virtue of physical principles [154]. The morphological and kinematic resemblance of cooperating humans is also beneficial for synchronization [31, 155], which has positive effects in return for increasing emotional empathy [156] and social connectedness and rapport in general [157].

Perceptual contact is the most natural form of coupling between agents in a group. It obviously plays a crucial role, as the emergence and stability of a particular group structure heavily depend on how individuals are perceptually coupled, through mechanical [158], optical [159], or acoustical exchanges [160]. Visual and auditory couplings are the most pervasive forms of perceptual interaction in human groups, either separately [161] or combined, for instance during a meeting or when playing in an orchestra [162, 163]. Of interest for the present research is the recent discovery that certain topologies of the spatial organization of members in the group affect the strength and symmetry of perceptual coupling.

In these and other examples, perceptual connection among participants is often temporarily lost. In this Chapter, we target this powerful capacity of humans to maintain regimes of synchronization despite a transient loss of perceptual (i.e., visual) coupling. This phenomenon occurs for instance when a group of people continue to walk at the

same pace even after they separate, or when dancers in a choreographic performance maintain body synchronization during a transient lack of visual connection. This capacity is a solid contributor to a wide range of social performances, in sport or at work. It relies on our practical ability to internalise previously-produced movement patterns in a social context, and to maintain them when alone for a certain amount of time. Besides these alternative and not necessarily exclusive explanations, the memory effect has only been experimentally studied in dyadic situations, and its dynamics in various spatial configurations remains unknown. Addressing this issue is of pressing interest, not only for basic science, but also for its potential consequences toward the acquisition and mastering of cooperative patterns in a variety of domains such as daily work, sport, or music performance.

This chapter, whose contents have been published in [37], is devoted to the analysis of how the behaviour of a human ensemble, engaged in a specific coordination task, depends on the particular interaction pattern implemented (e.g., the topological structure of the visual pairings among its members), as well as on the group mechanical composition and individual synchronization abilities of the subjects involved. Specifically, we investigate the dynamics of voluntary synchronization, in groups composed of seven participants, manipulating their similarity, spatial organization, and the presence or duration of visual coupling (see Section 3.1). Participants were engaged in an intentional group synchronization task and had to swing a pendulum in order to achieve unison in space and in time (phase synchronization). This task was selected as (i) it is extremely easy to learn and perform, (ii) it has been documented before in a dyadic context [159], and (iii) it allows a simple yet precise control over each participant's natural frequency. Our data analysis- fully described in Section 3.2- confirms and unravels interesting attributes of human group motor synchronization, which are detailed in Section 3.3. In addition, in Section 3.4 in order to evaluate the contribution of memory (and of which type, individual or social) to synchronization persistence after visual interruption, we describe three versions of a dynamical model capturing the essence of our experimental data, with the potential for generalization to various group situations during which perceptual contact is transiently lost. At the end, a summary of the main findings will be given in Section 3.5.

3.1 Task and conditions

We considered two different experimental setups to investigate the unknown aspects of human synchronization dynamics.

In Experiment 1, we explored the influence of participants' similarity (i.e., homogeneity) on the emergence and quality of group coordination. Mechanical similarity was controlled by manipulating the pendula's inertia and hence the natural frequency of the players' oscillatory motion.

In Experiment 2, homogeneity among the players was manipulated at a different scale, by comparing groups of novices with groups of certified dancers. Since ballet and ballroom dancers encounter various neural [164], cognitive [165] and motor [166] changes during their years of practice, they can be considered as experts in sensorimotor synchronization compared to non-dancers [167–169].

Two groups of volunteers took part in our experiments and were grouped as follows:

- **Experiment 1.** A group of 7 participants, selected among 30 tested students at the University of Montpellier took part in the experiment (5 males, 2 females, all right-handed; mean age 21.2 y ± 1.5 y). They had no expertise in sensori-motor synchronization activities (e.g. music or dance).
- **Experiment 2.** A total of 28 right-handed volunteers were recruited among students at the University of Montpellier. They were divided into two macro-groups according to their dancing experience. The dancers (**D**) had more than 5 hours of practice per week over the past 10 years, and all possessed the French Dance EAT certificate (Dance professorship). The non-dancers (**ND**) had performed physical activities or sport less than three hours per week, and had never practiced dance or music before. Participants were assembled in four groups of seven individuals each. Specifically,
  - two groups of dancers: **D1** (5 females, mean age 25.6 y ± 3.1 y) and **D2** (6 females, mean age 22.4 y ± 2.4 y);
  - two groups of non-dancers: **ND1** (3 females, mean age 20 y ± 2.6 y) and **ND2** (4 females, mean age 21.9 y ± 2.27 y).

Both studies were carried out according to the principles expressed in the Declaration of Helsinki, and were approved by the EuroMov ethical committee. All participants provided their written informed consent to participate in the study, and this consent was also approved by the ethical committee.

In both experiments, the volunteers, seated in a circle in a quiet room with no distractions, were asked to oscillate a pendulum, in synchronization with each other (Fig. 3.1(a)-(c)). The instruction was "*Synchronize the movement of your pendulum back and forth with the movement of the others, as naturally as possible, as if you could do it for* 30 *minutes*". A demonstration was performed to make sure that the task was understood by each participant, and to clarify that synchronization in phase, and not only in frequency, was expected. Each group performed the experiments in four different interaction patterns among players (i.e., *topologies*), implemented through the combination of the spatial location of each participant and the use of home-made goggles limiting the field of vision to the desired location. Namely, the four topologies were

- **Complete graph**: participants had all the other players in their field of vision;
- **Ring graph**: each participant could only see the motion of the pendulums of their two closest neighbors;
- **Path graph**: this topology is similar to the ring graph, with the exception of two participants who could visualize the motion of only one neighbor;
- **Star graph**: this topology prescribes the presence of a hub, that is, a player who could see the motion of all the other players, who, in turn, could only see the motion of the hub.

See Figure 3.1(d).

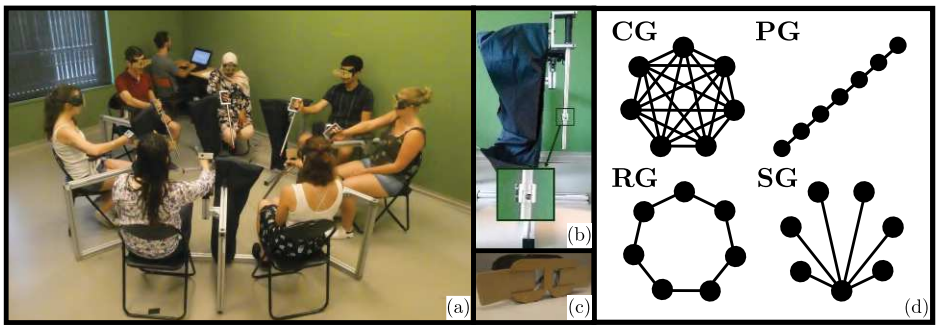

Figure 3.1: **Experimental set up.** Experimental set up with (a) seven participants, (b) details on one aluminium pendulum showing the additional mass, (c) in-house goggles controlling the field of view; (d) complete, ring, path, and star graphs tested.

In each topology, each group performed 5 trials of 75 s each in Experiment 1, and of 90 s each in Experiment 2. The trials alternated absence or presence of visual contact as follows:

- **Eyes-closed period 1 (EC_1).** The participants were asked to first swing the pendulum with their preferred hand at their own comfortable tempo during 15 s (Experiments 1) or 30 s (Experiments 2), while keeping their eyes closed.
- **Eyes-open period (EO).** Once the baseline was established in EC_1, the participants were instructed to open their eyes, synchronize their pendulums, and maintain this synchronization regime during 30 s;
- **Eyes-closed period 2 (EC_2).** The participants were then instructed to close their eyes again, and to keep on swinging their pendulum for 30 s. For the subsequent analyses, the eyes-closed period 2 is split into two periods of equal length, denoted by EC_{2a} and EC_{2b}, respectively.

An acoustic signal notified the requested change between visual conditions. The comparison between the first two conditions allowed us to evaluate the role of perceptual contact in creating synchronization patterns. The comparison between the two eyes-closed periods (before vs. after visual exchange) allowed the evaluation of the transient persistence of synchronization in the absence of visual contact.

In Experiment 1, these analyses were repeated in three different *Homogeneity* conditions. Indeed, the 7 participants were selected among 30 volunteers based on pre-tests that were run to compute their natural frequencies. Specifically, each participant was asked to sequentially oscillate 7 pendulums characterized by 7 different eigenfrequencies (4.71 rad/s, 4.78 rad/s, 4.84 rad/s, 4.96 rad/s, 5.03 rad/s, 5.09 rad/s, and 5.15 rad/s, respectively), obtained by adding additional masses of 96 g at different locations of the pendulums' arm (see Fig. 3.1(b)). For each pendulum, 5 trials of 20 s each were performed to select the 7 participants of Experiment 1, based on the frequency of their natural movement and their stability across time and trials. This enabled the design of the three *Homogeneity* conditions:

- **Matched.** By appropriately placing the additional masses, the different natural frequencies of the 7 participants were compensated so that their swinging frequency coincided (5.34 rad/s). The selected value of 5.34 rad/s corresponds to the group average of all the individual frequencies recorded during the pre-tests.
- **Matched-but-one.** The six most stable participants at pre-tests (characterized by an individual coefficient of variation in the range 0.33% – 2.75%) were set at the same swinging frequency of 5.34 rad/s, while the seventh participant (the most unstable, coefficient of variation 4.50%) was set at a different frequency (6.28 rad/s). This condition was used to test to what extent and under which interaction topology the introduction of one outlier would destabilize an otherwise homogeneous network.
- **Natural.** Here, all the additional masses were removed, and the 7 participants performed the task at their own natural frequency, ranging from 5 rad/s to 6.13 rad/s.

3.2 Data analysis

Data collected in each experimental setup were processed following two steps: preprocessing and metrics computation.

3.2.1 Preprocessing

Each pendulum was equipped with a calibrated analog potentiometer to record its angular motion at $f_s = 200$ Hz. The position time series were then smoothed out through a Moving Average filter with a time window of 10 samples ($\Delta t_w = 0.05$ s). The Hilbert transform method [170] was applied on the filtered positions to extract the time series of the phases.

3.2.2 Data analysis and relevant metrics

Denoting T as the number of samples in each trial and N as the number of players, we can define $\theta_i(k)$ as the phase of the i-th pendulum at the k-th sampling instant, for all $i = 1, \ldots, N$ and $k = 1, \ldots, T$. The following set of metrics were used to capture the relevant features of the human group interactions recorded in our experiments:

- **Individual frequencies and group frequency**
  At each time step, we computed the angular velocity of each player by applying finite differences (*forward Euler method*) to the extracted phases:

$$\omega_i(k) = \frac{\theta_i(k+1) - \theta_i(k)}{\Delta t}, \qquad i = 1, 2, \ldots, N \quad , \tag{3.1}$$

  with $\Delta t = 1/f_s$ being the sampling time. This allowed us to characterize the frequency of each participant and its stability. Then, the average frequency of the group, $\omega_{\text{group}}(k)$, was extracted as the time-average of $\omega_i(k)$.
- **Group synchronization metrics**
  To quantify and characterize the level of synchronization among the players, we used the following metrics:

– *Phase-synchronization index*: for each trial, we evaluated the extent of synchronization in the group at each sampling time k through the order parameter $r(k)$, defined as

$$r(k) = \left| \frac{1}{N} \sum_{i=1}^{N} e^{j\theta_i(k)} \right| \qquad \forall k \in \{1, \ldots, T\}, \tag{3.2}$$

where j is the imaginary unit. Note that $r(k)$ belongs to the interval $[0, 1]$, and it is 1 when the phases coincide at time k. Then, we computed the average order parameter in the trial $\bar{r}$, and that is,

$$\bar{r} = \frac{1}{T} \sum_{k=1}^{T} r(k). \tag{3.3}$$

– *Levels of group phase synchronization*: to allow for a proper comparison of the extent of synchronization in the group in the various conditions introduced in the main document, we discretized the order parameters into four *phase-synchronization levels* (see Fig. 3.2):

$$\text{Level}_r(k) = \begin{cases} 1, \text{ if } r(k) < 0.70 & \textbf{(not in sync)}, \\ 2, \text{ if } 0.70 \leq r(k) < 0.85 & \textbf{(weak synchronization)}, \\ 3, \text{ if } 0.85 \leq r(k) < 0.95 & \textbf{(medium synchronization)}, \\ 4, \text{ if } 0.95 \leq r(k) \leq 1 & \textbf{(high synchronization)}. \end{cases} \tag{3.4}$$

Note that $\text{Level}_r(k) = 1$ (not in sync) means that the phase of the pendula at time k cannot be grouped in a circular sector of angle π rad.

– *Time-To-Synchronization and Time-In-Synchronization*:
Figure 3.2 illustrates how data were classified in order to compute the *Time-To-Synchronization* (**TTS**) and the *Time-In-Synchronization* (**TIS**).

  * **Eyes-open** *(EO)***: computing** TTS. For a given trial, we denote $T_{\text{sync},i}$ as the number of sampling instants k such that $\text{Level}_r(k) = i$, and the corresponding fraction $F_{\text{sync},i} = T_{\text{sync},i}/T$, for $i = 1, \ldots, 4$. We computed TTS only for trials in which $F_{\text{sync},1} \leq 0.5$ in order to exclude from the analysis the trials in which synchronization was only occasionally achieved. The remaining trials were classified as follows:

    1. if $F_{\text{sync},2} + F_{\text{sync},3} > 0.75(1 - F_{\text{sync},1})$, then the trial was considered as an instance of *Medium* synchronization;
    2. if $F_{\text{sync},3} + F_{\text{sync},4} > 0.75(1 - F_{\text{sync},1})$, then the trial was considered as an instance of *High* synchronization;
    3. if neither condition 1 nor 2 are satisfied, then the trial is considered as an instance of *Weak* synchronization.

    Depending on the above classification, TTS was defined as the first time instant such that Level_r became 2 (for trials of weak synchronization), 3 (for trials of medium synchronization), or 4 (for trials of high synchronization).

∗ **Eyes-closed (EC_2): computing** TIS. TIS was the first time instant such that $\text{Level}_r < 1$ if the players stayed in sync ($\text{Level}_r > 1$) after closing their eyes for at least 3 consecutive periods of length $2\pi/\omega_{\text{group}}$, where ω_{group} is the mean frequency of the players in the trial. Otherwise, we set TIS= 0.

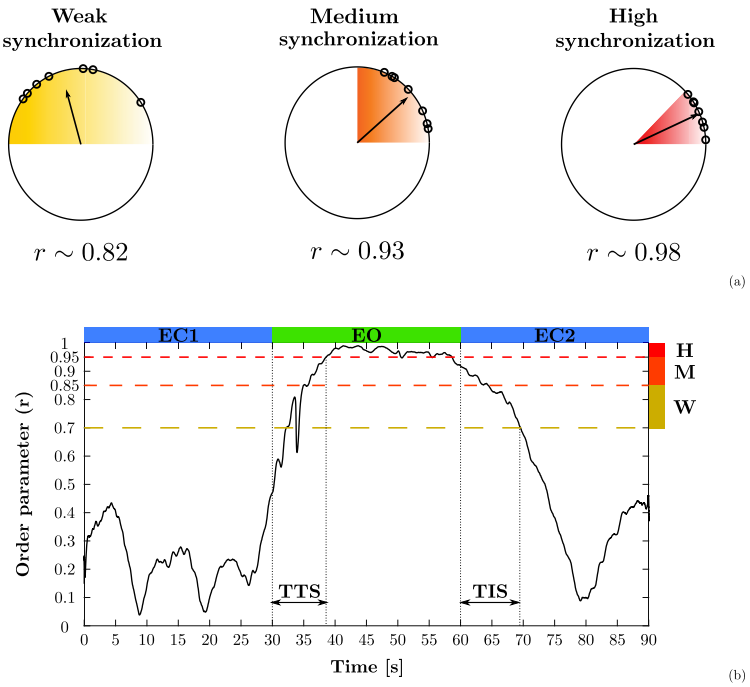

Figure 3.2: **Levels of phase synchronization.** Three levels of synchronization — Weak (W), Medium (M), and High (H) — characterized by the value of the order parameter r, used to determine Time-To-Synchronization (TTS) and Time-in-Synchronization (TIS). *EO*: Eyes Open; *EC*: Eyes Closed.

3.3 Synchronization results

3.3.1 Experiment 1: mechanical similarity

Individual and group frequencies

We computed the average ω_{group} recorded during the interaction across the three Homogeneity conditions and compared them with the average individual frequency, which we called ω_{solo}, that the players displayed during the pre-test session. On average, these frequencies were measured to be 5.34 rad/s (SD: 0.05), 5.23 rad/s (SD: 0.03), 5.31 rad/s (SD: 0.02), and 5.33 rad/s (SD: 0.03) in Solo, Matched, Matched-but-one, and Natural

conditions respectively, and were affected by our manipulation. A repeated-measures ANOVA detected a general Homogeneity effect ($F(3, 12) = 9.48$. $p = 0.002$, $\eta^2 = 0.70$) showing that swinging movements slowed down when performed in the groups. This slowing down was however observed only in the Matched condition (post-hoc Bonferroni difference between Solo - Matched $p = 0.002$, Matched - Matched-but-one $p = 0.02$, Matched - Natural $p = 0.004$), at first sight a surprising result. However, as the homogeneous (Matched) condition was also the condition exhibiting the highest synchronization performance, both in frequency and in phase, this suggests that our players modulated their behaviour in that condition, i.e., slowed down, in order to maximize perceptual coupling and increase performance (the group values reported here are those extracted from the eyes-open periods).

Movement similarity increases phase synchronization during and after visual interaction

The values recorded in the 5 trials performed by the group in each condition were considered independent samples in a within-subjects analysis of variance (repeated-measures ANOVA) with *Homogeneity* [Matched, Matched-but-one, Natural], *Topology* [Complete, Path, Ring, Star] and *Vision* [EC_1, EO, EC_{2a}, EC_{2b}] as factors. The three way (Homogenity $\times$ Topology $\times$ Vision) repeated-measures ANOVA on r values, with all degrees of freedom corrected using the Greenhouse-Geisser estimate of sphericity, showed a main effect of Vision ($F(1.17, 4.67) = 53.4$, $p < 0.001$, $\eta_p^2 = 0.93$), indicating that visual coupling induced phase synchronization. This main effect was completed by a Homogeneity $\times$ Vision interaction ($F(1.89, 7.54) = 7.52$, $p = 0.017$, $\eta_p^2 = 0.65$), see Figure 3.3(a) (left panel), suggesting that movement similarity increased the visual advantage. Particularly interesting for the present research is the transient persistence of phase synchronization, after vision has been removed (EC_{2a} condition). This is witnessed by significant post-hoc Bonferroni comparisons between EC_1 and EC_{2a} ($p = 0.001$), and between EC_{2a} and EC_{2b} ($p < 0.001$). This was the case in all homogeneity conditions, with a clear advantage of fully similar movements compared to the other two homogeneity types ($p < 0.001$). In short, group phase synchronization persisted for around 7 seconds after visual interaction had been interrupted, a persistence that was strongly reinforced when the participants' motion was homogeneous.

Topology modulates phase synchronization and its persistence after visual interruption

The ANOVA presented above also revealed an effect of Topology ($F(3, 12) = 9.54$, $p = 0.002$, $\eta_p^2 = 0.70$), showing that Complete and Star graphs yielded higher synchronization than Ring and Path graphs (post-hoc Bonferroni comparisons: Ring different from Complete, $p = 0.007$, and from Star, $p = 0.004$). This confirmed a result previously obtained for different types of movement [25]. More important is the finding that phase persistence after visual interruption was reinforced for the two leading topologies (Complete and Star graphs) compared to the Ring and Path graphs (see Figure 3.3(a), right). This is shown by the significant Topology $\times$ Vision interaction ($F(2.23, 8.93) = 10.8$, $p = 0.004$, $\eta_p^2 = 0.73$), and by the subsequent post-hoc analyses (Complete and Star topologies differ from Path and Ring topologies in EO ($p < 0.001$) and in EC_{2a}

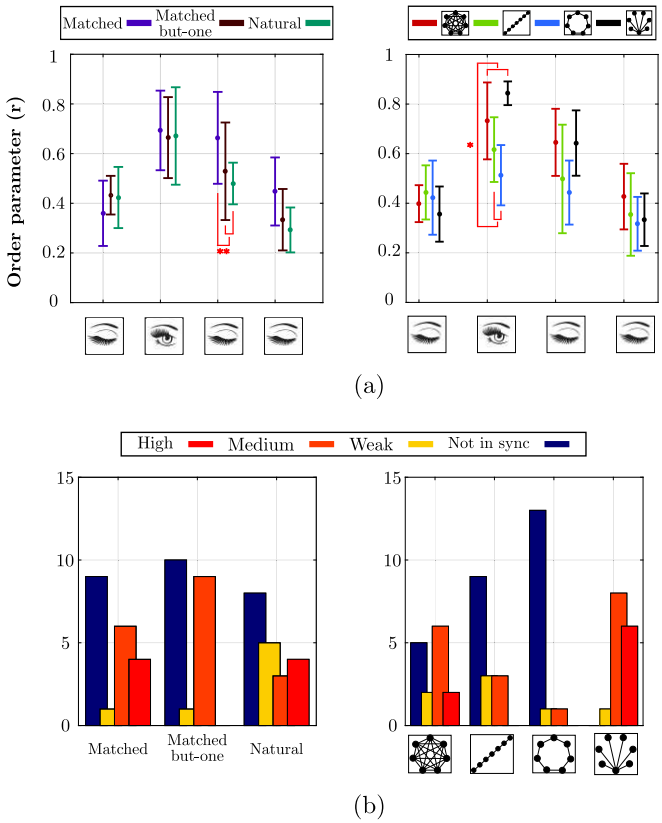

Figure 3.3: **Main results of Experiment 1.** (a) Mean and standard deviation of phase synchronization across homogeneity (left panel) and topology conditions (right panel); (b) distribution of phase synchronization levels for Similarity (left panel) and Topology (right panel).

($p < 0.001$); Complete topology differs from Star ($p = 0.02$), from Path ($p = 0.01$), and from Ring topologies ($p = 0.03$) in EC_{2b}).

Synchronization quality through the order parameter r

To assess the quality of synchronization among conditions, we defined four levels of coordination based on the order parameter values: (i) not-in-sync ($r < 0.7$), (ii) weak ($0.7 \leq r < 0.85$), (iii) medium ($0.85 \leq r < 0.95$), and (iv) strong ($0.95 \leq r \leq 1$). In order to test for Homogeneity and Topology effects, we ran the log-likelihood version of χ^2, the $G-$test, on the distribution of these four levels, encoded by a variable denoted by Level_r. We found that the distributions were indeed different. Homogeneity exhibited weak synchronization when an outlier was present in the group (matched-but-one condition) ($G^2(6) = 14.08$, $p = 0.02$, Cramer's $V = 0.34$) (Figure 3.3(b), left panel). Topology

showed an increase in occurrence of medium and high phase values for the Complete and Star graphs ($G^2(9) = 41.15$, $p < 0.001$, Cramer's $V = 0.48$) (Figure 3.3(b), right panel).

Time-To-Synchronization (TTS) and Time-In-Synchronization (TIS)

To complete our analyses, we evaluated the effect of homogeneity in individual frequencies on the temporal aspects of the various synchronization regimes. This was performed by focusing on two variables, (i) the time to synchronization (TTS), capturing the time necessary for all participants to reach phase synchronization once they had opened their eyes, and (ii) the time remaining in synchronization (TIS) after eye closure, quantifying the memory effect (see Figure 3.2). Since the normality assumption was not met for TTS, we analysed the *Homogeneity* effect through the Kruskal-Wallis statistical test instead of an ANOVA whereas for TIS, the normality assumption was met but the data were not homoscedastic. We ran the Welch's ANOVA on TIS, together with Games-Howell post-hoc tests for pairwise comparisons.

TTS did not differ between conditions but TIS did, showing a group effect ($F(2, 19.66) = 15.30$, $p < 0.001$, $\eta_p^2 = 0.61$), more precisely a difference between the Natural condition (5.32 s) and the two other conditions, Matched (9.95 s, $p = 0.001$) and Matched-but-one (8.20 s, $p = 0.003$), see Tab. 3.1.

Table 3.1: **Time-To-Synchronization** (TTS) **after eyes opening and Time-In-Synchronization** (TIS) **after eyes closing in Experiments 1.**

	Mean TTS	**Mean** TIS
Matched	8.66 s	9.95 s
Matched-but-one	8.18 s	8.20 s
Natural	6.25 s	5.32 s

3.3.2 Experiment 2: influence of participants' expertise

While Experiment 1 manipulated similarity between participants at the fast temporal scale of pendulum dynamics, Experiment 2 investigated similarity at a much more extended temporal scale. The group synchronization metrics were compared between novice and expert dancers, again across topologies and visual interaction.

Complete and Star graphs increased synchronization and persistence

Here as well we evaluated the synchronization performance reached by our participants in the group through the order parameter reflecting phase synchronization. A preliminary analysis of the *Group* factor [**D1**, **D2**, **ND1**, **ND2**] showed that the two groups of dancers (and of two non-dancers) were not statistically different and, for this reason, the sub-groups were combined to form the *Expertise* factor [**D**={**D1** ∪ **D2**}, **ND**={**ND1** ∪ **ND2**}]. Therefore, the values recorded in the 10 trials performed by each group (**D/ND**) in each *Vision* and *Topology* condition were considered as independent samples in a mixed repeated-measures analysis of variance with one between factor — *Expertise* [Dancers/Non dancers] — and two within-factors — *Topology* [Complete, Path, Ring, Star], and *Vision* [EC_1, EO, EC_{2a}, EC_{2b}]. As the Mauchly's test indicated non sphericity of the values of r for Topology ($\chi^2(5) = 17.6$, $p = 0.004$) and for the Topology × Vision interaction ($\chi^2(44) = 64.2$, $p = 0.03$), degrees of freedom were corrected using the Greenhouse-Geisser estimate of sphericity (Topology: $\epsilon = 0.59$, Topology × Vision: $\epsilon = 0.54$). The ANOVA revealed a main effect of Topology ($F(1.78, 32.1) = 27.8$, $p < 0.001$, $\eta_p^2 = 0.61$), again suggesting that the Complete and Star graphs increased synchronization by about 15%. It also revealed a general vision effect ($F(3, 54) = 196$, $p < 0.001$, $\eta_p^2 = 0.92$), suggesting a clear memory effect for both samples of participants during the first 15 s following visual occlusion (EC_{2a}). Interestingly, the Topology × Vision interaction (Figure 3.4(c)) was significant ($F(4.83, 87) = 14.7$, $p < 0.001$, $\eta_p^2 = 0.45$), indicating that this memory effect was prolonged after 15 s for the Complete graph, i.e., during EC_{2b} (all post-hoc $p < 0.03$).

Dancing increased synchronization and persistence

A main effect of Expertise was also found ($F(1, 18) = 34.2$, $p < 0.001$, $\eta_p^2 = 0.66$), indicating that dancers were in general more synchronized than novices, a clear anticipated effect of expertise visible in this simple pendulum oscillation task. More importantly for our research is the significant interaction found between expertise and the other factors (Figure 3.4(a)-(c)). First, the Expertise × Vision interaction ($F(3, 54) = 16.7$, $p < 0.001$, $\eta_p^2 = 0.48$), Figure 3.4(a), revealed that dancers exhibited a higher phase synchronization in EO (post-hoc $p = 0.002$) and in EC_{2a} than non dancers (post-hoc $p = 0.002$), the two conditions revealing the memory effect. Second, the Expertise × Topology interaction ($F(1.78, 32.1) = 3.63$, $p = 0.04$, $\eta_p^2 = 0.17$), Figure 3.4(b), revealed that the advantage of the complete graph at facilitating group synchronization benefited more to the dancers than to the novices (post-hoc $p = 0.002$).

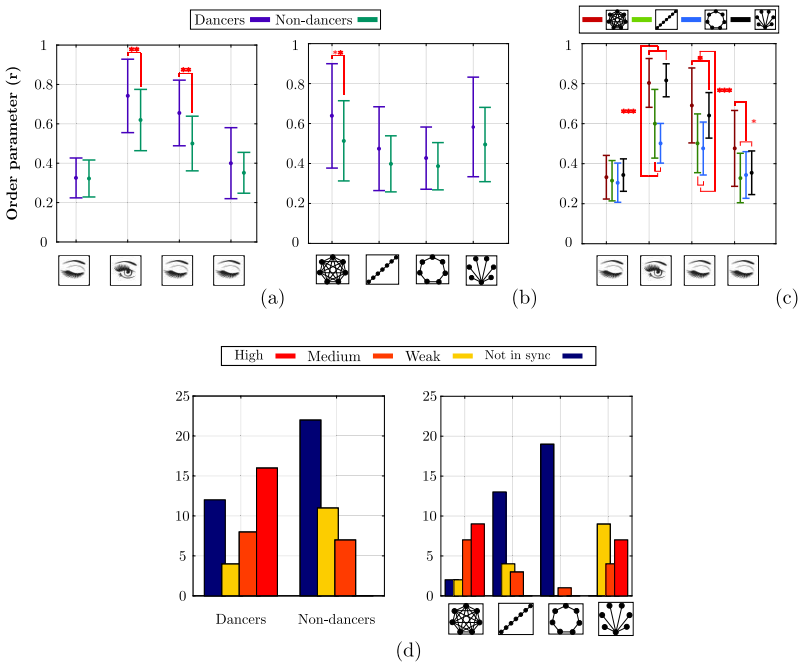

Figure 3.4: **Main results of Experiment 2.** Mean and standard deviation of Phase synchronization r in Experiment 2 as a function of (a) Vision × Expertise, (b) Expertise × Topology, (c) Vision × Topology); (d) distribution of phase synchronization levels across categories of robustness for Expertise (left panel) and for Topologies (right panel).

Synchronization quality analysis through the order parameter r

As in Experiment 1, we evaluated the extent of phase synchronization by grouping the values of the order parameter into four levels (from absent to strong synchronization), and compared the obtained distributions of Level$_r$ values using χ^2 tests. The analysis confirmed the general results obtained in Experiment 1. Indeed, distributions were different for Expertise ($\chi^2(3) = 22.28$, $p < 0.001$, Cramer's $V = 0.53$), with a higher occurrence of poor synchronization levels for novices compared to experts (Figure 3.4(d), left panel). They were also different for Topology ($G^2(9) = 77.29$, $p < 0.001$, Cramer's $V = 0.57$) (Figure 3.4, right panel), showing higher synchronization levels for Complete and Star graphs when compared to Ring and Path graphs.

Time To Synchronization (TTS) and Time In Synchronization (TIS)

Since the normality assumption was met neither for TTS nor TIS, we used the Mann-Whitney test instead of a $t-$test. Here again, we observed that *TTS* did not differ between groups. However, dancers were found to remain synchronized for a longer time interval after visual occlusion (in EC_{2a}) compared to non-dancers, 8.81 s and 6.26 s respectively ($U = 143$, $p = 0.007$, $r = 0.39$), consistent with the memory effect observed above (see Tab. 3.2).

Table 3.2: **Time-To-Synchronization** (TTS) **after eyes opening and Time-In-Synchronization** (TIS) **after eyes closing in Experiments 2.**

	Mean TTS	**Mean** TIS
Dancers	8.99 s	8.81 s
Non dancers	7.21 s	6.26 s

3.4 Modelling group synchronization and memory effect

Next, we present a modelling framework to capture the experimental observations and to test different hypotheses in order to explain the persistence of synchronization observed in groups when visual coupling is suddenly lost.

Due to the oscillatory nature of the tasks that the volunteers were asked to carry out, the mathematical model we employ to account for the dynamics of the group observed in the these experiments and for the rest of this thesis work is a network of nonlinearly coupled heterogeneous Kuramoto oscillators [38]. Such model is described by:

$$\dot{\theta}_i(t) = \omega_i + c \sum_{j=1}^{N} a_{ij} \sin\left(\theta_j(t) - \theta_i(t)\right) \tag{3.5}$$

with θ_i representing the phase of the motion of the preferred hand of the i-th human subject in the ensemble, ω_i their own natural frequency of oscillation when not coupled with the others (i.e., preferred rhythm recorded in the eyes-closed sessions), and N the number of players. Each participant is modelled with a different value of ω_i, so as to account for human heterogeneity, and is influenced by the interaction with her/his neighbours modelled by the second term in the right hand side of Eq. 3.6. In particular, $a_{ij} = a_{ji} = 1$ if the topology being studied involves a visual connection between players i and j when eyes are open, whereas $a_{ij} = a_{ji} = 0$ if it does not. Parameter c, here assumed to be constant and equal for all nodes in the network, models the intensity of interaction among the subjects, i.e., when visual coupling was established.

In this work, in a first attempt, following [25], we modeled the group dynamics as a network of Kuramoto oscillators, coupled through the graph topologies used in the experiment and we embedded the transition between 'eyes closed' and 'eyes open' by setting the coupling gain c instantaneously to zero so that the motion of each player in the group is modeled as

$$\dot{\theta}_i(t) = \begin{cases} \omega_i + c \sum_{j=1}^{N} a_{ij} \sin\left(\theta_j(t) - \theta_i(t)\right), & \text{if eyes open,} \\ \omega_i, & \text{if eyes closed,} \end{cases} \tag{3.6}$$

In the following, we will refer to this model as the **Static Coupling** model (**SC**).

Two additional versions of the model were contrasted to better understand the origin of the memory effect following visual interruption: the individual memory (**IM**) version, and the social memory (**SM**) version. Similarly to the **SC** model, these two versions predict a decay rate in synchronization metrics when vision is removed. However, the **IM** version predicts that the decay is based on the individual motion features of each participant, whereas the **SM** version predicts a decay dependent upon the synchronization strength at the time of visual interruption. In the first model extension, the **Individual Memory** model (**IM**), we assume that the motion frequency exhibited by each player at time t_a of visual occlusion remains first as similar as possible to the last frequency $\dot{\theta}_i(t_a)$ exhibited with eyes open, and then, after some time lag, relaxes back to the natural frequency of the player, ω_i. The model then becomes:

$$\dot{\theta}_i(t) = \begin{cases} \omega_i + c \sum_{j=1}^{N} a_{ij} \sin\left(\theta_j(t) - \theta_i(t)\right), & \text{if eyes open,} \\ \omega_i + \phi(t)(\dot{\theta}(t_a) - \omega_i), & \text{if eyes closed,} \end{cases} \tag{3.7}$$

with $\phi(t) = \exp\left(-(t - t_a)/\tau\right)$; τ being the estimate of the decay time observed experimentally once visual contact among the participants is lost.

We contrasted the model above with the predictions of a different model, the **Social Memory** model (**SM**). In this model, we assume that participants maintain longer synchronization times at eye closure by internalising the aggregate group dynamics. These dynamics are captured by the modulus $r_i(t)$ and phase $\psi^i_{\text{ref}}(t)$ of the local order parameter computed by player i, using information received from the visually coupled players before closing their eyes. In this case we have

$$\dot{\theta}_i(t) = \begin{cases} \omega_i + c \sum_{j=1}^{N} a_{ij} \sin\left(\theta_j(t) - \theta_i(t)\right), & \text{if eyes open,} \\ \omega_i + c\phi(t) r_i(t_a) \sin\left(\psi^i_{\text{ref}}(t) - \theta_i(t)\right), & \text{if eyes closed,} \end{cases} \tag{3.8}$$

where $\psi^i_{\text{ref}}(t) = \dot{\psi}^i_{\text{ref}}(t_a)(t - t_a) + \psi^i_{\text{ref}}(t_a)$ and $\phi(t)$ is the decay function defined above.

3.4.1 Models parameterization

To test the model validity, we parameterized the model from experimental data as described here, and then computed the average TIS after switching the coupling c to zero.

Selection of coupling strength c

For a given group and topology, we varied c between 0 and 1 with step 0.01 and, for each value of c, we ran 50 simulations of the Static Coupling (**SC**) model described in equation (1) of the main document. Each of the 50 simulations differed for the selection of the frequency ω_i and for the initial phase $\theta_i(0)$, $i = 1, \ldots, 7$. Specifically, the frequency of the i-th player was extracted from a Gaussian distribution with the mean and variance corresponding to the sample estimation performed in EC_1. The initial phases were selected from a uniform distribution in $[0, 2\pi]$. For each value of c, we computed the average order parameter $\bar{r}(c)$ in the 50 corresponding trials. Then, we chose c as

$$\arg\min_{c} |\bar{r}_{\text{exp}} - \bar{r}(c)|, \tag{3.9}$$

where $\bar{r}_{\text{exp}}$ is the mean order parameter in EO across all the trials for the selected group and topology. The procedure was iterated to associate a value of c to each group and topology, see Table 3.3.

Table 3.3: **Coupling gains in Experiments 1 and 2.**

	c Complete	c Path	c Ring	c Star
Exp.1				
Matched	0.04	0.20	0.16	0.28
Matched-but-one	0.07	0.20	0.11	0.38
Natural	0.08	0.41	0.10	0.72
Exp.2				
Dancers 1	0.08	0.43	0.10	0.50
Dancers 2	0.12	0.40	0.09	0.50
Non dancers 1	0.07	0.14	0.07	0.25

Selection of decay time τ

For each group, we varied τ such that $1/\tau$ ranges between 0.02 and 1 with step 0.02 and, for each value of τ, we ran 50 simulations of the **IM** model (equation (2) in the main document) differing for the initial phases and natural frequency of the player (selected as above). For each value of τ, we computed the average time in synchronization $\overline{\text{TIS}}(\tau)$ in the 50 corresponding trials. Then, we chose τ as

$$\arg\min_{\tau} \left| \overline{\text{TIS}}_{\text{exp}} - \overline{\text{TIS}}(\tau) \right|, \tag{3.10}$$

where $\overline{\text{TIS}}_{\text{exp}}$ is the mean TIS across all trials where TIS was statistically different from the TIS obtained from simulations of the **SC** model (Mann-Whitney test). The procedure was iterated to associate a value of τ to each group. The same steps were followed to tune τ in the Social Memory **SM** model (equation (3) of the main document). All the identified values of τ in the **SC** and **SM** models are reported in Table 3.4.

Table 3.4: **Decay time τ estimated from data for each group and memory model in Experiments 1 and 2.**

	τ_{IM}	τ_{SM}
Exp.1		
Matched	12.50	8.33
Matched-but-one	10	12.50
Exp.2		
Dancers 1	8.33	6.25
Dncers 2	8.33	8.33

3.4.2 Comparing models

We observed that the **SC** model was unable to capture the relatively longer TIS measured experimentally, with model predictions being consistently shorter than expected in all conditions except in the natural condition (see Table 3.5). Significant differences were indeed found between data and simulations for Matched ($U = 222$, $p = 0.001$, $r = -0.37$) and Matched-but-one conditions ($U = 75$, $p = 0.003$, $r = -0.43$), while the model agreed with the data in the Natural condition ($U = 43$, $p = 0.17$, $r = -0.30$). When used to explain the observations in Experiment 2, the same model did capture the synchronization dynamics of the non-dancers ($U = 405$, $p = 0.41$, $r = -0.01$). However, it failed to capture the longer TIS exhibited by the dancers' group during the experimental trials ($U = 917$, $p < 0.001$, $r = -0.38$). Therefore, a more sophisticated model is required to adequately capture the experimental observations.

Table 3.5: **Comparison of the Static Coupling, Individual Memory and Social Memory models with the experimental results: average (with standard deviation) experimental Time-In-Sync $\overline{\text{TIS}}_{\text{exp}}$ versus average (with standard deviation) simulated Time-In-Sync $\overline{\text{TIS}}_{\text{sim}}$; **$p < 0.01$, ***$p < 0.001$.**

	Conditions	Experimental results $\overline{\text{TIS}}_{\text{exp}}$	Static Coupling $\overline{\text{TIS}}_{\text{sim}}$	Individual Memory $\overline{\text{TIS}}_{\text{sim}}$	Social Memory $\overline{\text{TIS}}_{\text{sim}}$
Exp. 1	Matched	9.95 ± 3.71 s	6.52 ± 2.88 s **	9.73 ± 3.72 s	9.71 ± 3.67 s
	Matched-but-one	8.20 ± 1.94 s	5.94 ± 2.77 s **	8.26 ± 2.55 s	8.16 ± 3.23 s
	Natural	5.32 ± 1.17 s	4.74 ± 1.06 s	-	-
Exp. 2	Dancers	8.81 ± 3.42 s	5.92 ± 2.11 s ***	8.90 ± 2.97 s	8.97 ± 3.36 s
	Non dancers	6.26 ± 2.43 s	5.66 ± 2.07 s	-	-

More specifically, the longer TIS exhibited in both experimental scenarios suggests that some memory mechanism was present, allowing the groups to stay in sync for longer than predicted by a sudden memory-less transition from eyes-open to eyes-closed.

Both the **IM** model ($M = 2.05$, $SD = 1.58$ error across topologies) and the **SM** model ($M = 1.38$, $SD = 1.84$ error across topologies) were found to capture the experimental data (mean difference= -0.67, $t(6) = -1.98$, $p = 0.09$, $r^2 = 0.40$). In Experiment 2, the **IM** model ($M = 0.96$, $SD = 1$ error across topologies) was found to better capture the experimental data than the **SM** Model ($M = 1.74$, $SD = 1.53$ error across topologies, mean difference= -0.79, $t(7) = -2.87$, $p = 0.02$, $r^2 = 0.54$). This would explain the residual synchronization found in dancers. For both models, and for all of the four topologies top $\in$ {Complete, Path, Ring, Star}, we computed the error $e_{\text{top}} = \left|\overline{\text{TIS}}_{\text{exp,top}} - \overline{\text{TIS}}_{\text{sim,top}}\right|$ where $\overline{\text{TIS}}_{\text{exp,top}}$ is the average TIS observed in the experiments, while $\overline{\text{TIS}}_{\text{sim,top}}$ is the average TIS obtained from the simulations. To evaluate the model that better fitted the data, a $t-$test was then run to assess the differences between the values of e_{top} observed in the **IM** and **SM** models, which are reported in Table 3.6.

Table 3.6: **Experimental and Simulated Time-In-Synchronization** (TIS) **for each group, memory model and topology (in Path Matched-but-one, players did not stay in sync for at least 3 consecutive periods of length** $2\pi/\omega_{\text{group}}$**).**

	$\overline{\text{TIS}}_{\text{exp}}$	$\overline{\text{TIS}}_{\text{IM}}$	$\overline{\text{TIS}}_{\text{SM}}$
Exp.1			
Complete Matched	9.41 s	9.64 s	9.31 s
Complete Matched-but-one	9.02 s	9.27 s	8.31 s
Path Matched	12.50 s	8.60 s	8.31 s
Path Matched-but-one	No-sync	No-sync	No-sync
Ring Matched	4.90 s	9.14 s	8.88 s
Ring Matched-but-one	7.39 s	7.22 s	6.23 s
Star Matched	10.39 s	10.86 s	10.98 s
Star Matched-but-one	7.78 s	8.16 s	9.91 s
Exp.2			
Complete D1	8.98 s	8.60 s	6.98 s
Complete D2	13.79 s	10.58 s	9.28 s
Path D1	7.53 s	7.83 s	6.95 s
Path D2	6.56 s	7.99 s	9.82 s
Ring D1	6.23 s	6.43 s	5.92 s
Ring D2	6.38 s	5.75 s	6.76 s
Star D1	7.88 s	7.40 s	8.65 s
Star D2	9.56 s	10.58 s	11.68 s

3.5 Summary

In this Chapter, we analysed our ability to move in unison as function of our spatial configuration, similarity in behaviour, expertise and amount of visual exchange. In two experiments we demonstrated that Complete and Star graphs were the most solid topologies prone to facilitating synchronized behaviours, reinforced by inertial homogeneity between participants and their expertise in perceptuo-motor synchronization. Importantly, we also demonstrated that group synchronization can be maintained for a certain amount of time (about 7 seconds) after informational exchanges have been interrupted, again more so in the two dominant topologies, and in a stronger way for experts.

We investigated the origin of this "social memory" effect by modelling our behavioural results with three different versions of networks of Kuramoto oscillators. A memory effect had to be introduced in the model to account for the strong persistence of synchronization when the visual exchange was lost, for two of the three homogeneity conditions, as well as for the coordination experts. An advantage was found in this population for the Individual Memory version compared to the Social Memory version of the model. Taken all together,

these results help to better understand why behavioural cohesion is easier to maintain when perceptual exchanges are lost and how perceptuo-motor expertise can reinforce this cohesion.

Obviously, ordinary situations, such as team rowing, everyday working meetings, or musical ensemble performance, are far richer than the pendulum experiments performed here, both on the action side and on the perception side. How multiple and coexisting configurations, within and across our senses, modulate our collaborative behaviours, in those and other situations, remains largely unknown and constitute a promising research line for future studies. Contrasting the proposed modelling strategies in a variety of situations, where perceptual and topological parameters are manipulated, would help to better characterize their respective contribution and their possible complementary nature.

In the next Chapter, we present some extensions of the classical Kuramoto model to capture one notable observation from our experiments, the fact that when players coordinate their motion, their common oscillation frequency is typically lower than their individual tempos when playing solo.

4 Capturing human slowing down during group interaction: modified Kuramoto models

Cognitive responses during human group interaction can be explained both in terms of the so-called *theory of mind* and as the motor responses driven by the sensory feedbacks of the interaction [23, 24, 171]. However, while human interactions have been systematically investigated over the last decades across different fields, see for instance the studies on mirror neurons [172], child development [135, 173] and joint action [174, 175], the contributions of the cognitive and motor responses to human group coordination are only partially understood. In particular, behavioural science is trying to understand how to promote a desired group behaviour by only entraining a subset of the group members [93]. This phenomenon is observed, for example, in music ensembles [160], rhythmic applause [22], team rowing [176], and has potential implications in group rehabilitation [15].

Networks of heterogeneous Kuramoto oscillators have been successfully employed to explain how synchronization may emerge in human groups performing oscillatory tasks. For instance, in [25] Alderisio et al. found that a rather simple mathematical model of coupled Kuramoto oscillators was able to capture the coordination levels, observed experimentally, of the ensemble depending on group homogeneity, as well as on the pattern of visual couplings. However, this model predicts synchronization to the average frequency of the individual characteristic frequencies, which is in contrast with our experimental observation that, when synchronizing, the group tends to consistently reduce their average frequency. These experimental findings are in agreement with previous observations in the joint-action literature. For instance, inhibition of the motor output pathway has been extensively studied in the context of action stopping, where a planned movement needs to be abruptly stopped, jointly or alone [177, 178]. These works explain how the brain selects actions, regulates movement initiation and execution, showing that joint action requires a more selective and slower mechanism compared to individual movements. This phenomenon has been observed across diverse tasks and applications, including in tapping experiments, where researchers found that participants tapped faster alone than when they are involved in cooperative tasks [179], or in human-robot interactions [180].

The significantly large temporal difference between interacting partners is necessary to gain time to see what the other person does during joint interaction. By slowing down, resources could be freed-up and the own and the other's movement could be judged [174].

Within the context of the mirror game [33], in this Chapter we propose three alternative modifications of the traditional Kuramoto model to explain the observed reduction in the synchronization frequency of the group. In particular, the three alternative models are grounded on three main neuroscientific hypotheses.

In what follows, we first describe the testbed scenario of interest (Section 4.1), we illustrate the metrics used in data analysis (Section 4.2), and discuss the main experimental finding on group synchronization (Section 4.3). Then, in Section 4.4 we detail the three different physiological hypotheses that could reasonably explain what we observed, and explain how they can be taken into account to modify the standard Kuramoto model. The proposed models are numerically validated in Section 4.5, and concluding remarks are given in Section 4.6.

Part of the results presented in this Chapter were the outcome of a collaboration with Mr Albert David Martinez from UPC Barcelona who carried out his MSc project as an Erasmus student at the University of Naples Federico II in autumn 2018.

4.1 Experimental set-up

Here, we considered a multi-agent extension of the mirror game [33]. We ran our experiments via a novel computer-based architecture Chronos developed at the University of Naples, in collaboration with the University of Bristol [34], consisting of different hardware/software devices. A central server unit receives position data from the client-players and broadcasts movement information to a subset of the others, according to the desired implemented spatial configuration, through a Wi-Fi network, as depicted in Fig. 4.1(a). The positions of each agent are captured by a Leap Motion device [181]- a low-cost position sensor- and appear on the screens of each individual personal computer (see Fig. 4.1(b)). This platform allows remote motor coordination between players in the absence of social (visual and/or acoustic) interaction.

4.1.1 Task description

Three groups of participants, each recruited from an initial pool of volunteers, employees and students at the University of Naples, at the Euromov center, and at University of Montpellier, took part in the experiments. They had no expertise in typical sensori-motor synchronization activities. Volunteers were divided in three groups as follows:

- group 1 (**G1**)- 1 female, 4 males;
- group 2 (**G2**)- 3 females, 3 males;
- group 3 (**G3**)- 4 females, 2 males.

Experiments were divided in two sessions. The first part, called solo session, involved only one participant. Participants were asked to carry out 5 trials in **G1** and 10 in **G2** and **G3**, each lasting 30s, to produce sinusoidal-like waves at their own preferred rhythm with

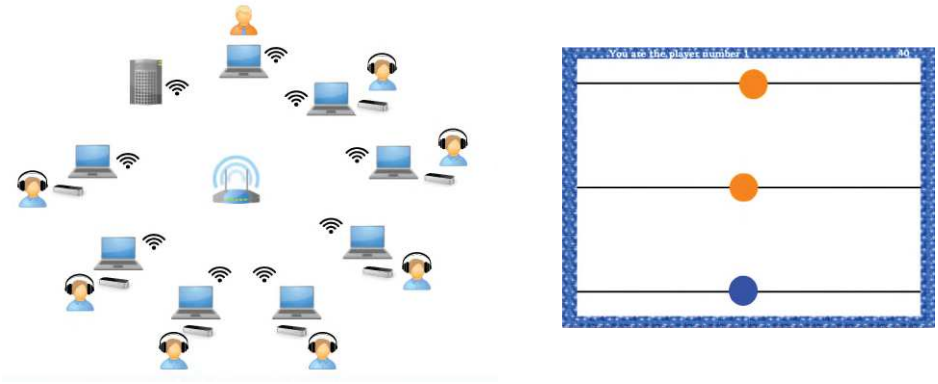

(a) (b)

Figure 4.1: **Details of Chronos architecture.** *N* clients (human players) send the server requests to carry out group experiments through their player modules, so that real-time interaction is initiated and data is appropriately saved (see panel (a)). The administrator assigns the interaction patterns and sets the trial duration in group experiments. All the devices are connected onto the same wireless local area network (WLAN) with the aid of a dedicated WiFi source. The client interface is shown in panel (b). Specifically, for each player: blue circle (her/his individual trace); orange circles (traces of the players s/he is connected to). Participants are provided with their own one-dimensional position trace and those of the others they are interconnected with, which are broadcast on their computer screen, respectively, while being visually and auditory uncoupled among them.

their favourite hand, in isolation. In so doing, the experimenter can record the movement of each single player alone in order to characterize her/his kinematic features. In Table 4.1 we report the average individual frequency for each of the three groups and computed their average value.

The second session of the experiments is devoted to investigate group synchronization. Participants were connected through the software platform Chronos and were asked to move their index finger on a leap motion controller so as to move a ball on the screen representing their own avatar, oscillating from left to right and vice versa, in a synchronized way with the others (see Figure 4.1(b)). Namely, each participant was given the following instruction: "*Synchronize the movement of your finger from left to right with the movement of the others, as naturally as possible, as if you could do it for 30 minutes*". A demonstration was performed to make sure the task was understood by each participant. Volunteers were separated by barriers and wore headphones playing white noise.

The Chronos platform allows to manipulate the structure of the information shared on the screen of each player so as to implement 4 different interaction topologies (Complete, Path, Ring and Star graphs, which were described in Chapter 3, Figure 3.1(d)). For the purpose of this analysis, we only considered the Complete topology since it represents the unbiased condition where all the players have access to the current position of each of the other players on their screen. Volunteers performed respectively 6 (**G1**) and 4 (**G2** and

Table 4.1: **Mean individual frequencies in each dataset.**

Group 1		**Group 2**		**Group 3**	
Player #	$\overline{\omega}_i$ Solo	Player #	$\overline{\omega}_i$ Solo	Player #	$\overline{\omega}_i$ Solo
1	3.40 ± 1.55 rad/s	1	5.01 ± 0.23 rad/s	1	3.83 ± 0.26 rad/s
2	3.04 ± 0.11 rad/s	2	1.73 ± 0.64 rad/s	2	3.95 ± 0.23 rad/s
3	6.36 ± 0.58 rad/s	3	3.68 ± 0.49 rad/s	3	3.76 ± 0.47 rad/s
4	3.34 ± 0.21 rad/s	4	4.22 ± 0.14 rad/s	4	4.28 ± 0.30 rad/s
5	9.91 ± 0.68 rad/s	5	2.84 ± 0.20 rad/s	5	4.26 ± 0.36 rad/s
		6	6.39 ± 0.54 rad/s	6	3.54 ± 0.35 rad/s
Average	5.21 ± 2.96 rad/s		3.98 ± 1.64 rad/s		3.94 ± 0.29 rad/s

G3) trials of 30 seconds each.

Each experiment was carried out according to the principles expressed in the Declaration of Helsinki, and was approved by the local ethical committee. All participants provided their written informed consent to participate in the study, and such consent was also approved by the local ethical committee.

4.2 Data analysis

Data collected in each experimental setup were preprocessed and then sychronization metrics were computed, following the same processing routine described in Chapter 3, Section 3.2. The position time-series of each player collected through Chronos is sampled at 10 Hz and then interpolated through a spline to obtain a 100 Hz sampling. Then, the position time-series were filtered through a Butterworth filter with a cutoff frequency equal to twice the typical human natural movement frequency (~ 3 Hz). For each dataset, the Hilbert transform [170] was employed to reconstruct the phase associated to each agent from its position time series. As in Section 3.2, we denote T as the number of samples in each trial and N as the number of players and we define $\theta_i(k)$ as the phase of the ith player at the kth sampling instant, for all $i = 1, \ldots, N$ and $k = 1, \ldots, T$.

The following set of metrics were computed to capture the relevant features of the human group interactions recorded in our experiments:

- the average individual frequencies $\bar{\omega}_i$ (see Eq. (3.1)) and group frequency $\bar{\omega}_{\text{group}}$ defined in Section 3.2;
- the average phase-synchronization index $\bar{r}$ (see Eq. (3.2)) and the average frequency-synchronization index $\bar{\rho}_g$. This latter metric is used to quantify and analyse the level of frequency coordination among multiple agents, and is a modification of the index proposed in the context of human group coordination [114].
  Specifically, let $\theta_i(k) \in [-\pi, \pi]$ be the phase of the ith agent, extracted from the position signal by making use of the Hilbert transform, and let $\psi(k)$ be the phase

associated to the order parameter at each sampling time k, defined as

$$r(k) = \left| \frac{1}{N} \sum_{i=1}^{N} e^{j\theta_i(k)} \right| \qquad \forall k \in \{1, \ldots, T\}, \tag{4.1}$$

$$\psi(k) = \tan^{-1} \frac{\mathrm{Im}\{r\}}{\mathrm{Re}\{r\}}, \tag{4.2}$$

which can be regarded as the average phase of the group at time k. Let $\phi(k) := \theta_i(k) - \psi(k)$ be the relative phase between the ith agent and the group at time k. Differently from the arithmetic mean proposed in [114], this quantity can be averaged considering a moving average over a time window w as follows:

$$\bar{\phi}_i'(k) := \frac{1}{w} \sum_{l=k-w}^{k} e^{j\phi_i(l)}, \qquad \forall k \in \{w+1, \ldots, T\}, \tag{4.3}$$

$$\bar{\phi}_i(k) := \tan^{-1} \frac{\mathrm{Im}\{\bar{\phi}_i'\}}{\mathrm{Re}\{\bar{\phi}_i'\}} \tag{4.4}$$

The level of frequency coordination of the entire ensemble at sampling time k can be quantified as follows:

$$\rho_g(k) := \frac{1}{N} \left| \sum_{i=1}^{N} e^{j\Delta\phi_i(k)} \right|, \qquad \forall k \in \{w+1, \ldots, T\} \tag{4.5}$$

where $\Delta\phi_i(k) := \phi_i(k) - \bar{\phi}_i(k)$.
The index $\rho_g(k)$ gives information on the variability of the phase mismatches among all the agents: the closer $\rho_g(k)$ is to 1, the more the frequencies of the players are synchronised at time k. Its value can be averaged over the whole time interval $[w+1, T]$ in order to have an estimate of the mean coordination level of the group during the total duration of the performance:

$$\bar{\rho}_g := \frac{1}{T-w+1} \sum_{k=w+1}^{T} \rho_g(k), \qquad \forall k \in \{w+1, \ldots, T\} \tag{4.6}$$

In this study, we selected $w = 3/T_g$, where T_g is the period of the average oscillation in the group, computed as $T_g = \frac{2\pi}{\bar{\omega}_{\text{group}}}$, with $\bar{\omega}_g$ being the average frequency in the group.

4.3 Collective slowing down

The analysis of data collected during group cooperation sessions revealed an interesting result that represents the central topic of this chapter. Comparing Tables 4.1 and 4.2, we observe that participants reduce the frequency of their oscillations when they try

to coordinate with their partners. Independent t-tests run between solo and group frequencies in each group showed significant differences ($t(11) = 17.07,\ p < 0.001$, **G1**; $t(12) = 5.07,\ p < 0.001$, **G2**; $t(12) = 8.28,\ p < 0.001$, **G3**). Also, we observed that this approach was successful since participants reached a synchronization level different from chance. This was ascertained by comparing the values of the recorded order parameter with the value of the index computed on phases randomly extracted from a uniform distribution in $[0, 2\pi]$. The levels of phase cohesiveness reached by each ensemble could not be obtained by chance- $r = 0.40 \pm 0.20$ for $\mathrm{N}_{\mathrm{agents}} = 5$, $r = 0.37 \pm 0.18$ for $\mathrm{N}_{\mathrm{agents}} = 6$.

Table 4.2: **Details of indices of interest.**

Group #	Group sync frequency ($\bar{\omega}_g$)	Order parameter (r)	Frequency sync index ($\bar{\rho}_g$)
1	2.97 ± 0.08 rad/s	0.90 ± 0.08	0.97 ± 0.01
2	3.23 ± 0.25 rad/s	0.78 ± 0.09	0.96 ± 0.03
3	2.88 ± 0.39 rad/s	0.78 ± 0.13	$0.98 \pm 5 \cdot 10^{-3}$

Building on the work of [25], we first modeled the dynamics of the group interaction in the mirror game as a network of nonlinearly coupled heterogeneous Kuramoto oscillators [38]:

$$\dot{\theta}_i = \omega_i + c \sum_{j=1}^{N} \sin(\theta_j(t) - \theta_i(t)), \tag{4.7}$$

where the values of the players' natural oscillation frequencies ω_i were estimated by considering the trials recorded in solo session. In the numerical exploration of the model, we assumed that each ω_i was randomly extracted from a Gaussian distribution whose mean $\mu = \overline{\omega}_i$ and standard deviation $\sigma^2 = SD_i^2$ are taken from the "solo" experiments (see Table 4.1) whereas the initial phases were picked from a uniform distribution in $[0, 2\pi]$. A sample simulation using data from **G1** is reported in Figure 4.2. We notice that, by construction, this model predicts synchronization to the average frequency of the individual characteristic frequencies [125], thus failing to reproduce the salient experimental observation of a reduction in the group oscillation frequency.

In what follows, we first identify three possible neuroscientific hypotheses that could explain the experimental observation, and then, for each hypothesis we propose a subsequent modification of the Kuramoto model, to finally validate them against the collected experimental data.

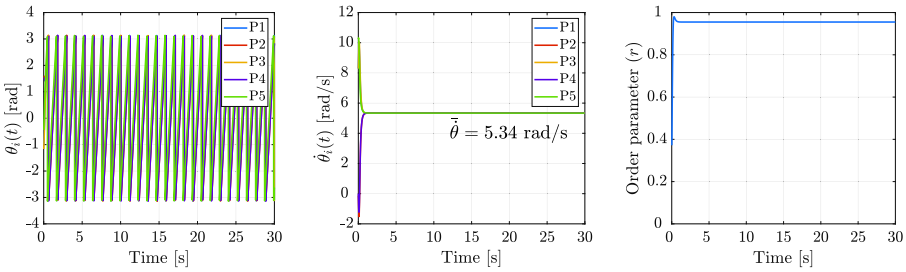

(a) (b) (c)

Figure 4.2: **Simulation results for a network of N = 5 heterogeneous Kuramoto oscillators (Eq. 4.7) tuned to behave like agents in Group1.** Phase trajectories $\theta_i(t)$ (a), angular velocities $\dot{\theta}_i(t)$ (b) and Kuramoto order parameter r (c) are shown for Group1. Different colours refer to different players. The parameters and the initial conditions are set as follows: $c = 1.6$, $\theta(0) = [-1,\ 1.60,\ -1.17,\ 1.53,\ 0.44]$ rad, $\omega = [8.29,\ -0.13,\ 8.29,\ -0.003,\ 10.24]$ rad/s, $\bar{r} = 0.95$ over the trial.

4.4 Neuroscientific hypotheses and proposed mathematical modeling

The complexity of the processes underlying joint interaction lies in the interaction of several different mechanisms that allow individuals to share representations, to observe and predict actions, and to integrate the predicted effects of own and others' actions such as joint attention, task sharing, action coordination [174]. In particular, each individual possesses certain tracking skills, which are enhanced through suitable behavioural strategies aimed at minimizing the tracking error. A lesser ability to execute these strategies could lead to poorer performance by older adults [182].

In the current study, we considered three possible neuroscientific explanations of the slowing down during group coordination observed in our experiments. Each of them is grounded in the literature on human group interaction which highlights that our motor system is characterized by plasticity and by the inherent presence of delays. In particular, the first and second possible explanations of our observation are both related to plasticity. The former hypothesis posits that the individual behaviour adapts as a function of the aggregate performance of the group, whereas the latter considers that each player weights differently the information sensed from each neighbor. Finally, the third mechanism considers that information is processed with a certain delay.

For each of the three plausible explanations, we present a corresponding extension of the traditional Kuramoto model. Each modification acted on one of the three salient components of a complex system (see Fig. 2.4) that is, the **individual dynamics**,the **interaction topology**, and **the communication protocol**, respectively.

In the following, we provide a description of our hypotheses and detail the possible modelling solutions to replicate experimental results.

4.4.1 Hypothesis 1: behavioural plasticity as individual adaptivity

Sensorimotor synchronization is observed in different forms of coordination in daily human life, especially in social contexts like coordinated dancing, rhythmic clapping, or simply when walking together. In such complex scenarios, behavioural plasticity is essential, since the partner's decisions and actions cannot be accurately predicted and the ongoing interactions constantly change. Therefore, precision and flexibility in the movements represent crucial features to achieve coordination. In addition, interpersonal entrainment has a wide variety of social consequences, in particular the de-individuation, and the formation of a common group identity amongst partners [183]. Group coordination leads an individual to think of themselves and the other in less individualised and more interdependent ways. The sense of belonging arising from moving together leads to pro-social behaviours and makes the agent more incline to adopting the ideology of the team and, therefore, to adapt. Anticipatory mechanisms that support temporal prediction of sequences that contain tempo changes are not sufficient to explain how people effectively coordinate their joint actions during everyday activities and adaptive error correction process should be considered [184]. Indeed, our motor system requires the capacity to deal with, for example muscular fatigue, external loads, or changes in the sensory systems guiding the movement [185, 186].

Adaptivity is a key-aspect in cooperation tasks since each individual moves differently from everyone else (faster/slower, harder/smoother, etc.). Indices of variability, such as the individual motor signature (IMS) [79], are able to capture the differences in the way each of us moves and to demonstrate evidence of the behavioural plasticity that coordination between two individuals performing a joint-action task requires. Specifically, by behavioural plasticity it is meant that in order to cooperate people are willing, to a different degree, to disregard their individual preferences and adjust their kinematic characteristics when interacting with others. As pointed out by Ganesh et al. [187], behavioural plasticity arises even when individuals are not consciously aware of being physically connected. The authors of the study investigated how a partner adapts the interaction forces and observed the motor adaptations during physical interactions to be mutually beneficial, such that both the most and the least skilled among the interacting partners improved motor performance. These benefits could not be explained only in terms of multi-sensory integration by an individual, but also required an adaptation process. This adaptation is often associated with a slowing down of the individual motion, so as to favor synchronization. Studies have shown that, to achieve the accuracy necessary for a successful interaction with the environment, specific strategies are employed, with specific components of movement execution being slowed down [173].

Modelling-wise, we propose to mimic the slowing down associated with this adaptive mechanism through a reduction of the individual natural frequency, until a desired degree of phase synchronization, quantified by the order parameter r (assumed to be different from zero), is achieved by the group. The standard Kuramoto model is then modified as follows:

$$\dot{\theta}_i = \omega_i(t) + c \sum_{j=1}^{N} \sin(\theta_j(t) - \theta_i(t)), \tag{4.8}$$

with

$$\dot{\omega}_i(t) = \begin{cases} -\frac{1}{r^2(t)}\omega_i(t), & \text{if } r(t) < r_d, \\ 0, & \text{otherwise,} \end{cases} \tag{4.9}$$

where r_d is some desired synchronization level the group wishes to achieve. Note that the more the group will be far from the desired level of coordination, the more the individual frequencies will decrease. In what follows, we refer to Eqs. (4.8)-(4.9) as **Model 1**.

4.4.2 Hypothesis 2: behavioural plasticity as a result of selective attention

An alternative hypothesis sees behavioural plasticity as the result of a differentiated way to pay attention to "what the others do" and to their personality or kinematic features, with these aspects influencing the way we accomodate to interact with the others. Here, we hypothesize that the heterogeneity in the motor repertoire of the group may foster the emergence of a specific player catching the attention of the others.

Selective attention-the ability to concentrate on one source of information while disregarding others [188]- is a key-element in effective cognitive and behavioural functioning for children and adults, and dysfunctions of this process are paired with diverse developmental psychopathology [189]. Indeed, the perceptual world presents too much information compared to our limited processing abilities, and an act of selection must take place at some point. Beyond this point, only some of the available information is handled, while disturbing irrelevant sensory information are actively suppressed [190]. Among the multiple behavioural consequences of attentional selection, researchers highlight higher accuracy levels, enhanced sensitivity, but also a better communication among neuronal groups in spatially distant areas, enhancing effective interactions and processing relevant information [191].

Selective attention becomes relevant during group interactions as it has been often highlighted in the literature. Capozzi et al. [192] observed that previous group interactions can shape leader/follower identities in subsequent social attention episodes. Individuals who do not guide group attention in exploring the environment are ineffective social attention directors in later interactive tasks. Thus, the role played in previous group social attention interactions modulates the relative weight assigned to others' gaze. Similarly, experiments with mixed-race groups helped the authors to show that aspects of the perceiver's social identity shape social attention [193].

Concerning the mathematical framework, we encode the selective attention through the following model:

$$\dot{\theta}_i = \omega_i + c \sum_{j=1}^{N} w_{ij} \sin(\theta_j(t) - \theta_i(t)), \tag{4.10}$$

where $w_{ij} \geq 0$ weights the attention that player i devotes to player j, and represents the ij-th element of a weighted (rather than binary) adjacency matrix W.

A question naturally arises about the selection of the elements of W. Here, we assume that they are related to motor variability, which is a central topic in human movement theory and has become an object of study in its own right during the last

century. Bernstein [194] used the expression "repetition without repetition" when he described consecutive attempts at solving a motor task. Each repetition of an act is unique, with nonrepetitive neural and motor patterns [195].

Traditionally, movement variability is considered an indicator for sensorimotor malfunctioning, associated to performance decrements and pathology. But functional movement variability is also a result of compensation mechanisms e.g. to account for prior movement deviations, to cope with perturbations, reduce injury risk, and facilitate changes in coordination patterns [196]. Empirical evidence demonstrate that variability can also play a functional role in the detection and exploration of postural stability in aging and movement disorders, with special emphasis on the Parkinson's disease [197]. For this reason, variability and noise are a natural part of the neuromuscular system, and can occur at multiple levels. Obviously, individual differences, for instance in terms of expertise, influence variability of the neuromuscular system. The analysis of functional variability during motor learning of a complex cyclic task showed that movement variability of the result parameter decreased significantly with increasing expertise [198]. Many other studies on the influence of expertise on the variability have been carried out in literature in different sport domain as triple jumpers, javelin, discus throwing, basketball shooting, locomotion, expert gymnasts [196, 199–201]. The analysis of the influence of expertise on the coordination variability was consistent with a U-shaped curve, resulting in the emergence of different types of action in seeking to achieve the same task goal, as opposed to the concept of "optimal" movement patterns, and fewer exploratory movements. In contrast, beginners display lower levels of functional intra-individual variability of motor organization.

Researchers suggested that slower speeds are associated with increased locomotor variability, and increased variability has traditionally been equated with loss of stability [202]. If the latter were true, this would suggest that slowing down, as a locomotor control strategy, should be completely antithetical to the goal of maintaining stability. Neuropathic patients instead exhibit slower walking speeds and better local dynamic stability of upper body movements supporting the hypothesis that reductions in walking speed are a compensatory strategy used to maintain dynamic stability of the upper body during level walking.

The importance of quantifying motor variability for understanding the biomechanics of human movement has been highlighted in several works [203–205]. Therein, standard deviation has been shown to be a good measure for the analysis of variability, far from being a source of error, optimal for healthy and functional movement. Here, we consider standard deviation of the oscillation frequency recorded in solo session as a proxy for the movement repertoire and for the individual tendency to adapt to the others. These elements help the partners to weight the interactions with the others, as in general happens during strategy selection characterizing human group interaction where synchronization emergence affects how people subsequently adjusted their performance [206–208].

Specifically, from a modelling point of view, we consider two alternative scenarios where the elements of the weighted matrix are defined as:

1. **Flexibility scenario** where
$$w_{ij} = \frac{\mathrm{SD}_i}{\mathrm{SD}_j} \tag{4.11}$$
the more player i is plastic than player j, the more player i corrects their mismatch (in a scenario where the agents are supposed to coordinate);
2. **Stubborness scenario**
$$w_{ij} = \frac{\mathrm{SD}_j}{\mathrm{SD}_i} \tag{4.12}$$
the more player i is plastic than player j, the less they adapt to them.

In what follows, we refer to Eqs. (4.10)-(4.11) as **Model 2a**, and to Eqs. (4.10)-(4.12) as **Model 2b**.

4.4.3 Hypothesis 3: delays in information processing

Multilevel crosstalk represents the neural basis for motor control [209]. Multisensory processing involves participation of individual sensory streams (e.g. vision, hearing) to facilitate perception of environmental stimuli [210]. Since any natural process is not instantaneous, a motor model should incorporate time delays, which are known to induce temporal coupling between functional elements to modulate perception and stabilize or destabilize a particular mode of coordination. The time delays associated with these pathways and their signal processing are deduced from a variety of data: interhemispheric transfer time has been estimated to be about 5 ms [211] based on behavioural [212,213] and physiological studies [214], including intracranial recordings in humans [215], whereas the maximum possible delay for the cortico-thalamocortical loop has been estimated to be about 20 ms [211]. Although in most circumstances transmission delays in the brain do not exceed 100 ms [216], for the visual system they can reach 150 ms [217].

Previous works have used delays when modelling replicating oscillatory behaviour [218–220]. For instance, Slowinsky et al. [218] showed how two Haken–Kelso–Bunz (HKB) oscillators coupled through a delayed communication protocol, were able to replicate both a drop in the oscillation amplitude and the loss of anti-phase stability.

With the different goal of capturing the reduced frequency observed in groups of individuals synchronizing their oscillations, we propose to embed delays in cross-talk motor system within a modified Kuramoto model of the form:

$$\dot{\theta}_i = \omega_i + c \sum_{j=1}^{N} \sin(\theta_j(t-\tau) - \theta_i(t)) \tag{4.13}$$

where the cross-talk delays are captured by the parameter τ, which corresponds to the time that an agent i requires to track the position of an agent $j \neq i$ and to process this information.

In what follows, we refer to Eq. (4.13) as **Model 3**.

4.5 Validating the proposed models

4.5.1 Tuning the parameters

All the proposed models depend upon the selection of one or more parameters. Let us denote with Π_m, $m \in \{1, 2a, 2b, 3\}$, the set of parameters of model m that needs to be tuned. Namely, we have $\Pi_1 = \{c, r_d\}$, $\Pi_{2a} = \Pi_{2b} = \{c\}$, and $\Pi_3 = \{c, \tau\}$. Further, we denote $\mathcal{A}_m$ the set of the admissible values for the set of parameters of model m. Specifically,

- the coupling gain c is varied between 0 and 2 with step equal to 0.1,
- the threshold r_d is varied between 0.40 and 0.95 with step equal to 0.05,
- the information delay τ is varied between 0.01 and 0.35 with step equal to 0.01.

The parameter ranges were chosen as follows. The selected coupling gain interval encompasses the values of the optimal couplings obtained when considering the original Kuramoto model, see Table 4.3. As for the threshold r_d, we used 0.40 as the minimum value based on the values of the order parameter obtained by chance (see Section 4.3), whereas the maximum value was set to 0.95, which corresponds to all phases within an angle of $\frac{\pi}{3}$ rad. The choice of the information delay interval was based on the different transmission delays in the sensorimotor system found in literature (see Section 4.4.3).

For each proposed model, combination of the parameters, and experimental group $g \in \{\mathbf{G1}, \mathbf{G2}, \mathbf{G3}\}$, we performed ten simulations. In particular, in each simulation the initial phases are randomly picked from a uniform distribution in $[0, 2\pi]$, and the natural frequency ω_i of player i is picked from a Gaussian distributions with mean and standard deviation corresponding to their sample estimates computed in the solo conditions. For each simulated scenario, we computed $\overline{\omega}_{\mathrm{g,sim}}$, $\overline{r}_{\mathrm{g,sim}}$ and $\overline{\rho}_{\mathrm{g,sim}}$ representing the average values of the metrics described in Section 4.2.

In order to calibrate the parameters of each model for each experimental group, we considered the following cost function:

$$J_{\mathrm{gm}}(\Pi_m) = \left(\frac{\overline{\omega}_{\mathrm{g,exp}} - \overline{\omega}_{\mathrm{g,sim}}(\Pi_m)}{\overline{\omega}_{\mathrm{g,exp}}}\right)^2 + \lambda\left(\frac{\overline{r}_{\mathrm{g,exp}} - \overline{r}_{\mathrm{g,sim}}(\Pi_m)}{\overline{r}_{\mathrm{g,exp}}}\right)^2 + (1-\lambda)\left(\frac{\overline{\rho}_{\mathrm{g,exp}} - \overline{\rho}_{\mathrm{g,sim}}(\Pi_{\mathrm{m}})}{\overline{\rho}_{\mathrm{g,exp}}}\right)^2 \tag{4.14}$$

for all g $\in \{\mathbf{G1}, \mathbf{G2}, \mathbf{G3}\}$, m $\in \{1, 2a, 2b, 3\}$. This cost function is composed by three terms. The first term is used to evaluate the ability the model has of capturing the average group frequency, whereas the other two terms are a measure of the agreement in the phase and frequency synchronization between simulations and experiments. The parameter λ is set to 0.30 to bias the parameter choice towards a better agreement on the average ρ_g.

Then, for each group and model, we picked the parameter combination that returned the lowest value of Π_m, that is,

$$\Pi^*_{\mathrm{m,g}} = \underset{\Pi_{\mathrm{m}} \in \mathcal{A}_m}{\arg\min}\, J_{\mathrm{g}}(\Pi_m), \quad \forall m \in \{1, 2a, 2b, 3\}, \quad \forall g \in \{\mathbf{G1}, \mathbf{G2}, \mathbf{G3}\}, \tag{4.15}$$

Figure 4.3 shows for each model how the value of the cost function J_{gm} defined in (4.14) changes as the model parameters are varied over the range of interest. We notice

that, when model 3 is selected, the level curves of $J_{gm}(c, \tau)$ are hyperbolic, implying that similar performance is obtained by setting a small delay and a large coupling gain or viceversa, see panels (1e-3e).

Not surprisingly the weighted models (panels (1c-3c) and (1d-3d)) behave similarly to the original model (panels (1a-3a)).

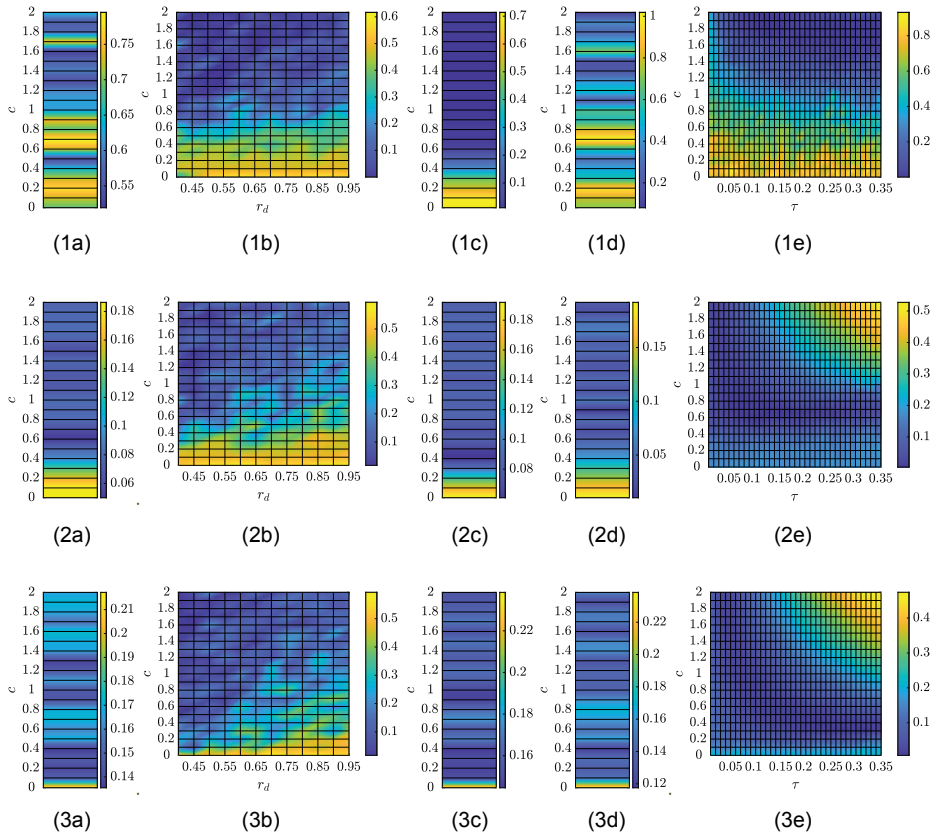

Figure 4.3: **Cost function J_{gm} as a function of the parameter selection.** Each panel corresponds to a specific dataset and model. In particular, the panel number identifies the dataset (e.g., 1 corresponds to dataset **G1**), whereas the letter identifies the proposed mathematical models. Specifically, letter (a) corresponds to the Standard Kuramoto, (b) to Model 1, (c) to Model 2a, (d) to Model 2b, and (e) to Model 3, respectively.

In Table 4.3, we report the parameter values corresponding to the optimal values of the parameters for each model in each group dataset.

Table 4.3: **Parameters corresponding to the optimal values.**

	Standard Kuramoto	**Model 1**		**Model 2a**	**Model 2b**	**Model 3**	
	c^*	c^*	thr*	c^*	c^*	c^*	τ^*
Group1	1.6	1.3	0.55	1.1	2	1.9	0.17
Group2	0.6	0.9	0.45	0.4	0.7	0.6	0.11
Group3	0.4	1.7	0.40	0.1	0.4	0.4	0.31

4.5.2 Comparing the proposed models

Denoting $\mathrm{N}_{\mathrm{trials}(g)}$ the number of trials of the experimental group g, we compare how the tuned models capture our experimental data by computing the following cost function in each trial l:

$$J_{\mathrm{gm},l} = \left(\frac{\omega_{\mathrm{g,exp},l} - \omega_{\mathrm{gm},l}(\Pi^*_{gm})}{\omega_{\mathrm{g,exp},l}}\right)^2 + (1-\lambda)\left(\frac{\rho_{\mathrm{g,exp},l} - \rho_{\mathrm{m},l}(\Pi^*_{gm})}{\rho_{\mathrm{g,exp},l}}\right)^2 + \lambda\left(\frac{r_{\mathrm{g,exp},l} - r_{\mathrm{m},l}(\Pi^*_{gm})}{r_{\mathrm{g,exp},l}}\right)^2, \tag{4.16}$$

for all g $\in \{\mathbf{G1}, \mathbf{G2}, \mathbf{G3}\}$, $m \in \{1, 2a, 2b, 3\}$, $l \in \{1, \ldots, \mathrm{N}_{\mathrm{trials}}(g)\}$ where Π^*_{gm} are the optimal parameters reported in Table 4.3, $\omega_{\mathrm{g,exp},l}$, $\rho_{\mathrm{g,exp},l}$ and $r_{\mathrm{g,exp},l}$ represent, respectively, the group frequency, the frequency synchronization index and the order parameter recorded in each experimental trial, whereas $\omega_{\mathrm{g,m},l}$, $\rho_{\mathrm{m},l}$ and $r_{\mathrm{m},l}$ are the corresponding simulated values. We removed the outliers and ran an ANOVA test on $J_{\mathrm{gm},l}$ to capture significant improvement provided by the proposed models. We considered 20 permutations of the pairing between simulated and experimental trials.

Figure 4.4 shows the models' performances. The results confirm that the Standard Kuramoto model (**Model 1**) does not fully match the experimental data and that a modelling extension is needed. In particular, the figure reveals that the adaptive model (**Model 2**) always returns the worst values in terms of $J_{\mathrm{gm},l}$ whereas **Model 3** always returns low values that are significantly different from the same cost function computed for the other models (see also Table 4.4). In addition, in Figure 4.5 we compare the dynamics in a sample trial of both the Standard Kuramoto model and the **Model 3** in the first experimental group. The asymptotic frequency value reached by the group with the Standard Kuramoto is far from the experimental value (see Table 4.2) met by the delayed model.

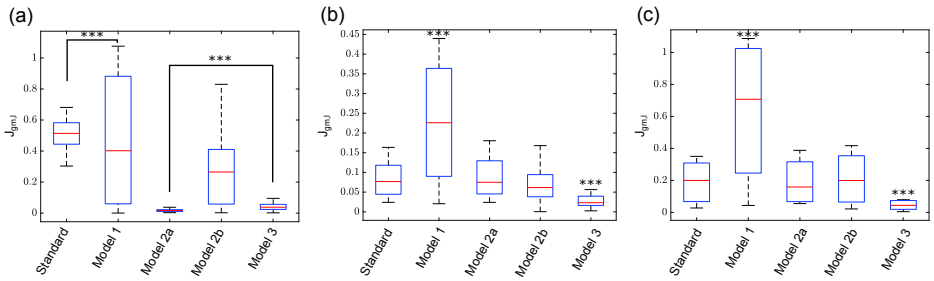

Figure 4.4: **Boxplots of $J_{\mathrm{gm},l}$ for G1(panel a), G2(panel b) and G3(panel c).** A triple star corresponds to $p < 0.001$

Table 4.4: **Details of models' performances in terms of $J_{\mathrm{gm},l}$ as plotted in Figure 4.4.**

	Anova results	Standard Kuramoto	Model 1	Model 2a	Model 2b	Model 3
Group1	$F(4,556) = 114.87, p < 0.001$	0.52 ± 0.11	0.47 ± 0.38	0.02 ± 0.01	0.34 ± 0.35	0.04 ± 0.02
Group2	$F(4,387) = 78.22, p < 0.001$	0.08 ± 0.04	0.22 ± 0.15	0.08 ± 0.05	0.06 ± 0.04	0.03 ± 0.02
Group3	$F(4,395) = 90.28, p < 0.001$	0.19 ± 0.13	0.64 ± 0.41	0.19 ± 0.13	0.21 ± 0.15	0.05 ± 0.03

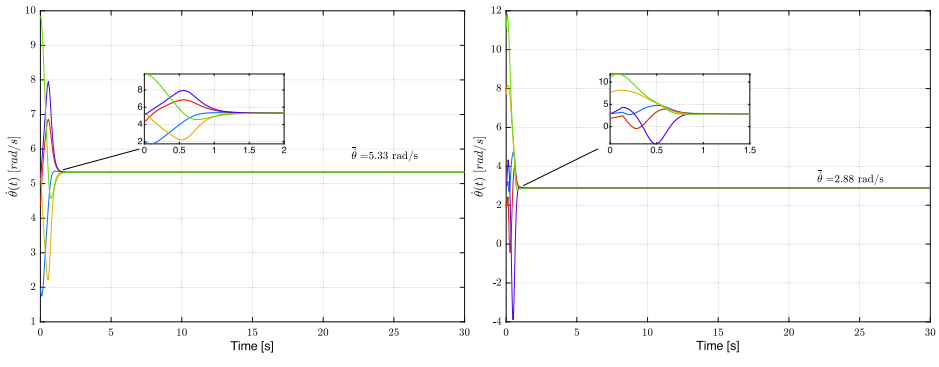

Figure 4.5: **Comparison between the Standard Kuramoto and Model 3 in a sample trial from G1.** Panel (b) shows how players in **Group1** can achieve frequency synchronization to the experimental recorded value with the delayed model (average group frequency $\bar{\dot{\theta}} = 2.88\mathrm{rad/s}$), better than the results of the Standard Kuramoto model (panel a, average group frequency $\bar{\dot{\theta}} = 5.33\mathrm{rad/s}$).

4.6 Summary

In this Chapter, we investigated the possible reasons why human agents slow down while executing a cooperative motor task and proposed three different models based on different neuroscientific hypotheses underlying sensorimotor group synchronization. We found that a model accounting for delays in information processing is the one that best captures the reduced frequency of oscillation observed in our experiments when compared to solo trials. The sensorimotor control system requires coordinating different forms of sensory and motor data and these data are generally in various *formats*. Transformations between these coordinate systems allow the motor and sensory data to be related, closing the sensorimotor loop [221]. Therefore, to generate skilled actions, the sensorimotor control system must find solutions to several problems, including coping with the nonlinear nature of our motor system, together with delays, redundancy, and noise [222]. Motor control can be divided into feedforward and feedback control strategies. Feedforward control includes all techniques for controlling a motor apparatus without reference to one or more controlled variables describing the current state of the motor system. In contrast, feedback control uses some knowledge of the controlled variables to determine the outgoing motor commands. Such control is robust but its principal disadvantage is that it is sensitive to intrinsic delays in the sensorimotor loop and this reduces the speed of its response [223]. In particular, neural delay has been shown to play a significant role in the muscle control system [224, 225]. This delay can be defined as the total time interval between the presentation of a stimulus and the evocation of a response. It can be influenced by the length of the neural path between the receptor organ and the responding muscles, the time that the central nervous system requires to process the information, and the time it takes for a muscle to react. For this reason, four sequential components play a key role in the neural delay: sensation, perception, conduction, and execution. These delays combine to give an unavoidable feedback delay within the negative feedback control loop, which ranges between about 30 ms for a spinal reflex up to 200–300 ms for a visually guided response [226] [171].

Tuning our simple yet effective model 3, which explictly accounts for these intrinsic delays, we found delay values that are in line with the typical range evidenced in the literature, and specifically between 110ms and 310ms.

In the following Chapter, we examine how leadership emergence occurs in a set of experimental group coordination tasks, showing the occurrence of some "leadership patterns" that seem to explain the observed behaviour.

5 Patterns of leadership emergence organize coordinated motion in human groups

The main objective of this chapter, whose results were presented in [227], is to shed light on leadership emergence during movement synchronisation in groups of interacting agents. Leadership is a complex yet fascinating phenomenon that plays an essential role in several human activities, as for example economics, politics, music and sport. In this chapter, we investigate if and how leadership emerges within the context of human groups motor coordination, which is observed for instance when people walk together or move at unison. More specifically, we consider groups of humans performing a joint motor task, that is, the multi-agent extension of the *mirror game*, described earlier in Chapter 2, as implemented in Figs. 5.1 and 5.3. From a mathematical point of view, the problem of leadership emergence has been studied with the aid of dynamical systems theory in the case of animal groups [39, 63–66], whereas less attention has been focused on the case of human ensembles.

Different metrics have been used to investigate leader-follower relationships; most notably, the phase of each agent has been used to identify who is lagging behind whom in the analysis of oscillatory tasks [20, 27], whereas information theoretic quantities such as transfer entropy have been employed to reconstruct the mutual influence among the interacting agents [56, 228]. Here, we combine both these metrics to investigate which leadership patterns emerge and how they affect the level of coordination in the group.

In addition, to assess whether the social dimension affects the emergence of leadership in the group, we repeat our experiments via our computer-based architecture Chronos described in Section 4.1, removing any type of direct visual or auditory communication between the group members so that subjects do not know the identity of the others they are interacting with. In so doing, we also explore the emergence of leadership within groups performing a different coordination task providing further evidence of our findings.

The contents of this Chapter is organized as follows. In Section 5.1 we describe the task we assigned in our experiments and we illustrate the two experimental setups. Then, in Section 5.2 we decribe the data analysis pipeline to achieve our results that are fully presented in Section 5.3. Finally, a summary of the main findings and related implications

are presented in Section 5.4.

5.1 Experimental setup

Six groups of voluntary participants were involved in two different types of experiments as described in what follows.

5.1.1 Experiment 1: social cooperation

For this scenario, we considered the data described in Section 3.1- Experiment 2 of Chapter 3 and will be analysed here in terms of leadership emergence. In particular, since in this analysis we are not interested in the influence of the motor expertise, there is no need to distinguish between dancers and non dancers. Therefore, the groups of participants will be here addressed with more general labels as **G1** (**D1**), **G2** (**D2**), **G3** (**ND1**), **G4** (**ND2**).

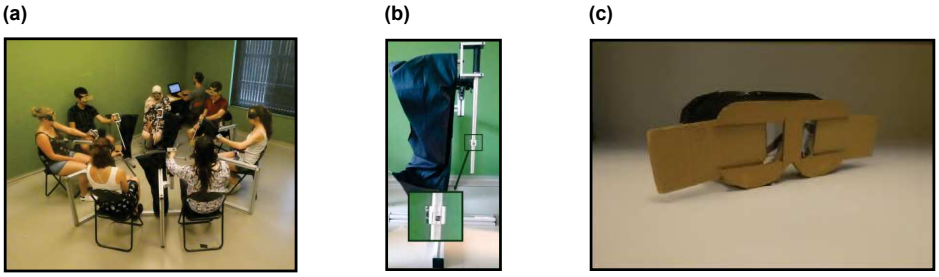

Figure 5.1: **Experimental setup (1).** Panel (a) describes the first setup (*Experiment 1: social cooperation*), where each player was asked to move a pendulum with their own preferred hand and try to synchronize its movement with the others. Panel (b) shows the pendulum used to run experiments. Although masses could be added on the rod to modulate the inertia of the pendulum, we did not use this feature of the setup as we did not add any additional mass. Each participant was asked to wear handmade goggles (see panel (c)) to manipulate the field of vision and implement the different topologies of interest.

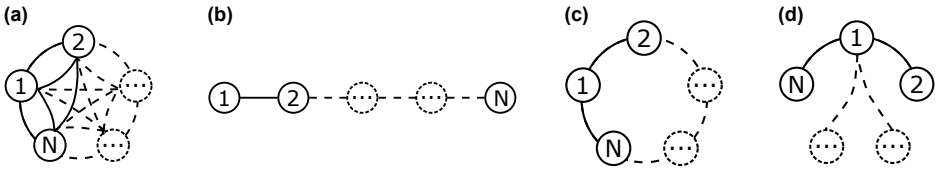

Figure 5.2: **Spatial distribution.** In panels (a-d) we plotted the four configurations (*topologies*) implemented in the experiments: *complete graph* (a), *path graph* (b), *ring graph* (c), and *star graph* (d), with N being the number of players involved in the experiments. In the *complete graph*, each participant can see all the others; in the *path graph*, every player can see the trajectories of two neighbours with the exception of the two external participants (the head and tail of the chain) that are constrained to visualize the motion of only one neighbour; in the *ring graph*, each player can see the motion of only two neighbours; in the *star graph*, all the players observe the motion of one central player who, conversely, sees the motion of all the others.

5.1.2 Experiment 2: group performance in the absence of social interaction

Two groups of six participants, each recruited from an initial pool of fourty volunteers, employees and students at the Euromov center and at University of Montpellier, took part in the experiment (all right-handed). They had no expertise in typical sensori-motor synchronization activities (music or dance). Volunteers were divided in two groups as follows:

- group 1 (**CG1**)- mean age = 22.5 ± 4.04, 3 females, 3 males;
- group 2 (**CG2**)- mean age = 26 ± 12.07, 4 females, 2 males.

Participants were connected through the software platform Chronos developed at the University of Naples Federico II, in collaboration with the University of Bristol [34], as part of the European project AlterEgo (`www.euromov.eu/alterego/`). Specifically, volunteers were asked to move their index finger on a leap motion controller so as to move a ball on the screen representing their own avatar (Figure 5.3), oscillating from left to right and vice versa, in a synchronized way with the others. Namely, they were instructed to "*Synchronize the movement of your finger from left to right with the movement of the others, as naturally as possible, as if you could do it for 30 minutes*". A demonstration was performed to make sure the task was understood by each participant. The Chronos software allowed to manipulate the structure of the information shared on the screen of each player so as to implement the 4 different interaction topologies depicted in Figure 5.2. Moreover, participants were separated by barriers and wore headphones playing white noise (see Figure 5.3(b),(c)). In each configuration, volunteers performed 4 trials of 30 seconds each.

Both studies were carried out according to the principles expressed in the Declaration of Helsinki, and were approved by the local ethical committee.

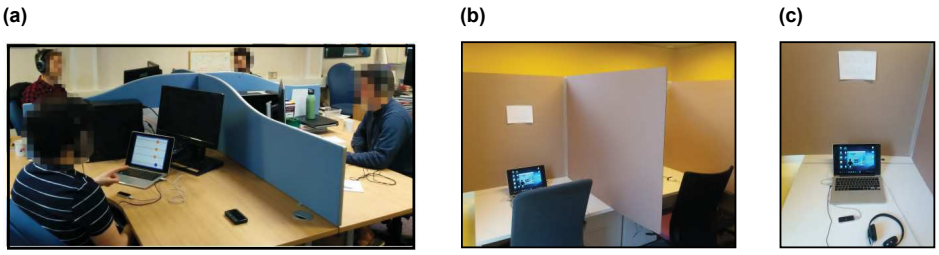

Figure 5.3: **Experimental setup (2).** Panel (a) shows the second setup (*Experiment 2: group performance in absence of social interaction*), where participants had to oscillate and synchronize the index finger of their preferred hand over a Leap Motion controller (Leap Motion, Inc. [181]) while being virtually connected with the others through the platform Chronos [34]. The main difference with the previous setup is the absence of visual and acoustic coupling among the players. Cardboards were used to visually isolate participants and headphones playing white noise were during each trial to ensure acoustic isolation between participants, see panel (b). Each participant was sitting in front of a laptop pc equipped with headphones and a leap motion controller (as shown in panel(c)).

5.2 Data analysis

5.2.1 Data preprocessing

Before performing data analysis, we preprocessed data.

Experiment 1. Potentiometers were used to compute the projection of the hand motions on the floor through a voltage-divider formula. The position time-series were smoothed out through a moving average filter with time window equal to 10 samples, that is, with a time-step $\Delta t = 0.05$s.

Experiment 2. The Chronos architecture is a computer-based platform consisting of different hardware/software devices. The positions of each agent are captured by a Leap Motion device- a low-cost position sensor- and appear on the screens of each individual personal computer. The position time-series of each player is sampled at 10 Hz.

In this study, data were interpolated through a spline to obtain a 100 Hz sampling. Then, the position time-series were filtered through a Butterworth filter with a cutoff frequency equal to twice the typical human natural movement frequency ($\sim$ 3 Hz).

For both datasets, the Hilbert transform method [170] was employed to reconstruct the phase associated to each agent from its position time series.

5.2.2 Leadership metrics

To uncover leadership emergence we propose the combined use of two indices. The first, which we term as "phase leadership" index, identifies who is leading whom in phase in the group. The other, termed as "influence leadership" index is based on the computation of the net causation entropy between players. Such an information theoretic concept is used to infer causality by extracting the directional information flows from the position (or phase) time-series acquired from the group players during the experiments [228].

We describe below how each of the indices we adopt in our investigation is defined.

Mean phase leadership index. For every individual, say i, we reconstructed from data the time-series of the phase of their motion. We then determined the phase leadership index, say $H_i(t)$, of that individual in the group at every time instant. Namely, the value of $H_i(t)$ ranges from 1 to 7, with 1 (7) corresponding to player i being followed (led) in phase by all the other player. We then computed the average phase index of individual i over the entire trial ($\overline{H_i}$) to quantify their tendency to lead in phase.

Knowledge of the phase of all the players at each time instant t_k allows to compute the phase difference among every pair of agents, that is,

$$\phi_{ij}(t_k) = \theta_i(t_k) - \theta_j(t_k) \quad \forall i, j = 1, \ldots, N_{\text{players}}, \quad \forall k = 1, \ldots, N_{\text{instants}}, \tag{5.1}$$

where N_{instants} is the number of time steps of duration Δt, that is the sampling period, of the trial of duration $T = N_{\text{instants}}\Delta t$. We say that player j is *ahead* of i at time t_k when $\phi_{ij}(t_k) < 0$. Then, we denote $\mathcal{L}_i(t_k)$ the set of players that are ahead of player i at time t_k, that is,

$$\mathcal{L}_i(t_k) = \{j | \phi_{ij}(t_k) \leq 0\} \quad \forall i = 1, \ldots, N_{\text{players}}, \quad \forall k = 1, \ldots, N_{\text{instants}}. \tag{5.2}$$

The phase leadership index of player i at time instant t_k, $H_i(t_k)$, is given by the cardinality of the set $\mathcal{L}_i(t_k)$, i.e.

$$H_i(t_k) = |\mathcal{L}_i(t_k)| + 1 \quad \forall i = 1, \ldots, N_{\text{players}}, \quad \forall k = 1, \ldots, N_{\text{instants}}. \tag{5.3}$$

In every trial of each experiment, we compute the mean phase leadership index $\overline{H_i}$ of player i as the time average of $H_i(t_k)$:

$$\overline{H_i} = \frac{1}{N_{\text{instants}}} \sum_{k=1}^{N_{\text{instants}}} H_i(t_k), \quad \forall i = 1, \ldots, N_{\text{players}} \tag{5.4}$$

Net causation entropy. To complement the analysis and uncover who is influencing whom in terms of the information flow between group members, we evaluated the causation entropy [229] between every pair of agents in the group from the time series of the phases of their motion. Then, we computed the net predicted information flow, NetCaus_i, from agent i to the rest of the group. This index defines the ability of each agent of influencing the motion of the whole group.

Given a discrete random variable V, the Shannon information content associated to V can be computed as

$$H(V) = -\sum_{v} p(v) \log p(v). \tag{5.5}$$

where $p(v)$ is the probability mass function of V. $H(V)$ is called the *Shannon entropy* (from now on, simply *entropy*) associated with V [230].
Given two (discrete) stochastic processes $X(t_k)$ and $Y(t_k)$, it is possible to define the *transfer entropy* [231] as:

$$T_{X\to Y} = H(Y(k+\tau)|Y(k)) - H(Y(k+\tau)|X(k), Y(k)). \tag{5.6}$$

$T_{X\to Y} \geq 0$ represents the information that flows from X to Y over the time interval $[k, k+\tau]$. In other words, transfer entropy measures the uncertainty reduction in inferring the future state of the process Y when, in addition to its current state $Y(k)$, also the current state $X(k)$ of the process X is known.

Transfer entropy successfully detects the directionality of the information flow and, therefore, it may be used to detect causality between two processes. However, when other processes affect both Y and X, the causal relationship between X and Y might be poorly related with the transfer entropy [228]. In other words, the transfer entropy is a bi-factor measure, so it is unable to distinguish direct versus indirect influences when three or more stochastic processes may be involved. For this reason, in multi-agent systems with more than 2 interacting entities, *causation entropy* is used to neutralize the effect on transfer entropy of the other entities, whose state is encoded in a third (vector) process $Z(k)$:

$$C_{X\to Y|(Y,Z)} = H(Y(k+\tau)|Y(k), Z(k)) - H(Y(k+\tau)|X(k), Y(k), Z(k)). \tag{5.7}$$

In the context of the mirror game, we use causation entropy to compute the net information flow among the players. Specifically, given two players i and j, we compute $w_{ij} = C_{i\to j|(j,\mathcal{P}\setminus j)}$, where $\mathcal{P}$ is the set of players participating to the game. Then, for all players $i = 1, \ldots, N_{\text{players}}$, we compute the outgoing and the incoming information flow as $\delta_{\text{i,out}} = \sum_{j=1, j\neq i}^{N_{\text{players}}} w_{ij}$ and $\delta_{\text{i,in}} = \sum_{j=1, j\neq i}^{N_{\text{players}}} w_{ji}$, respectively. Finally, we defined the *Net Causation Entropy* (NetCaus) score for each player as

$$\text{NetCaus}_i = \delta_{\text{i,out}} - \delta_{\text{i,in}} \quad \forall i = 1, \ldots, N_{\text{players}}. \tag{5.8}$$

NetCaus_i quantifies the net information flow between player i and all the other players and therefore is taken as the *influence leadership index* in this study. Thus, the "influence leader" is defined as the participant with the highest value of NetCaus.

To reconstruct the influence indices across the players, we followed the oCSE algorithm [57]. We select as input of the oCSE algorithm the time-series of the positions of each player. As described in Eq. (5.7), a parameter that needs to be selected is the time-lag τ. We set τ to 0.25 seconds, which corresponds to 50 samples in Experiment 1 and to 25 samples in Experiment 2. The selected value of τ corresponds to the average human response time in processing information [232–234]. The oCSE algorithm then uses the Kraskov-Strogbauer-Grassberger estimator [235] to estimate causation entropy from

time-series. Specifically, it is a non parametric estimator based on κ-nearest neighbors. In this study, following [236], we selected κ as the square root of the sample size of the joint variables, which corresponds to setting $\kappa = 75$ in Experiment 1 and $\kappa = 55$ in Experiment 2. The computed causation entropy are then used to calculate the weights w_{ij}. To determine whether or not these positive weights are significantly different from zero, shuffle tests with significance level $\alpha = 0.01$ in both the forward (discovery) and backward (removal) phases of the oCSE algorithm are used. We ran 100 trials in Experiment 1 and 500 trials in Experiment 2 per each hypothesis tests. The different number of trials is explained by the different length of the time series in the two experiments.

5.2.3 Level of coordination

As the joint task used as a paradigmatic case of study in the paper is oscillatory, we quantified the level of coordination among the agents by means of the instantaneous *cluster phase* or *Kuramoto order parameter, z*, introduced for the first time by Kuramoto [38]. This index is defined, for each trial j, as follows:

$$z_j(t_k) = \left| \frac{1}{N_{\text{players}}} \sum_{i=1}^{N_{\text{players}}} e^{j\theta_i(t_k)} \right| \quad j = 1, \ldots, N_{\text{trials}} \quad k = 1, \ldots, N_{\text{instants}}. \tag{5.9}$$

It is equal to 0 for pairwise agents in phase opposition and it becomes 1 when the players are perfectly overlapped in phase, reaching the highest level of coordination. We considered the mean value in each trial:

$$\bar{z}_j = \frac{1}{N_{\text{instants}}} \sum_{k=1}^{N_{\text{instants}}} z_j(t_k) \quad j = 1, \ldots, N_{\text{trials}}. \tag{5.10}$$

5.3 Results

5.3.1 Leadership emerges in three different patterns when people move together

Analyzing the results of experiment 1, we found that coordination was achieved through three main leadership patterns. In **Pattern 1**, the individual who is the most influential, as assessed by computing the causation entropy between each pair of group members, is also the one leading the rest of group motion in phase (see Fig. 5.4(a),(b)). This type of leadership pattern is reminiscent of one often found in the animal kingdom, where young pet animals follow the motion of their parents when flocking together, see Fig. 5.4(c). In **Pattern 2**, the most influential player is the one lagging behind all the others in phase, see Fig. 5.4(d)-(f). This leadership pattern often emerges in team sports, as for example in cycling where domestiques work for the benefit of the team leader, who, although moving behind all the others, determine the pace of the group. Finally, shared leadership constitutes a third possible pattern (**Pattern 3**), where the highest influence leadership index is shared by the two players with the highest and lowest phase leadership index

respectively. This leadership pattern is often observed in nature. For example, in animal migrations, the movement of the entire group towards the next destination is influenced by the animal in front who knows the route (*phase leader*) as well as by the pace of the slowest member, who will be in the back of the group, see Figure 5.4(i).

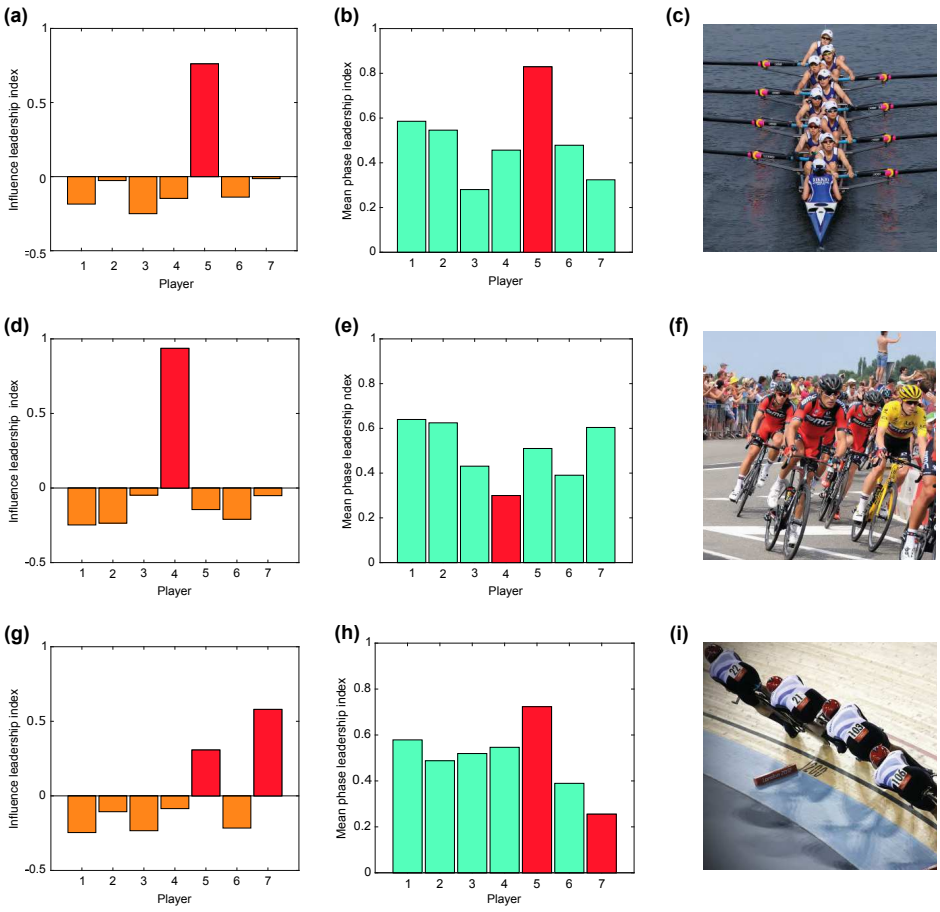

Figure 5.4: **Description of the leadership scenarios.** In the first column, each bar represents the value of the influence leadership index. The central column shows the mean phase leadership index for each player. The red bars identify the relationship between these two metrics typical of each pattern (Pattern 1- top row, Pattern 2- middle row, Pattern 3- bottom row). The third column displays an example for each leadership scenario from sports world. In particular, Panel (c) reports an example of the first scenario, where the role of a coxswain is to steer the boat and coordinate the rhythm of the team members. Panel (f) depicts professional road cyclists racing at the *Tour de France*. It is a paradigmatic example of leadership assigned to the participant lagging behind all the others, since the team leader typically drafts the wheels of her/his teammates (domestiques) but is pivotal for determining the team strategy. Panel (i) shows an example of shared leadership observed during team pursuit in track cycling, where the fastest player in front sets the pace, but also accounts for the position of the third lagging player, since the final time for the team is taken when the third team member crosses the finish line.

More specifically, the experimental trials could be classified into 4 different groups, one where no patterns emerged and the other three associated to each of the leadership scenarios described above. In the first collection, the participant who obtained the highest NetCaus was also the person with the highest mean phase leadership index. In the second group the person with the highest NetCaus was instead the one with the lowest value of the phase leadership index, while in the third two players, the ones with the highest and lowest phase pleadership index values were those with the two highest values of NetCaus. A geometric interpretation of these three patterns can be obtained by plotting the net predicted information flow against the mean ranking in phase.

The results of our analysis are summarized in Fig. 5.5. To analyse each scenario, we removed outlier data from the data points. A first order (linear) polynomial regression analysis shows that, in the trials where the phase leader emerges as the most influential (**Pattern 1**), ranking in phase and influence are positively correlated ($r(19) = 0.33$, $R^2 = 0.11$, $p < 0.001$). Instead, when leadership is assumed by the player most lagging in phase (**Pattern 2**), the opposite is observed ($r(12) = -0.48$, $R^2 = 0.23$, $p < 0.001$). Interestingly, a linear fitting ($R^2 = 0.02$, $p = 0.17$) cannot capture **Pattern 3**, where two players share leadership, and a parabolic interpolation is required to depict the coexistence of the lagging and phase leaders ($R^2 = 0.24$, $p < 0.001$). Visual inspection of the QQ-plots and Lilliefors tests on residuals show that the null hypothesis of normality of data cannot be rejected ($D(127) = 0.08$, $p = 0.06$ for Pattern1, $D(80) = 0.07$, $p = 0.50$ for Pattern2, and $D(123) = 0.06$, $p = 0.32$ for Pattern3).

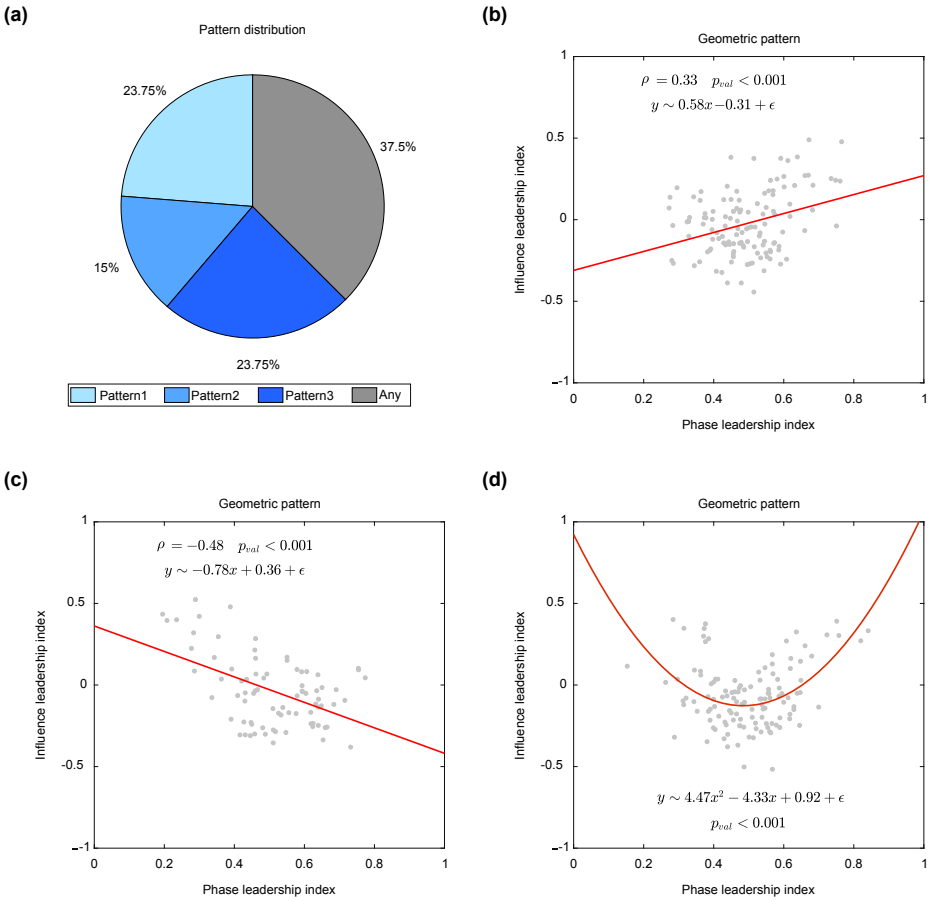

Figure 5.5: **Distribution and characterization of the leadership patterns in Experiment 1.** In Panel (a) the pie chart depicts how the three patterns were distributed among the trials of Experiment 1. A correlation analysis between the net information flow NetCaus and the mean position ranking $\overline{H}$ in the trials where Pattern 1 and 2 were observed is reported in Panels (b) and (c), respectively. The linear fitting is represented by a red solid line. In Pattern 3, the relationship between NetCaus and $\overline{H}$ is instead captured by a parabolic curve fitting, which is the red solid line in Panel (d).

5.3.2 Leadership emergence aids coordination

We found that one of the three leadership patterns described above emerged in the 62.50% of all the trials in Experiment 1. We ascertained that the frequency of occurrence of one of the three patterns was different from chance by comparing it with the expected frequency of occurrence (28.57%) using a χ^2-test ($\chi^2(3) = 83.54$, $p < 0.001$). Most importantly, we found that the level of coordination in the group was significantly higher in those trials where leadership emerged than in those where it did not. In particular, we computed the group order parameter z to be equal to 0.73 on average when leadership emerged ($M_1 = 0.73$, $SD_1 = 0.17$) while being equal to 0.60 otherwise ($M_2 = 0.60$, $SD_2 = 0.17$). An independent t-test calculated on these values showed significant synchronization differences in the scenarios (independent t-test, $t(78) = 3.37$, $p < 0.001$, *Cohen's* $d = 0.78$).

5.3.3 Leadership emergence patterns are independent of direct visual/auditory coupling

We performed a second set of experimental trials (denoted Experiment 2 in Section 5.1) to assess whether the emergence of the identified leadership patterns persisted also in the absence of direct visual and auditory coupling. Specifically, in Experiment 2 we used Chronos (see Figure 5.3) and we found again that in 62.50% of the trials one of the three leadership patterns emerged. A χ^2-test revealed that the frequency of occurrence of the leadership patterns was different from chance ($\chi^2(3) = 18.81$, $p < 0.001$), thus suggesting that these emergent patterns are still present in the absence of direct visual/auditory coupling among group.

Again, the average order parameter in the trials where these patterns are observed is higher than that observed in the remaining trials ($M_1 = 0.68$, $SD_1 = 0.16$ versus $M_2 = 0.55$, $SD_2 = 0.14$), and this difference is found to be significant (independent t-test, $t(30) = 2.23$, $p = 0.03$, *Cohen's* $d = 0.82$). Also, the geometric interpretation of the three patterns in this second experiment was qualitatively the same as in the experiments where players were physically present in the same room, see Figures 5.6(b)-(d). Our findings confirm that leadership emergence occurs even in the absence of social interaction between the group members and therefore that some type of unintentional communication encoded in the motion of each group member causes its occurrence to achieve a prior common goal. Lilliefors tests on residuals shows that the null hypothesis of normality of data cannot be rejected ($D(55) = 0.08$, $p = 0.49$ for Pattern1, $D(24) = 0.18$, $p = 0.05$ for Pattern2, and $D(35) = 0.11$, $p = 0.28$ for Pattern3).

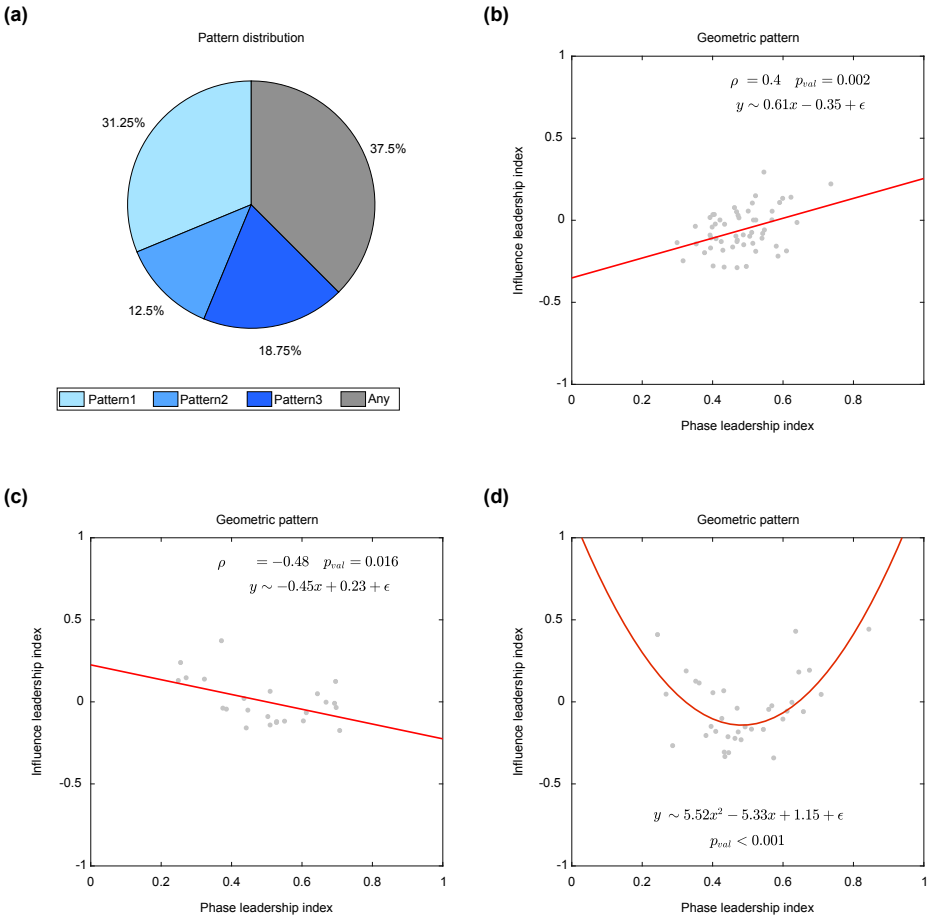

Figure 5.6: **Distribution and characterization of the leadership patterns in absence of social interaction.** In Panel (a) the pie chart depicts how the three patterns were distributed among the trials of Experiment 2. A correlation analysis between the net information flow NetCaus and the mean phase ranking $\overline{H}$ in the trials where Pattern 1 and 2 were observed is reported in Panels (b) and (c), respectively. The linear fitting is represented by a red solid line. In Pattern 3, the relationship between NetCaus and $\overline{H}$ is instead captured by a parabolic curve fitting, which is the red solid line in Panel (d).

5.3.4 Spatial distribution influences leadership emergence

We manipulated the group interaction structure to assess whether different topologies had an effect on leadership emergence. A χ^2 test revealed that the distribution of the three leadership patterns across the topologies is different from uniform ($\chi^2(3) = 10.88$, $p = 0.012$). In particular, we observed a higher occurrence of leadership emergence when all players were interacting with everyone else (complete graph topology, Fig. 5.2(a)) or when a central player was interacting with the rest of the group (star graph structure, Fig. 5.2(d), see Tabs. 5.1-5.2). These topologies are also those that were found in previous work to facilitate the onset of motor coordination in the group ($F(3, 76) = 31.55$, $p < 0.001$, $\eta^2 = 0.55$). This is a further confirmation that the emergence of leadership is associated to improved levels of coordination among the participants.

Table 5.1: **Distributions of the leadership Patterns in each topology (Experiment 1).** The last line represents the expected percentages if agents phase and influence leadership ranking are both extracted from a uniform distributions.

Topology	Pattern1	Pattern2	Pattern3	None
Complete	25%	5%	50%	20%
Path	25%	15%	10%	50%
Ring	25%	5%	10%	60%
Star	20%	35%	25%	20%
Expected	11.90%	11.90%	4.77%	71.43%

Table 5.2: **Distributions of the leadership Patterns in each topology (Experiment 2).** The last line represents the expected percentages if agents phase and influence leadership ranking are both extracted from a uniform distributions.

Topology	Pattern1	Pattern2	Pattern3	None
Complete	37.5%	12.5%	25%	25%
Path	50%	0%	12.5%	37.5%
Ring	12.5%	0%	25%	62.5%
Star	25%	37.5%	12.5%	25%
Expected	13.33%	13.33%	6.67%	66.67%

5.3.5 Distribution of leader role across players

The authors of [74] posited the existence of two diverse leadership structures. Specifically, in a group with a centralized leadership structure, a single member of the group acts as a leader, while all the other players enable and reinforce the leader identity. In opposition to this paradigm, leading actions can be distributed among group members across time. As we observed that the identity of the leaders emerging in the three patterns identified in the main text was not always the same, we used the Gini index [237] to discriminate between *distributed leadership* across the players or *centralized leadership* [74] emerged.

For each of the six groups of participants (4 for Experiment 1, and 2 for Experiment 2), we focused on the trials where one of the three patterns was observed, and we computed for each player, say i, the percentage x_i of trials where s/he acted as a either a phase or an influence leader. The agents were indexed in non-decreasing order with respect to x_i, that is, for all i, $x_i \leq x_{i+1}$. After normalizing such that $\sum_i x_i = 1$, we then obtained 6 distributions of x_i for each group, on which we computed the Gini index $0 \leq I_g \leq 1$, $g = 1, \ldots, 6$, where the subscript g identifies the specific group considered. Originally introduced in economics to measure inequalities in the wealth distribution within a country, in this context the Gini index quantifies whether leadership is shared among the players, with $I_g = 1$ corresponding to a single agent consistently leading in all the trials, and $I_g = 0$ to all agents leading in the same number of trials. Specifically, for each of the six groups, the Gini index can be computed as

$$I_g = 1 - \frac{2}{N_{\text{players}} - 1}\left(N_{\text{players}} - \frac{\sum_{i=1}^{N_{\text{players}}} i x_i}{\sum_{i=1}^{N_{\text{players}}} x_i}\right). \tag{5.11}$$

The values of the Gini indices depicted in Figures 5.7-5.8 (it ranges between 0.50 and 0.63) suggest that, although some players tends to lead more than others, leadership is generally shared among the group members.

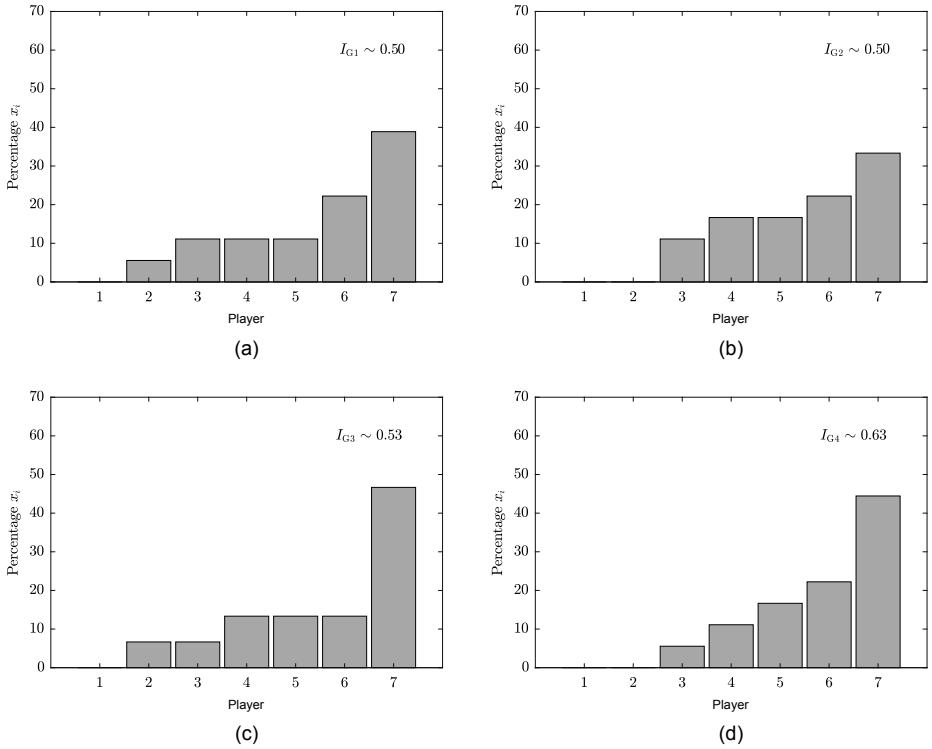

Figure 5.7: **How leadership distributes among the players (Experiment 1).** Each panel shows the percentage x_i of trials where player i acted as a leader, for all $i = 1, \ldots, 7$. The agents are sorted so that x_i is non-decreasing. Panel (a), (b), (c), and (d) refer to group **G1**, **G2**, **G3**, and **G4**, respectively (see the Experimental setup section for details on how players were clustered in each group). The value of the Gini index for each group is reported in the top-right corner of each panel.

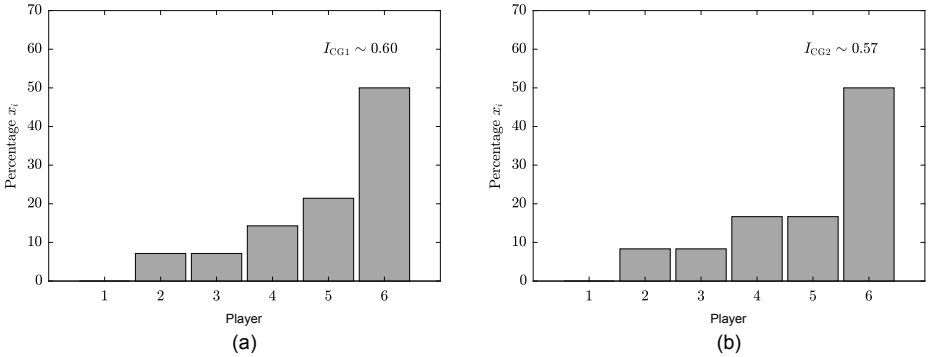

Figure 5.8: **How leadership distributes among the players (Experiment 2).** The two panels show the percentage x_i of trials where player i acted as a leader, for all $i = 1, \ldots, 6$. The agents are sorted so that x_i is non-decreasing. Panel (a) and (b) refer to group **CG1** and **CG2**, respectively. The value of the Gini index values ($I_{\mathrm{CG1}} \sim 0.60$, $I_{\mathrm{CG2}} \sim 0.57$) given in the top-right corner of every panel suggests that there is no particular group member always assuming a leadership role but that in different trials different players took such role.

5.4 Summary

In this Chapter, we focused on the problem of studying leadership emergence and its effects in human groups involved in a joint motor task. We found that leadership emergence does indeed foster coordination and is therefore a natural phenomenon occurring in human groups even when it is not established a priori. Interestingly, with the combined use of two metrics- phase leadership and net causation indices-, we uncovered three main patterns through which leadership emerges. One, where the most influential player is the one ahead in phase, an other, where the lagging one is the most influential, and the third, where a shared leadership arrangement emerges between the players ahead or lagging in phase. Crucially, these three scenarios can be immediately related to some analogous ones that have been uncovered in the animal kingdom confirming that leadership emergence is a naturally occurring organizing phenomenon when coordination is the goal of the group.

Our results also highlighted how the emergence of these leadership patterns fosters coordination in the group, with the order parameter being significantly lower in those trials where these patterns were absent. This observation was found to be independent of the presence of physical perceptuo-motor interaction among the players. Indeed, the results were validated and confirmed via a set of experiments, where the participants could only perceive each other's motion through a laptop screen. The persistence of the leadership patterns we uncovered in different conditions, combined with the observation that they appear to promote synchronization, suggest that this is a self-organizing phenomenon emerging when a group needs to perform a cooperative task.

In the following Chapter, we present preliminary experimental evidence showing that coordination and leadership emergence in a group can be perturbed ad hoc by introducing an artificial agent in the group of humans performing a joint motor task.

6 Preliminary investigation on the effect of virtual players on group coordination

Investigations on sensorimotor synchronisation introduced in the previous chapters included experimental setups within ensembles composed only by human agents. The presence of a virtual player can influence and steer the overall group dynamics towards a certain level of coordination. The introduction of artificial agents in a human group is relevant to aid the design of innovative [139, 141] and personalized rehabilitation therapies in those impairments where the imitation and movement synchronization mechanisms fail [15, 16, 136, 238].
Researchers in Social Neuroscience proposed the use of a new interaction paradigm termed as Human Dynamic Clamp (HDC) [239]. Inspired by the neuronal dynamic clamp [240], the HDC allows to directly manipulate in real time the interaction or coupling between a human and an avatar constructed to behave like a human, driven by well-established models of coordination dynamics. This novel interaction paradigm allows to explore a wide repertoire of human behavior and shed light on those features that cannot be easily accessed in standard human interactions.

In our work, inspired by the human dynamic clamp paradigm, we used our hardware-software platform *Chronos* [34] to include artificial agents in a group of humans performing a joint motor task to analyse how they influenced the emergence of human coordination. Indeed, several behaviours and hypotheses can be explored and investigated on human group coordination by varying the mathematical model of the artificial agent and playing with its parameters.

This chapter presents preliminary results, describing the influence of a stubborn artificial agent on individual and group synchronization dynamics, and on the emergence of the leadership patterns introduced in Chapter 5.

Specifically, in Section 6.1 we formalize our research questions. In Section 6.2 we describe the task and the different sessions of the experiment. Then we present the individual kinematic characterization in solo session and the experimental synchronization results obtained in groups both with and without the addition of a virtual player (Section 6.3). Finally, an interpretation of the main findings and contributions of the virtual player

on the emergence of leadeship patterns is presented in Section 6.4. Finally, a summary of the key results investigation is given at the end of the Chapter in Section 6.5.

6.1 Research questions

The goal of our study was to address some open research questions about group synchronization, leadership emergence and the influence of an external virtual agent. Specifically, by introducing and manipulating the virtual agent dynamics we aimed at investigating:

1. which group synchronization frequency emerges;
2. whether the players' positions in a given group topology influence the group dynamics (configuration effect);
3. if the virtual player can steer the synchronization group dynamics in a desired manner;
4. if a virtual agent influence the leadership patterns emerging in the group.

We report below a first attempt at investigating the issues above.

6.2 Task and procedure

In order to analyse the influence of an avatar on the group synchronization performance we employed the Chronos platform (see 4.1) in three scenarios including solo and group experiments in an ensemble of 5 agents, with and without a Virtual Player (VP). All the experiments involve participants moving their favourite hand above their respective position sensors (Leap Motion [181]), along a 1D direction parallel to the floor. The experimental setup presented here is the same described in Chapter 5. Data was originally stored with a frequency rate of 10Hz, and then underwent cubic interpolation with a sampling frequency equal to 100Hz. 5 volunteers took part in the experiments (4 males and 1 female). All the subjects were right handed, and none of them had physical and mental illnesses or disabilities. They were M.Sc. and Ph.D. students from the University of Naples- Federico II. The experiments took place in three different sessions. All subjects gave written informed consent in accordance with the Declaration of Helsinki.
Seven different group structures were implemented (see Fig. 6.1): complete (a), path (b-d), ring (e) and star graph (f-g, for a detailed description of each graph see Chapter 3). In particular, for path and star graphs multiple configurations were tested. As for the path graph, three versions of the topology were considered, specifically:

- PG_{12345}: random arrangement of the participants disregarding the individual kinematic features (see Tab. 6.1);
- PG_{12534}: the random disposition is split by placing the slowest (but also the most coherent) player in the middle;
- PG_{53214}: in this configuration we positioned the two slowest players at the endpoints of the group.

Regarding the star graph, we explored two configurations. Namely:

- SG_{3cen}: the fastest player acted as hub;
- SG_{5cen}: the slowest player was the central node.

For each topology, 7 experiments lasting 45s each were carried out.

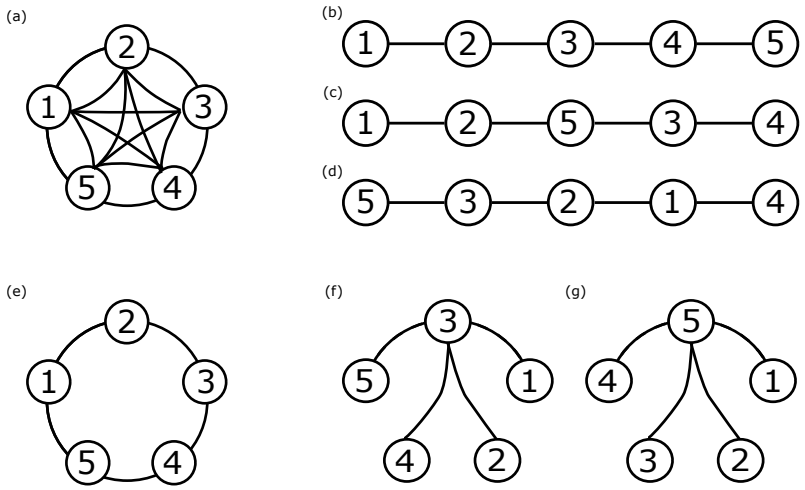

Figure 6.1: **Topologies of interest.** Panels (a-g) show the four topologies implemented in the second session of experiments: complete graph(a), path graph(b-d), ring graph(e), and star graph(f-g). In the complete graph, each participant can see all the others; in the path graph, every player can see the trajectories of two neighbours with the exception of the two external participants (the head and tail of the chain) that are constrained to visualize the motion of only one neighbour; in the ring graph, each player can see the motion of only two neighbours; in the star graph, all the players observe the motion of one central player who, conversely, sees the motion of all the others. In addition, for path and star graphs we ran trials with additional configurations to test any possible effect of how the players are combined in a given constrained topology. In particular, for the path graph we considered the fastest and the slowest players in the middle (respectively in panels (b) and (d)) in the same way of the star topology ((f) and (g)). In addition, in the path graph we tested also the effect of the slowest players at the head and tail of the chain.

6.2.1 Deployment of a virtual player through Chronos platform

The problem of entraining a human group is relevant in many scenarios like, for instance, in orchestra performance, in rowing teams or in the field of rehabilitation robotics. With the support of data analysis and ad-hoc mathematical models, it could be possible, in principle, to observe and assign at will leadership in a human group by deploying virtual agents [241, 242]. Indeed, virtual players with specific values of natural oscillation frequency could be appropriately connected to a subset of the agents in the ensemble and influence their motion so as to control the group collective behaviour.

In this work, we deployed the virtual agent implemented in the Chronos platform whose dynamics is described as follows. Denote with $x(t) \in \mathbb{R}$ the position of the VP at time t. The mathematical description modelling its dynamics is given as follows:

$$\ddot{x}(t) = f(x(t), \dot{x}(t)) + u(t) \tag{6.1}$$

where f represents the behaviour of the artificial agent in isolation (i.e., not connected to other agents), $\dot{x}$ and $\ddot{x}$ are its velocity and acceleration, and u represents the control input modelling the coupling interaction between the virtual agent and some other individuals in the group. The Chronos platform makes it possible to choose several combinations of inner dynamics and coupling functions to generate the movements of the virtual player. In our experiments we set the VP model as follows:

- **Inner dynamics model.** The nonlinear HKB model was selected to describe the internal dynamics of the avatar. Here:

$$f(x, \dot{x}) = -(\alpha x^2 + \beta \dot{x}^2 - \gamma)\dot{x} + \omega^2 x \tag{6.2}$$

  with α, β, γ characterising the damping and friction coefficients, and ω influencing the frequency of oscillation, respectively.
- **Control signal.** Different options can be selected for the coupling contribution u to describe the interaction between the VP and another agent. We selected an adaptive control strategy. Namely, in the case of the virtual player acting as a follower, u is set as:

$$u = [\psi + \chi(x - y)^2](\dot{x} - \dot{y}) - Ce^{-\delta(\dot{x}-\dot{y})^2}(x - y) \tag{6.3}$$

  where

$$\dot{\psi} = -\frac{1}{\psi}[(x - y)(\dot{x} - \dot{y}) + (x - y)^2] \tag{6.4}$$

$$\dot{\chi} = -\frac{1}{\chi}(\dot{x} - \dot{y})[f(x, \dot{x}) + u] \tag{6.5}$$

  with y, $\dot{y}$ being position and velocity of the agent connected with the artificial agent, C and δ being control parameters, and where ψ and χ are adaptive parameters.
  In the case of the virtual player acting as a leader, the control signal is described as:

$$u = \lambda\Big([\psi + \chi(x - \sigma_p)^2](\dot{x} - \sigma_v) - Ce^{-\delta(\dot{x}-\sigma_v)^2}(x - \sigma_p)\Big) + (1 - \lambda)K(y - x) \tag{6.6}$$

  with $\lambda := e^{-\delta|x-y|}$, K being a control parameter, and with σ_p and σ_v being reference profiles for position and velocity (kinematic signature) that allow the virtual agent to spontaneously produce motions.

In this work, we chose a VP acting as a leader with default parameter values: $\alpha = 3$, $\beta = 7$, $\gamma = 0.2$, $\omega = 1.75$, $C = 60$, $\delta = 0.5$, $\psi(0) = \chi(0) = -10$, $K = 40$. σ_p and σ_v are pre-recorded signatures chosen from the Chronos database. For more details on the available options for the virtual player setup to interact in a human-like fashion with its partners, see [34].

6.3 Synchronization results

In this section, we present the main results of the analysis on group interaction. All the metrics employed here to analyse and quantify the coordination level of the participants, have been defined in Section 3.2. In addition, we employ the coefficient of variation CV and the dyadic coordination metric.

The first is a measure of the level of dispersion of the natural rhythms of the participants of group, defined as

$$CV(\tilde{\omega}) = \frac{\sigma(\tilde{\omega})}{\mu(\tilde{\omega})} \tag{6.7}$$

where $\tilde{\omega} := [\mu(\omega_1)\mu(\omega_2)\dots\mu(\omega_5)]^T \in \mathbb{R}^5$ is the vector of the natural oscillation frequencies of the players in the group. Specifically, the higher the value of CV is, the more different are the frequencies of the participants of group from each other. Analogously, it is possible to define the individual coefficient of variation $CV(\tilde{\omega}_k)$ as a measure of the individual variability of the natural oscillation frequency of the k-th player.

As for the dyadic coordination level, denoting with $\phi_{i,j}(k) := \theta_i(k) - \theta_j(k)$ the relative phase between two participants in the group at the sampling time k, it is possible to estimate their level of dyadic coordination, that is how stable ($\rho_{d_{i,j}} = 1$) or variable ($\rho_{d_{i,j}} = 0$) their phase mismatch is over the total duration N_T of the trial.

$$\rho_{d_{i,j}} := \frac{1}{N_T}\left|\sum_{k=1}^{N_T} e^{j\phi_{i,j}(k)}\right| \quad \in [0,1], \tag{6.8}$$

Note that $\rho_{d_{i,j}} = \rho_{d_{j,i}}$, and that low dyadic coordination levels can coexist with high group coordination values.

6.3.1 Kinematic characterization of the players

Solo trials were performed in the first session. This kind of experiment involves only one participant. Participants were asked to carry out 7 trials, each lasting 30s, to produce sinusoidal-like waves at their own preferred rhythm with their favourite hand, in isolation. In so doing, the movement of each single player alone can be recorded in order to characterize her/his kinematic features. In Tab. 6.1 we synthesize the individual characteristics of the players. A one-way ANOVA run on the frequencies recorded across the seven trials in isolation revealed a significant difference among almost all the players ($F(4,30) = 84.21$, $p < 0.001$, $\eta^2 = 0.92$). In particular, post-hoc Bonferroni tests showed that participant number 2 is not significantly different from player 1 ($p = 0.21$) and from player 3 ($p = 0.41$) whereas all the agents differ clearly ($p < 0.001$). Participant identified by number 3 represents the fastest and the most variable agent of the group (highest SD) whereas player number 5 shows the slowest velocity and the lowest value of motion variability in the ensemble. Our attention will be focused on these actors throughout the study.

Table 6.1: **Kinematic characterization of the players in solo condition.**

Player	$\bar{\omega_i}$	**std**	**CV**
1	7.10 rad/s	0.66	9.34%
2	7.78 rad/s	0.53	6.83%
3	8.31 rad/s	0.92	11.03%
4	5.42 rad/s	0.21	3.83%
5	3.42 rad/s	0.20	5.97%
mean	6.40 ± 1.99 rad/s		
CV	31.07%		

6.3.2 Group interaction

Group trials were carried out in the second session of the experiments involving several agents. In particular, any interaction pattern among the players can be assigned by the administrator, with the possibility of implementing both directed and undirected topological structures (see Section 4.1). In Figure 6.1 we illustrated the topologies that we examined. In the case of the Path and Star graphs, we studied different configurations of the same topology in order to take into account the influence of the position of the most interesting players- in terms of kinematic features-on group performance. In this experiment, human subjects were required to synchronise their oscillations with those of the circles shown on their respective computer displays, representing the motion of the players interconnected with them. However, players did not have global information on the interaction patterns.

Slowing down. As we showed in Chapter 4, when human agents are involved in a group synchronization interaction, they achieve synchronization not on the average value of their natural kinematic frequencies but on a lower value. In this study, we observed a further confirmation of this significant result (see Tab.6.2), showing that slowing down is not the result of the influence of specific players but it is a typical emergent dynamics of this coordination task. A one-way repeated measures ANOVA with Greenhouse-Geiser corrections ($\epsilon = 0.35$) run on the group frequencies captured in all the topologies indicated a considerable interaction effect ($F(7, 42) = 82.18$, $p < 0.001$, $\eta^2 = 0.93$). Specifically, in all the topologies players slowed down compared to the average frequency achieved in isolation ($p < 0.001$). Moreover, the third configuration of the path graph (**Path graph 53214**) led to the lowest frequency value reached by the group which was significantly different from the two additional **Path graphs** ($p = 0.03$), from the **Ring** ($p < 0.001$), and from **Star graph** with participant number 5 acting as the hub ($p = 0.03$). Furthermore, the frequency reached by the group in the Star graph with participant number 3 as a central player was significantly different from that achieved in the **Path graph 12534** ($p = 0.04$), in the **Ring** ($p = 0.002$), and in the **Star graph** with player 5 as a hub ($p = 0.02$).

Table 6.2: **Mean and standard deviation of the order parameter and synchronization frequency indices across the topologies during group interaction.**

	Order parameter	**Synchronization frequency**
Topology	mean±std	mean±std
Complete graph	0.93 ± 0.06	4.29 ± 0.03 rad/s
Path graph 12345	0.77 ± 0.13	4.55 ± 0.01 rad/s
Path graph 12534	0.84 ± 0.11	4.41 ± 0.02 rad/s
Path graph 53214	0.93 ± 0.02	4.18 ± 0.02 rad/s
Ring	0.90 ± 0.05	4.46 ± 0.01 rad/s
Star graph- 3 center	0.92 ± 0.04	4.22 ± 0.03 rad/s
Star graph- 5 center	0.91 ± 0.02	4.54 ± 0.03 rad/s

Configuration effect on phase synchronization index and frequency synchronization. A repeated-measures ANOVA test run on the order parameter recorded in the different configurations of the **Path group** topology shows an effect of the configuration on the synchronization results ($F(2,12) = 6.04$, $p = 0.02$, $\eta_p^2 = 0.50$). Normality and sphericity assumptions were met. In particular, LSD post-hoc test shows that the difference is due to the difference between Path graph **PG-12345** and **PG-53214** ($p = 0.03$). This result shows that there is no difference between putting the fastest or the slowest player in the middle ($p = 0.14$) and not between the topology with the slowest player in the middle and the two slowest players at the head and tail of the path ($p = 0.08$). These results say that to have a significant improvement it is important to remove the fastest player from the middle and put the slowest participants at the extremities of the path. A paired t-test on the order parameters recorded in the star graphs shows again that putting the fastest or the slowest player in the center has any effect on the synchronization performance ($t(6) = 0.47$, $p = 0.66$).

We ran again a repeated-measures ANOVA test on the frequency synchronization reached by the group recorded in the different configurations of the **Path topology**. Results show an effect of the configuration on the synchronization results ($F(2,12) = 8.47$, $p = 0.02$, $\eta_p^2 = 0.59$). Normality assumptions were met whereas Greenhouse-Geisser corrections were necessary for lack of sphericity. LSD post-hoc test shows that there is difference between Path graphs **PG-12345** and **PG-53214** ($p = 0.03$) and between Path graphs **PG-12534** and **PG-53214** ($p = 0.005$) but did not uncover any difference between putting the fastest or the slowest player in the middle ($p = 0.08$). These results show that putting the slowest participants at the extremities of the path guarantees a beneficial containment effect useful to make participants more cohesive in the chain. A paired t-test on the order parameters recorded in the various configurations of the Star graph shows again that having the slowest player as the central node has a more significant effect on the frequency than placing the fastest in the central role($t(6) = -3.33$, $p = 0.02$).

6.3.3 Group interaction with VP

The third and last session of the experiments involve the addition to the group of players described in in Section 6.3.2 of a Virtual Player described implemented through Chronos (see Section 6.2.1). However, players did not have information on the virtual nature of the sixth participant.

Figures 6.2 and 6.3 illustrate the topologies that we examined. For each topology, we explored different interconnection of the VP to the rest of the group. In particular, our attention focused on trying to influence the fastest and slowest players (number 3 and 5, respectively) and on players in specific positions of some topologies.

Influence of the virtual player on the synchronization frequency. In each topology, we ran an ANOVA to check if and how the influence of the avatar on the group interaction was detectable. One-way repeated measures ANOVA ran on the frequencies recorded in each topology (Tab. 6.3) showed an effect of the virtual player. All the post-hoc Bonferroni comparisons results for all the topologies are summarized in Table 6.4.

Specifically, in the **Complete graph** (see Fig.6.1(a)), normality and sphericity were met and the rANOVA displayed a VP effect ($F(2, 12) = 92.69,\ p < 0.001,\ \eta_p^2 = 0.94$). Post-hoc tests showed a significant slowing down in the presence of the VP with respect to the only human setup but any significant difference was detected between the scenarios where a player, i.e., the fastest (**CG-3pin**, see Fig.6.2(a1)) or slowest member in the group (**CG-5pin**, see Fig.6.2(a2)), was influenced by the artificial agent.

Then, in the **Path graph-12345** (see Fig.6.1(b)), normality and sphericity were met and the rANOVA displayed a VP effect ($F(3, 18) = 75.32,\ p < 0.001,\ \eta_p^2 = 0.93$). The presence of a virtual agent resulted in a significant decrease of the average group frequency. In addition, the analysis also showed a significant difference between **PG-12345-1pin** (see Fig.6.2(b1)) and **PG-12345-3pin** (see Fig.6.2(b2)), between **PG-12345-1pin** and **PG-12345-5pin**(see Fig.6.2(b3)), and between **PG-12345-3pin** and **PG-12345-5pin**. In other words, in the case of **Path graph** with fastest player in the middle, a stubborn artificial player made the group slowing down significantly but not in the same way accross the connected players: manipulating the behaviour of the head (**PG-12345-1pin**) or tail (**PG-12345-5pin**) had a stronger effect and slower the player influenced by the virtual agent, slower the group dynamics.

In the **Path graph-12534** (see Fig.6.1(c)), normality was met but all degrees of freedom were corrected using the Greenhouse-Geisser estimate of sphericity ($\epsilon = 0.56$). The repeated-measures ANOVA showed a VP effect ($F(1.12, 6.72) = 12.96,\ p < 0.001,\ \eta_p^2 = 0.93$). In the case of the **Path graph** with slowest player in the middle, post-hoc Bonferroni comparisons showed a significant slowing down when a persistent virtual player played in the group. Moreover, the difference between the two versions affected by the avatar (**PG-12534-1pin**, see Fig.6.2(c1), and **PG-12534-5pin**, see Fig.6.2(c2)) proved that the head/tail had a stronger effect than the player in the middle.

In the **Path graph-53214** (see Fig.6.1(d)), normality and sphericity were met and the rANOVA displayed a VP effect ($F(3, 18) = 28.55,\ p < 0.001,\ \eta_p^2 = 0.83$). In this configuration, pair Bonferroni tests showed that the external influence of the behaviour of a random player (see Fig.6.2(d1)) or that of the slowest participant (see Fig.6.2(d3)) did not

make the group slow down their frequencies in a significant way. In addition, influecing the behaviour of the central player (see Fig.6.2(d1)) helped steering the ensemble towards a slower motion.

Then, in the **Ring graph** (see Fig.6.1(e)), normality and sphericity were met and the rANOVA displayed a VP effect ($F(2, 12) = 265.24,\ p < 0.001,\ \eta_p^2 = 0.98$). Post-hoc Bonferroni comparisons showed that the players significantly reduced their average group frequency when the VP was connected to a human member but any difference was given by the choice of the player connected to the artificial agent.

In the **Star graph** with player 3 as hub (see Fig.6.1(f)), normality and sphericity were met and the rANOVA displayed a VP effect ($F(3, 18) = 240.64,\ p < 0.001,\ \eta_p^2 = 0.98$). The presence of a virtual agent resulted in a significant decrease of the average group frequency, but in this case, influencing the player acting as hub (**SG-3cen-3pin**, see Fig.6.3(f2)) or as one of the leaves (**SG-3cen-2pin**, see Fig.6.3(f1), or **SG-3cen-5pin**, see Fig.6.3(f3)) did not have any effect but there was a difference between affecting the leaves and the slowest player. Controlling the behaviour of the slowest player guaranteed a higher effect in the reduction of group frequency.

At the end, in the **Star graph** with player 5 as hub (see Fig.6.1(g)), normality and sphericity were met and the rANOVA displayed a VP effect ($F(2, 12) = 84.61,\ p < 0.001,\ \eta_p^2 = 0.93$). Pair Bonferroni tests showed a significant slowing down when there was an artificial agent in the group, whereas any difference was given by the selection of the player influenced by the avatar (**SG-5cen-3pin**, see Fig.6.3(g1), and **SG-5cen-5pin** (see Fig.6.3(g2)). This case confirmed what found in the previous Star Graph that is manipulating the behaviour of player in the hub or in the leaf did not make any difference.

These results show that the presence of a stubborn virtual agent has a significant effect on the reduction of the average frequency reached by the human group. In particular, our repeated measure analyses show that also the choice of the player controlled by the avatar, can amplify the reduction effect of the presence of the VP on the human group behaviour in almost all the topologies, depending both on the position and on the kinematic features of the manipulated participant.

Influence of the virtual player on the phase synchronization index. Also for the analysis of the VP influence on the group phase cohesiveness, we ran a one-way repeated measures ANOVA in each topology. In Table 6.5, we reported all the post-hoc Bonferroni comparisons results for all the topologies.

Specifically, in the **Complete graph**, normality and sphericity were met and the rANOVA displayed a VP effect ($F(2, 12) = 90.43,\ p < 0.001,\ \eta_p^2 = 0.94$). Pair Bonferroni tests revealed a significant decline of the phase cohesiveness among the members when a VP acted in the group, with respect to the only human setup. However, any significant difference was detected between the scenarios where the fastest or slowest player in the group was influenced by the artificial agent.

In the **Path graph-12345**, normality was met but all degrees of freedom were corrected using the Greenhouse-Geisser estimate of sphericity ($\epsilon = 0.58$). The repeated measures ANOVA displayed a significant VP effect ($F(1.74, 10.42) = 1.42,\ p = 0.02,\ \eta_p^2 = 0.41$). In particular, post-hoc comparisons showed that, in this case, the unique considerable

weakening of group phase synchronization was reached when the slowest player behaviour was manipulated by the artificial agent.

Following, in the **Path graph-12534**, normality and sphericity were met and the rANOVA displayed a VP effect ($F(2, 12) = 41.94,\ p < 0.001,\ \eta_p^2 = 0.87$). Post-hoc Bonferroni comparisons showed a significant reduction of the coordination levels when the stubborn artificial player was connected to a member in the group. Nonetheless, the choice of the player to manipulate in the group did not affect considerably the group cohesiveness.

Then, in the **Path graph-53214**, normality and sphericity were met and the rANOVA displayed a VP effect ($F(3, 18) = 64.66,\ p < 0.001,\ \eta_p^2 = 0.92$). The presence of the virtual agent resulted in a significant decrease of the group phase synchronization. In particular, in this case, influencing the central player (**PG-53214-2pin**, see Fig.6.2(d2)) led to a worse performance than influencing player in a random position (**PG-53214-1pin**, see Fig.6.2(d1)), different from the end-point (**PG-53214-5pin**, see Fig.6.2(d3)).

In the **Ring graph**, normality was met but the Greenhouse-Geisser correction ($\epsilon = 0.55$) was necessary. The rANOVA displayed a VP effect ($F(1.10, 6.62) = 6.34,\ p = 0.003,\ \eta_p^2 = 0.78$). As it happened in the Complete graph and in the **Path graph-12534**, post-hoc Bonferroni comparisons unveiled a significant worsening of the phase synchronization level reached by the ensemble agents when a stubborn artificial player played with a group member. However, any significant difference was detected between the scenarios where different players in the group were connected to the artificial agent.

In the **Star graph** with player 3 acting as hub, normality and sphericity were met and the rANOVA displayed a VP effect ($F(3, 18) = 4.07,\ p = 0.02,\ \eta_p^2 = 0.40$). However, post-hoc tests revealed that the phase cohesiveness achieved by the ensemble worsened in a significant way only when the virtual player was connected to the central agent (**SG-3cen-3pin**, see Fig.6.3(f2)).

Finally, in the **Star graph** with player 5 acting as hub, normality and sphericity were met and the rANOVA displayed a VP effect ($F(2, 12) = 41.75,\ p < 0.001,\ \eta_p^2 = 0.87$). Here again, pair post-hoc comparisons showed that when the VP played with a group member, the phase synchronization level reached by the ensemble agents worsened significantly. However, no considerable difference was detected between the scenarios where different players were influenced by the artificial agent (**SG-5cen-3pin** and **SG-5cen-5pin**).

These results show that the presence of a stubborn virtual agent causes a general and considerable worsening of level of the group cohesiveness reached by the human group. In particular, our repeated measure analyses show that, as for the average group frequency, special attention should be addressed to both the position and the kinematic traits of the manipulated participant, considering that the choice of the player manipulated by the avatar can increase the negative effect of the VP presence on the human group performance, in all the topologies.

Coefficients of variation and dyadic coordination. In Tables 6.6- 6.8 the frequencies and the coefficients of variation of group frequencies are reported with and without the VP in each topology whereas Figures 6.4- 6.6 show the average and the standard deviation of dyadic synchronization indices for each pair of players in each topology. The combination of these two indices provides an additional confirmation of the influence of the virtual player and how it is recognized as an external agent.

It is interesting to highlight that in the **Path graph-12345** we observed two different scenarios depending on what player is being influenced by the VP. Specifically, when player 1 was connected to the virtual agent (see Tab. 6.6c and Fig. 6.4(c)), the metrics computed on the group behaviour showed that the ensemble remained united and the avatar's dynamics was not recongnized as part of the group and then ignored. Differently, when participant 5 played also with the virtual player (see Tab. 6.6e and Fig. 6.4(f)), the dyadic synchronization index clearly showed that the avatar had an influence on the motion of the human players.

In Figure 6.6, there is another interesting example represented by the **Star graph** with player 5 as hub. When player 3 interacted with the avatar, almost all the dyads showed variability in the synchronization index. Differently, when the hub- participant 5- was connected to the virtual agent, all the players consistently avoided the external player and synchronized among themselves as observed in the **Complete** (Fig. 6.4(b)) and the **Ring** (Fig. 6.5(f)) graphs.

Again we observe that a stubborn virtual player spreads its influence in different ways according to the kinematic features and position in the group of the player it tried to influence. Also, we can observe a sort of bifurcation behaviour in participant number 5. When s-/he participated to a dyadic or triadic interaction, s-/he tried to integrate the information coming from the stubborn player represented by the virtual agent. Instead, when the number of partners was equal or greater than 3, s-/he completely ignored the virtual player and applied a majority rule [243–246]. Future work could be done to explore the costs and benefits of group membership as a function of the group size.

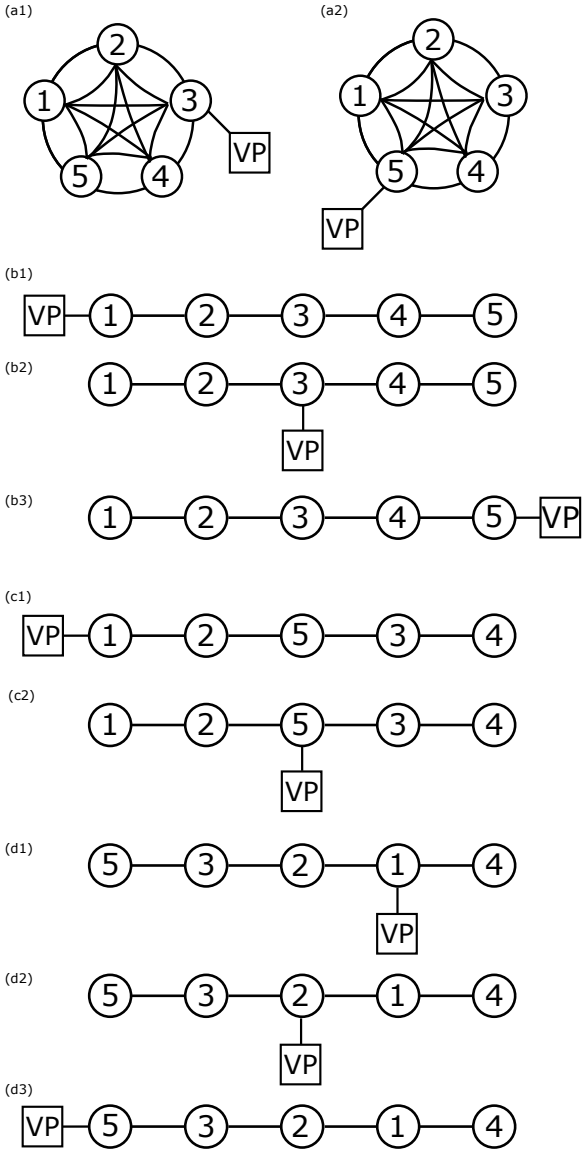

Figure 6.2: **Different connections of the Virtual Player to the human group (1).** Panels (a1-d3) show the topologies implemented in the third session of experiments where a virtual agent was added to influence the behaviour of different players in the human group. Specifically, circles correspond to human players whereas the square symbolizes the artificial agent in the group. In panels (a1-a2) we represented the Complete graph where both the fastest (a1) and the slowest (a2) players were reached by the action of the VP. Panels (b1-b3), (c1-c2) and (d1-d3) represent the three configurations of the Path graph, **PG-12345**, **PG-12534**, and **PG-53214**, respectively. In each configuration, different players at time interacted with the artificial player.

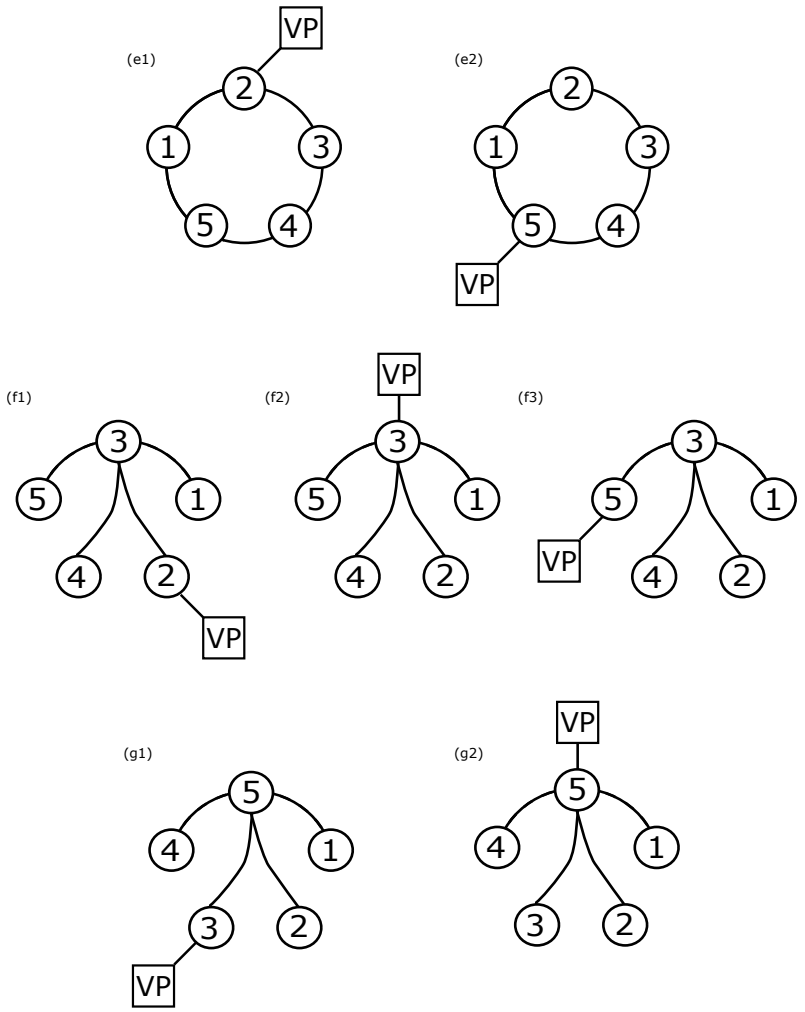

Figure 6.3: **Different connections of the Virtual Player to the human group (2).** Panels (e1-g2) show the topologies implemented in the third session of experiments where a virtual agent was added to influence the behaviour of different players in the human group. Specifically, circles correspond to human players whereas the square symbolizes the artificial agent in the group. In panels (e1-e2) we represented the Ring graph where both the player 2 (e1) and player 5 (e2) players were connected to the VP. Panels (f1-f3) and (g1-g2) represent the two configurations of the Star graph, SG-3cen and SG-5cen, respectively. In each configuration, different players at time were reached by the artificial player.

Table 6.3: **Mean and standard deviation of the order parameter and synchronization frequency indices of interests across the topologies during group interaction with a virtual agent.**

	Order parameter	**Synchronization frequency**
Topology	mean±std	mean±std
Complete graph		
- 3 pin	0.68 ± 0.05	3.55 ± 0.42 rad/s
- 5 pin	0.79 ± 0.02	3.59 ± 0.46 rad/s
Path graph-12345		
- 1 pin	0.70 ± 0.09	3.67 ± 0.50 rad/s
- 3 pin	0.63 ± 0.11	3.99 ± 0.53 rad/s
- 5 pin	0.58 ± 0.04	3.13 ± 0.38 rad/s
Path graph-12534		
- 1 pin	0.56 ± 0.08	3.56 ± 0.58 rad/s
- 5 pin	0.58 ± 0.09	4.00 ± 0.66 rad/s
Path graph-53214		
- 1 pin	0.65 ± 0.03	3.78 ± 0.55 rad/s
- 2 pin	0.56 ± 0.05	3.10 ± 0.27 rad/s
- 5 pin	0.62 ± 0.10	4.04 ± 0.56 rad/s
Ring graph		
- 2 pin	0.74 ± 0.03	3.30 ± 0.32 rad/s
- 5 pin	0.78 ± 0.06	3.15 ± 0.18 rad/s
Star graph- 3 center		
- 2 pin	0.79 ± 0.08	3.01 ± 0.06 rad/s
- 3 pin	0.82 ± 0.07	2.88 ± 0.05 rad/s
- 5 pin	0.79 ± 0.09	2.74 ± 0.05 rad/s
Star graph- 5 center		
- 3 pin	0.72 ± 0.06	3.03 ± 0.18 rad/s
- 5 pin	0.79 ± 0.02	3.29 ± 0.25 rad/s

Table 6.4: **Post-hoc Bonferroni comparisons run on average sychronization frequencies between different pairs of topologies.**

Topology	Complete graph	- 3pin	Path graph-12345	- 1pin	- 3pin	Path graph-12534	- 1pin	Path graph-53214	- 1pin	- 2pin	Ring graph	- 2pin	Star graph- 3cen	- 2pin	- 3pin	Star graph- 5cen	- 3pin
Complete graph																	
- 3pin	$p < 0.001$																
- 5pin	$p < 0.001$	$p = 0.70$															
Path graph-12345																	
- 1pin			$p = 0.004$														
- 3pin			$p = 0.03$	$p = 0.006$													
- 5pin			$p < 0.001$	$p = 0.003$	$p < 0.001$												
Path graph-12534																	
- 1pin						$p < 0.001$											
- 5pin						$p < 0.001$	$p = 0.03$										
Path graph-53214																	
- 1pin								$p = 0.11$									
- 2pin								$p < 0.001$	$p = 0.048$								
- 5pin								$p = 0.94$	$p = 0.98$	$p < 0.001$							
Ring graph																	
- 2pin											$p < 0.001$						
- 5pin											$p < 0.001$	$p = 0.06$					
Star graph- 3cen																	
- 2pin													$p < 0.001$				
- 3pin													$p < 0.001$	$p = 0.67$			
- 5pin													$p < 0.001$	$p = 0.003$	$p = 0.35$		
Star graph- 5cen																	
- 3pin																$p < 0.001$	
- 5pin																$p < 0.001$	$p = 0.06$

Table 6.5: **Post-hoc Bonferroni comparisons run on phase synchronization index between different pairs of topologies.**

Topology	Complete graph	- 3pin	Path graph-12345	- 3pin	- 3pin	Path graph-12534	- 1pin	Path graph-53214	- 1pin	- 2pin	Ring graph	- 2pin	Star graph- 1cen	- 2pin	- 3pin	Star graph- 5cen	- 3pin
Complete graph																	
- 3pin	$p < 0.001$																
- 5pin	$p = 0.002$	$p = 0.04$															
Path graph-12345																	
- 1pin																	
- 3pin			$p = 0.04$														
- 5pin																	
Path graph-12534																	
- 1pin						$p = 0.002$											
- 5pin						$p < 0.001$	$p = 0.87$										
Path graph-53214																	
- 1pin								$p < 0.001$									
- 2pin								$p < 0.001$	$p = 0.02$								
- 5pin								$p < 0.001$	$p = 0.98$	$p = 0.96$							
Ring graph																	
- 2pin											$p < 0.001$						
- 5pin											$p = 0.04$	$p = 0.54$					
Star graph-3cen																	
- 2pin																	
- 3pin													$p = 0.005$				
- 5pin																	
Star graph-5cen																	
- 3pin																$p < 0.001$	
- 5pin																$p < 0.001$	$p = 0.14$

Table 6.6: **Frequencies of the players during group interaction with a virtual player in each topology (1).**

Player	$\bar{\omega}_i$	std	CV
1	3.80 rad/s	0.07	1.87%
2	3.76 rad/s	0.20	5.22%
3	3.32 rad/s	0.27	8.19%
4	3.80 rad/s	0.10	2.74%
5	3.82 rad/s	0.11	2.98%
VP	2.78 rad/s	0	0%
average	3.55 ± 0.42		
average without VP	3.70 ± 0.21		
CV	11.89%		
CV without VP	5.81%		

(a) Complete Graph-3pin.

Player	$\bar{\omega}_i$	std	CV
1	3.76 rad/s	0.18	4.70%
2	3.76 rad/s	0.18	4.84%
3	3.78 rad/s	0.15	3.93%
4	3.80 rad/s	0.21	5.51%
5	3.80 rad/s	0.16	4.10%
VP	2.65 rad/s	$2e^{-3}$	0.08%
average	3.59 ± 0.46		
average without VP	3.78 ± 0.02		
CV	12.81%		
CV without VP	0.49%		

(b) Complete Graph-5pin.

Player	$\bar{\omega}_i$	std	CV
1	3.85 rad/s	0.16	2.73%
2	3.87 rad/s	0.06	2.58%
3	3.90 rad/s	0.15	3.30%
4	3.89 rad/s	0.17	3.15%
5	3.88 rad/s	0.12	3.20%
VP	2.65 rad/s	0	0%
average	3.67 ± 0.50		
average without VP	3.88 ± 0.02		
CV	13.61%		
CV without VP	0.56%		

(c) Path Graph-12345-1pin.

Player	$\bar{\omega}_i$	std	CV
1	4.12 rad/s	0.24	4.99%
2	4.16 rad/s	0.20	5.48%
3	4.22 rad/s	0.22	3.63%
4	4.27 rad/s	0.21	2.00%
5	4.26 rad/s	0.24	2.56%
VP	2.92 rad/s	0	0%
average	3.99 ± 0.07		
average without VP	3.88 ± 0.02		
CV	13.21%		
CV without VP	1.58%		

(d) Path Graph-12345-3pin.

Player	$\bar{\omega}_i$	std	CV
1	3.46 rad/s	0.13	3.68%
2	3.48 rad/s	0.14	3.98%
3	3.44 rad/s	0.16	4.55%
4	2.98 rad/s	0.34	11.36%
5	2.74 rad/s	0.16	5.75%
VP	2.65 rad/s	0	0%
average	3.13 ± 0.38		
average without VP	3.22 ± 0.34		
CV	12.21%		
CV without VP	10.51%		

(e) Path Graph-12345-5pin.

Player	$\bar{\omega}_i$	std	CV
1	3.11 rad/s	0.26	8.22%
2	3.28 rad/s	0.24	7.42%
3	4.12 rad/s	0.39	9.51%
4	4.08 rad/s	0.42	10.23%
5	4.00 rad/s	0.41	10.29%
VP	2.78 rad/s	0	0%
average	3.56 ± 0.58		
average without VP	3.72 ± 0.48		
CV	16.19%		
CV without VP	12.98%		

(f) Path Graph-12534-1pin.

Table 6.7: **Frequencies of the players during group interaction with a virtual player in each topology (2).**

Player	$\bar{\omega}_i$	std	CV
1	4.04 rad/s	0.30	7.37%
2	4.02 rad/s	0.34	9.01%
3	4.57 rad/s	0.14	3.00%
4	4.58 rad/s	0.16	3.48%
5	4.00 rad/s	0.36	9.07%
VP	2.78 rad/s	0	0%
average	4.00 ± 0.66		
average without VP	4.24 ± 0.30		
CV	16.40%		
CV without VP	7.19%		

(a) Path Graph-12534-5pin.

Player	$\bar{\omega}_i$	std	CV
1	4.00 rad/s	0.29	7.17%
2	4.01 rad/s	0.36	9.04%
3	4.01 rad/s	0.38	9.36%
4	4.04 rad/s	0.33	8.27%
5	3.94 rad/s	0.38	9.57%
VP	2.65 rad/s	0	0%
average	3.78 ± 0.55		
average without VP	4.00 ± 0.04		
CV	14.59%		
CV without VP	0.90%		

(b) Path Graph-53214-1pin.

Player	$\bar{\omega}_i$	std	CV
1	3.38 rad/s	0.34	9.97%
2	2.89 rad/s	0.23	7.94%
3	3.04 rad/s	0.30	9.81%
4	3.47 rad/s	0.27	7.85%
5	3.06 rad/s	0.24	7.93%
VP	2.78 rad/s	0	0%
average	3.10 ± 0.27		
average without VP	3.17 ± 0.24		
CV	8.70%		
CV without VP	7.73%		

(c) Path Graph-53214-2pin.

Player	$\bar{\omega}_i$	std	CV
1	4.25 rad/s	0.10	2.42%
2	4.34 rad/s	0.25	5.84%
3	4.40 rad/s	0.30	6.75%
4	4.27 rad/s	0.10	2.26%
5	4.04 rad/s	0.76	18.79%
VP	2.92 rad/s	0	0%
average	4.04 ± 0.56		
average without VP	4.26 ± 0.14		
CV	13.87%		
CV without VP	3.19%		

(d) Path Graph-53214-5pin.

Player	$\bar{\omega}_i$	std	CV
1	3.41 rad/s	0.11	3.14%
2	3.42 rad/s	0.11	3.10%
3	3.42 rad/s	0.11	3.15%
4	3.44 rad/s	0.13	3.80%
5	3.44 rad/s	0.10	2.96%
VP	2.65 rad/s	0	0%
average	3.30 ± 0.32		
average without VP	3.43 ± 0.01		
CV	9.58%		
CV without VP	0.40%		

(e) Ring Graph-2pin.

Player	$\bar{\omega}_i$	std	CV
1	3.22 rad/s	0.09	2.84%
2	3.20 rad/s	0.11	3.48%
3	3.25 rad/s	0.06	1.91%
4	3.22 rad/s	0.10	2.95%
5	3.22 rad/s	0.14	4.49%
VP	2.78 rad/s	0	0%
average	3.15 ± 0.18		
average without VP	3.22 ± 0.02		
CV	5.75%		
CV without VP	0.50%		

(f) Ring Graph-5pin.

Table 6.8: **Frequencies of the players during group interaction with a virtual player in each topology (3).**

Player	$\bar{\omega}_i$	std	CV
1	3.04 rad/s	0.16	5.38%
2	2.94 rad/s	0.06	1.89%
3	3.06 rad/s	0.15	5.06%
4	3.06 rad/s	0.17	5.66%
5	3.04 rad/s	0.12	3.93%
VP	2.92 rad/s	0	0%
average	3.01 ± 0.06		
average without VP	3.03 ± 0.05		
CV	2.10%		
CV without VP	1.66%		

(a) Star Graph-3cen-2pin.

Player	$\bar{\omega}_i$	std	CV
1	2.89 rad/s	0.24	8.16%
2	2.93 rad/s	0.20	6.71%
3	2.91 rad/s	0.22	7.52%
4	2.87 rad/s	0.21	7.32%
5	2.89 rad/s	0.24	8.15%
VP	2.77 rad/s	0	0%
average	2.88 ± 0.05		
average without VP	2.90 ± 0.02		
CV	1.79%		
CV without VP	0.79%		

(b) Star Graph-3cen-3pin.

Player	$\bar{\omega}_i$	std	CV
1	2.74 rad/s	0.13	4.84%
2	2.76 rad/s	0.14	5.23%
3	2.77 rad/s	0.14	5.11%
4	2.79 rad/s	0.19	6.91%
5	2.73 rad/s	0.10	3.54%
VP	2.65 rad/s	0	0%
average	2.74 ± 0.05		
average without VP	2.76 ± 0.02		
CV	1.73%		
CV without VP	0.81%		

(c) Star Graph-3cen-5pin.

Player	$\bar{\omega}_i$	std	CV
1	3.16 rad/s	0.11	5.45%
2	3.14 rad/s	0.11	6.22%
3	2.82 rad/s	0.11	4.70%
4	3.16 rad/s	0.13	6.20%
5	3.12 rad/s	0.10	6.25%
VP	2.78 rad/s	0	0%
average	3.03 ± 0.18		
average without VP	3.08 ± 0.15		
CV	5.90%		
CV without VP	0.81%		

(d) Star Graph-5cen-3pin.

Player	$\bar{\omega}_i$	std	CV
1	3.40 rad/s	0.15	4.54%
2	3.38 rad/s	0.13	3.92%
3	3.36 rad/s	0.13	3.73%
4	3.40 rad/s	0.11	3.27%
5	3.42 rad/s	0.11	3.08%
VP	2.78 rad/s	0	0%
average	3.29 ± 0.25		
average without VP	3.39 ± 0.02		
CV	7.60%		
CV without VP	0.63%		

(e) Star Graph-5cen-5pin.

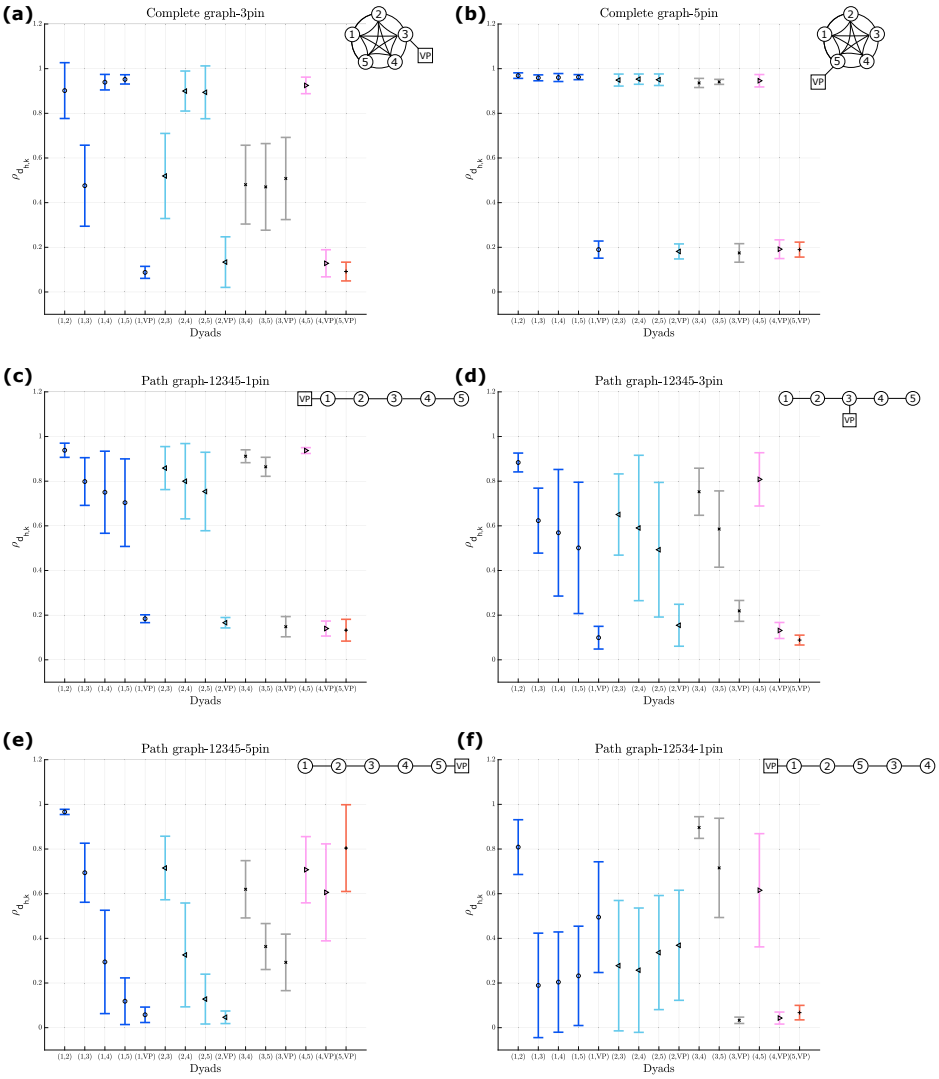

Figure 6.4: **Dyadic coordination levels observed experimentally in the presence of the virtual agent (1).** Symbols and error bars represent mean and standard deviation, across the total number of trials recorded during the third session, of the dyadic coordination levels $\rho_{d_{h,k}}$ for participants in in **Complete graph** (a-b), **Path graph-12345** (c-e) and **Path graph-12534**(f) respectively. Different colours and symbols refer to dyads related to different players. On the top right of each panel, a small schema of how players are phisically coupled, is depicted.

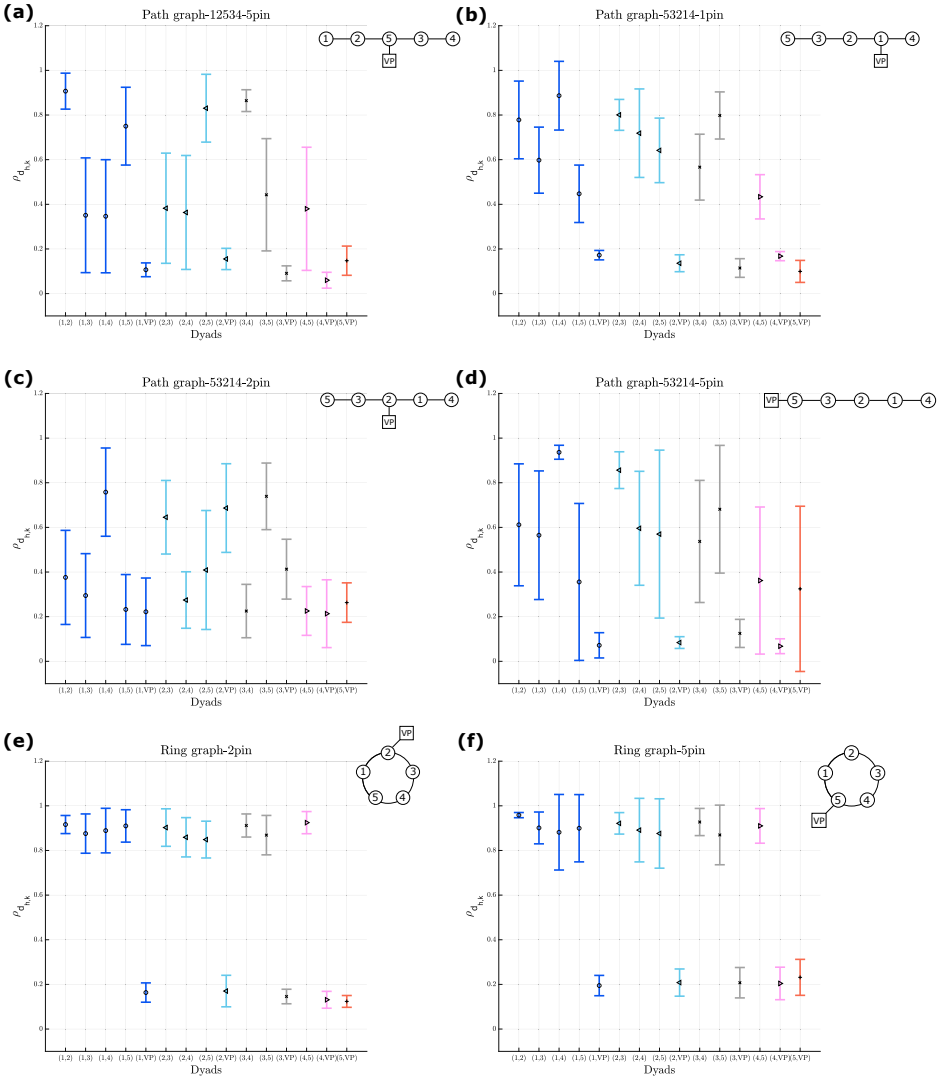

Figure 6.5: **Dyadic coordination levels observed experimentally in the presence of the virtual agent 21).** Symbols and error bars represent mean and standard deviation, across the total number of trials recorded during the third session, of the dyadic coordination levels $\rho_{d_{h,k}}$ for participants in **Path graph-12534** (a), **Path graph-12345** (b-d) and **Ring graph**(e-f) respectively. Different colours and symbols refer to dyads related to different players. On the top right of each panel, a small schema of how players are phisically coupled, is depicted.

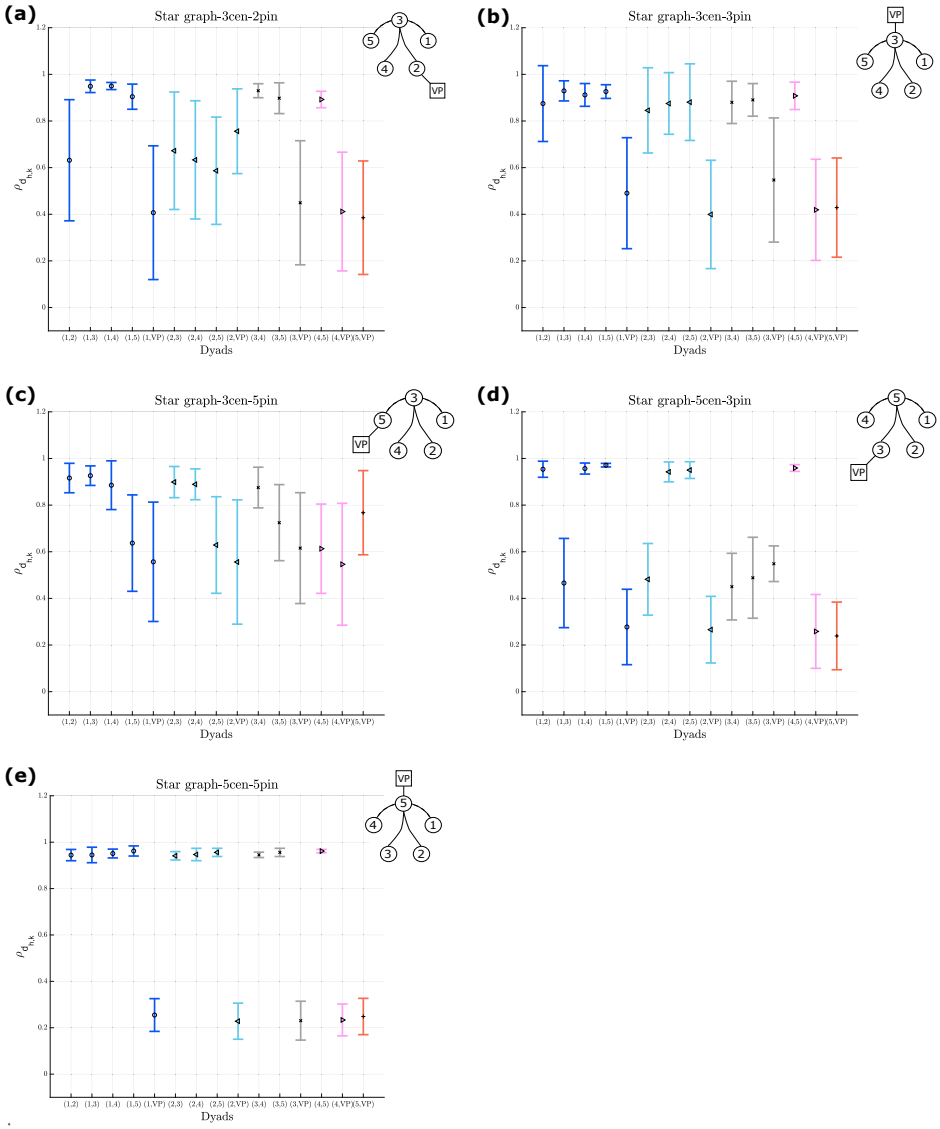

Figure 6.6: **Dyadic coordination levels observed experimentally in the presence of the virtual agent (3).** Symbols and error bars represent mean and standard deviation, across the total number of trials recorded during the third session, of the dyadic coordination levels $\rho_{d_{h,k}}$ for participants in in **Star graph-3cen** (a-c) and **Star graph-5 cen** (d-e) respectively. Different colours and symbols refer to dyads related to different players. On the top right of each panel, a small schema of how players are phisically coupled, is depicted.

6.4 Leadership analysis

In Chapter 5, we showed the emergence of three leadership patterns during human group synchronization. We also showed that these patterns are independent of the presence of social interaction but they are inherent in human coordination so that they emerge even in the absence of physical perceptuo-motor interaction among the players. In this section we tested the effect of the presence of a VP in the group on the quality of leadership patterns that emerged and on the distribution of it across the players. Specifically, we considered all the topologies where player 5 was reached by the VP, since it is the only player that was connected to the artificial agent in all the graphs. As detailed in Section 5.2 in Chapter 5, to quantitatively uncover each of these patterns we defined two indices, an influence index based on the computation of causation entropy, and a phase leadership index based on the phase analysis of the time series of the players' motion. The results of our analysis are summarized in what follows.

Influence of the artificial agent on leadership pattern emergence. As highlighted in Chapter 5, we found that the three leadership patterns described in Section 5.3.1 emerged in a significant number of trials (91.84%) and we ascertained that this occurrence was different from chance by comparing it with the expected frequency value (20%) with a χ^2-test($\chi^2(3) = 183.59$, $p < 0.001$).
A geometric interpretation of these three patterns can be obtained by plotting the net predicted information flow against the mean ranking in phase (see Fig. 5.5). A linear fitting shows that, in the trials where the phase leader emerged as the most influential (**Pattern 1**), ranking in phase and influence were positively correlated ($\rho(4) = 0.17$, $R^2 = 0.03$, $p = 0.41$), although the poor number of samples causes lack of significance. Instead, when leadership was assumed by the player most lagging in phase (**Pattern 2**), the opposite was observed ($\rho(4) = -0.63$, $R^2 = 0.40$, $p < 0.001$). Interestingly, a linear fitting ($R^2 = 0.001$, $p = 0.64$) cannot capture **Pattern 3**, where two players share leadership, and a parabolic interpolation is required to depict the coexistence of the lagging and phase leaders ($R^2 = 0.53$, $p < 0.001$).
In Figure 6.8 we represented the characterization of the leadership scenarios in the group interacting with the avatar. In almost 79.6% of trials we observed these scenarios (different from chance, $\chi^2(3) = 71.15$, $p < 0.001$) but the presence of the VP changed their distribution. In fact, a χ^2-test run on both the patterns distributions showed a significant difference ($\chi^2(3) = 16.33$, $p < 0.001$)- almost 40% of cases where **Pattern3** occurred in the absence of the VP were converted in the **Pattern1** (phase leadership) when the VP was present. Here again, in the trials where the phase leader emerged as the most influential, ranking in phase and influence were positively correlated ($\rho(16) = 0.43$, $R^2 = 0.18$, $p < 0.001$). Instead, when leadership was assumed by the player most lagging in phase (**Pattern 2**), the opposite was observed ($\rho(5) = -0.38$, $R^2 = 0.15$, $p = 0.02$). This result showed the weakening of the shared leadership supporting a stronger emergence of a phase leader. In addition, when two players shared leadership (**Pattern 3**), a parabolic interpolation was required to characterize the coexistence of the lagging and phase leaders ($R^2 = 0.37$, $p < 0.001$).

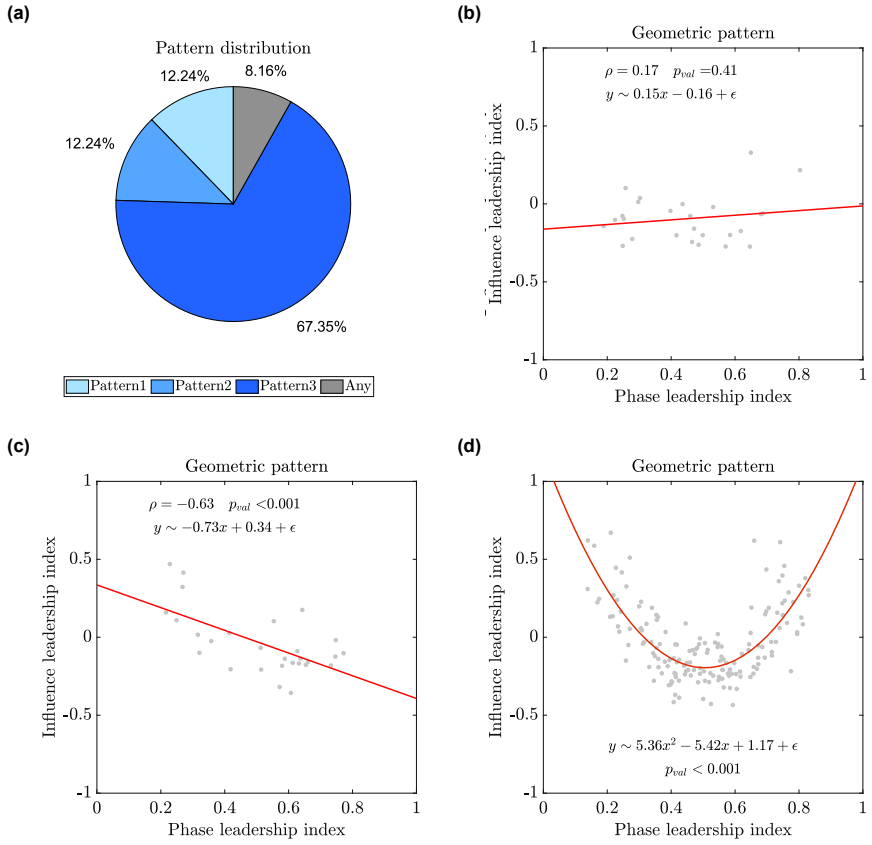

Figure 6.7: **Distribution and characterization of the leadership scenarios during group interaction without virtual player.** In Panel (a) the pie chart depicts how the three scenarios were distributed among the trials. A correlation analysis between the net information flow NetCaus and the mean phase ranking $\bar{H}$ in the trials where Pattern 1 and 2 were observed is reported in Panels (b) and (c), respectively. The linear fitting is represented by a red solid line. In Pattern 3, the relationship between NetCaus and $\bar{H}$ is instead captured by a parabolic curve fitting, which is the red solid line in Panel (d).

Effect of the virtual player on the leadership role of the players. Another way to capture the influence of the virtual player on the group dynamics is to see how it affects the distribution of the leadership role among group members. To do so, we computed the Gini indices [237] without and with the VP attached to player 5, as done in Section 5.3.5. Figure 6.9 clearly shows how the Gini index suggests a shift from shared leadership ($I_{\mathrm{G}} \sim 0.20$, see that $I = 0$ in uniform distribution) to a more centralized guidance ($I_{\mathrm{G+VP}} \sim 0.60$). As a result, the avatar contributed to define a more centralized scenario where player 1- not directly influenced by the virtual player- gained leadership in more than half of the trials where one of the three leadership patterns emerged. It is interesting to highlight that player 1 was neither the slowest, nor the fastest, the less or the most coherent player that emerged in the first session dedicated to the kinematic characterization of the participants. In addition, the virtual player was able to gain leadership in more than the 20% of the cases, representing the second most decisive player for the group interaction during the third experimental session.

Further investigations are needed to clarify how players takes advantage of the presence of the artificial agent to gain the leader role during group synchronization. These are left for future work.

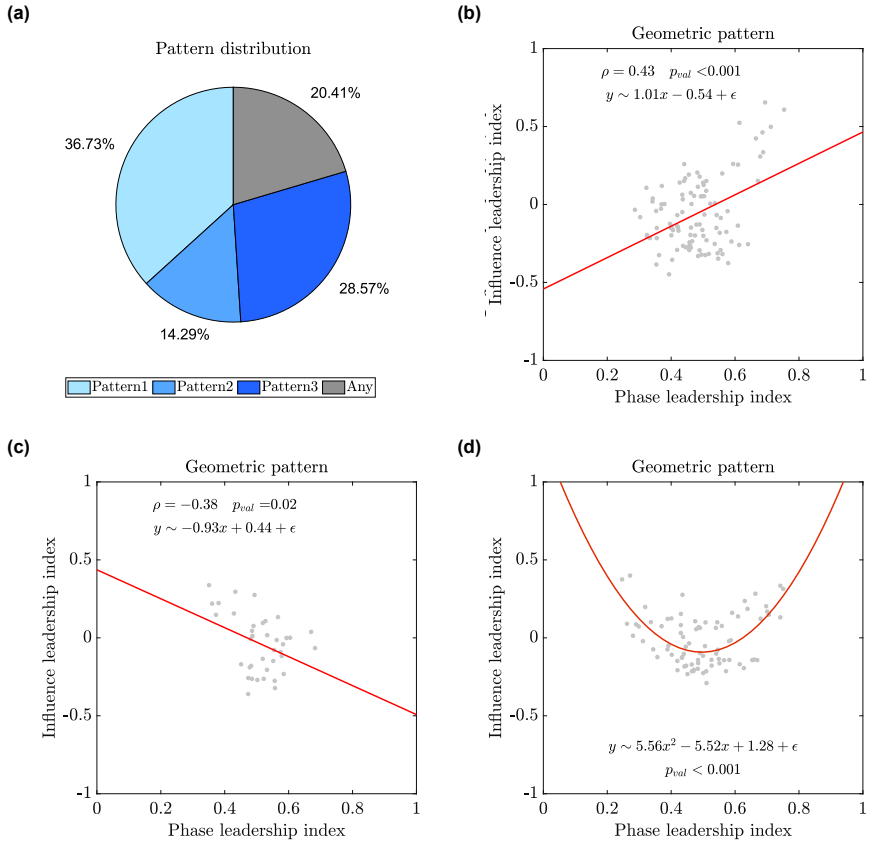

Figure 6.8: **Distribution and characterization of the leadership scenarios in presence of the virtual partner.** In Panel (a) the pie chart depicts how the three patterns were distributed among the trials with participant 5 pinned by the virtual player. A correlation analysis between the net information flow NetCaus and the mean position ranking $\bar{H}$ in the trials where Pattern 1and 2 were observed is reported in Panels (b) and (c), respectively. The linear fitting is represented by ared solid line. In Pattern 3, the relationship between NetCaus and $\bar{H}$ is instead captured by a parabolic curve fitting, which is the red solid line in Panel (d).

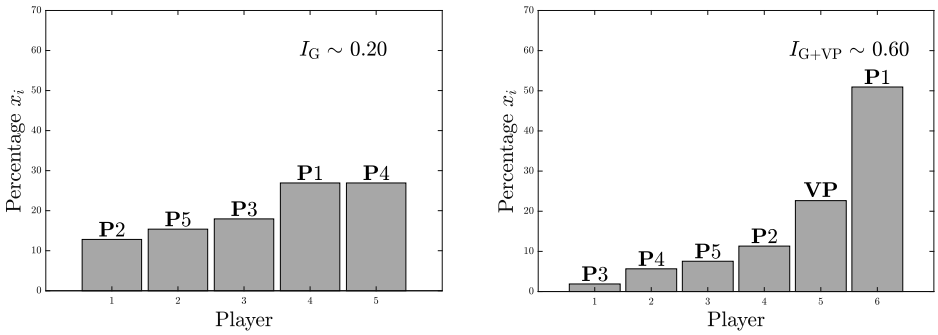

Figure 6.9: **How leadership distributes among the players.** The two panels show the percentage x_i of trials where player i acted as a leader, for all $i = 1, \ldots, 5$ in panel (a) and for all $i = 1, \ldots, 6$ in panel (b). The agents are sorted so that x_i is non-decreasing. Panel (a) and (b) refer to group interaction without and with virtual agent, respectively. The value of the Gini index when any player was pinned ($I_G \sim 0.20$, given in the top-right corner of the panel) clearly suggests that there is no particular group member always assuming a leadership role but that in different trials different players took such role, implementing a distributed version of leadership structure. Whereas when player 5 is pinned by the virtual agent, the Gini index ($I_{G+VP} \sim 0.60$) shows that it is able to steer the group towards a more centralized leadership structure where player 1 gains the role as leaders.

6.5 Summary

In this chapter, we compared the behaviour of an ensemble of human participants asked to synchronize their movement with and without the presence of a VP trying to influence the motion of some of them. Participants were unaware of the existence of a virtual player in the group. Experiments carried out using the hardware/software platform Chronos showed that the addition of a VP to the group changes the collective dynamics significantly. Our preliminary results also show that the leadership patterns emerging from the interaction are affected by the presence of the VP. The investigation of these and other observations reported in this chapter are left for future work.

7 Conclusion

Human coordination is a complex yet fascinating phenomenon common to a large number of different human activities. In this Thesis, features of coordination and emergence of leadership have been analysed by means of a combination of analytical, experimental, and numerical tools during human interpersonal coordination in the context of the paradigmatic mirror game task.

The work presented addressed the following key research questions:

i) establish how the interaction patterns among people in the group and their individual dynamics affect the coordination level of the ensemble;
ii) propose mathematical models to capture and analyse group coordination as observed experimentally;
iii) analyse formally and quantitatively how leadership in human group motor synchronization emerges through group interactions;
iv) explore whether levels of group cohesiveness and leadership agency distribution can be influenced by introducing some virtual players in the group.

7.1 Summary of the main results

After introducing the Thesis motivation in Chapter 1 and the key challenges discussed therein, a brief literature review of the main results on human coordination was given in Chapter 2. Specifically, works about human group interpersonal coordination and leadership emergence were reviewed, together with an overview of the models and data analysis' tools used in literature, placing emphasis on those shown to be useful to investigate and explore the synchronization processes arising in human group coordination.

The investigation of human group coordination then started with Chapter 3, where we focused on the properties characterising interpersonal coordination among multiple agents. Specifically, we analysed the human ability to move in unison with others as a function of the group spatial configuration, similarity in behaviour among the group members, expertise and amount of visual exchange. In two experiments we demonstrated that inertial homogeneity between participants and their expertise in perceptuo-motor synchronization were prone to facilitate synchronized behaviours, reinforced by specific configurations of the players in space. Importantly, we also demonstrated that cohesiveness can be maintained for a certain amount of time (about 7 seconds) after visual exchanges were

interrupted, and we investigated the origin of this strong persistence of synchronization by introducing a memory effect in three different extensions of networks of Kuramoto oscillators.

Indeed, networks of nonlinear oscillators were shown to be a good mathematical model to capture the experimental observations made in the literature on some representative human group coordination tasks. Additional modelling approaches were presented in Chapter 4. Therein, we investigated why human agents reduce their oscillation frequency while executing a joint motor task. We proposed three different models and we found that a model considering neural delays in information processing is the most able to capture the slowing down found in the experimental results. Our modelling results returned delays' values that are in the range typically evidenced in motor science literature [171, 226].

It is important to point out that both the data analysis and modelling results observed in Chapter 3 and 4 highlight how the "social" interpretation of these phenomena can be potentially misleading in this context. Our findings show how these processes reflect an underlying dynamics of "plastic" biological oscillatory systems coupled to other systems. Indeed, as the experiments which employ the Chronos platform suggest, these phenomena are observed also when people coordinate with dots on a screen, in addition to other research that demonstrated how individuals can reach synchronization when coupled to humans and artificial environment rhythms or stimuli [20, 58].

Next, in Chapter 5, we focused on the problem of studying leadership emergence and its effects in human groups involved in a joint motor task. We found that leadership emergence does indeed foster coordination and is, therefore, a natural phenomenon occurring in human groups even when it is not established a priori. Interestingly, with the combined use of two metrics- phase leadership and net causation indices-, we uncovered three main patterns through which leadership emerges. Crucially, these three scenarios can be immediately related to some analogous ones that have been uncovered in the animal kingdom confirming that leadership emergence is a naturally occurring organizing phenomenon when coordination is the goal of the group. These observations were found to be independent of the presence of physical perceptuo-motor interaction among the players. Indeed, the results were validated and confirmed via a set of experiments, in the absence of social interaction among the participants where the volunteers could only perceive each other's motion through a laptop screen.

Finally, Chapter 6 was devoted to presenting some preliminary investigation of the influence of a virtual player interacting within a human ensemble on the levels of group synchronization and leadership emergence. Virtual players with specific kinematic characteristics, appropriately connected to a subset of the participants in the ensemble, were found to be able to influence both group coordination and leadership emergence. These encouraging results show that artificial agents could used to influence and guide the collective behaviour, enhancing or disrupting coordination. With this respect, artificial agents could be effectively employed to offer complementary therapeutic methods for rehabilitating socially challenged people.

7.2 Possible applications and future work

Artificial agents represent a novel method to investigate human movement coordination and to explore the important principle in social psychology and to test such hypothesis numerically as well as through experiments with human partners. The availability of a mathematical model of human group coordination is of crucial importance to implement avatars interacting with other partners for rehabilitation purposes in the interaction with socially challenged people (e.g., schizophrenia or autism).

A mathematical description of human group coordination, as those explored in Chapters 3 and 4, is fundamental not only to shed light on the mechanisms underlying cooperation and synchronisation among numerous people, but also to predict the performance level achieved as function of interconnection structures or individual intrinsic behaviours for a better development of artificial entities. In this latter scenario, since leaders are those who influence the most the motion of the agents, it is sensible to put them in contact with a virtual player so as to promote a desired behaviour over the human group engaged in a rehabilitation exercise.

As regards possible future work, concerning modelling, possible extensions and improvements of the work presented in this study include the possibility of combining the adaptive and personalized parameters of the individual behaviour, as well as time-varying quantities as function of the real-time coordination level with the other partner, to enable virtual players to match experimental results on human group coordination even closer. However, there exists a plethora of different characteristics influencing collective behaviours that still deserve further investigation and contrasting the proposed modelling strategies in a variety of situations, where perceptual and topological parameters are manipulated, would help to better characterize their respective contribution and their possible complementary nature.

Also, the analytical investigation of leadership emergence in human group coordination presented in Chapter 5 could be applied to different and more complex movements. Ordinary situations, such as team rowing, everyday working meetings, or musical ensemble performance, are far richer than the than simple oscillatory tasks performed here, both on the action side and on the perception side. How multiple and coexisting configurations, within and across our senses, modulate our collaborative behaviours, in those and other situations, remains largely unknown and constitute a promising research line for future studies.

In spite of leadership being studied in this thesis in terms of motion dominance and influence over the others in the particular case of the mirror game, our preliminary experimental results in Chapter 6 can in general provide hints on how to select the members to be controlled by an artificial agent in order to obtain a desired behaviour, as for example during evacuation procedures, or when selecting coxswains in team rowing. An open problem left for further study is to investigate leadership emergence with a virtual agent in more systematic experimental setups to confirm our preliminary results.

Finally, the leadership strategies that we highlighted might be used to plan the motion of one or more artificial agents to enhance the performance of human-robot groups. This could be relevant, for instance, to aid the design of innovative artificial partners for

industrial applications, where a correct trade-off between robots autonomy and human intervention is necessary to maximise production but in a safe manner [247] or for search and rescue in hazard areas, not accessible for human beings [248].

Also, and more importantly, the results presented in this Thesis represent a sound basis to build upon in order to develop new exergames for the rehabilitation of patients with social disorders, such as autism that were described in Section 2.5 of this Thesis.

A From Individual to Group Motor Signature

Signatures play a key role in healthcare. They present a novel, low-cost and non-invasive potential diagnosis tool for different motor diseases, such as schizophrenia [35] and autism [249]. Clinical identification requires expert diagnostic training. Data analysis and machine learning allow a quicker biometric identification that distinguishes an individual from most other members of an ensemble. If each person had a unique movement signature it would be possible to identify this person on a subsequent testing session by his or her location in a multidimensional space.

Signatures are important especially in motor science [250] and for this reason they have been explored in the context of improvisation [251] and coordination [252]. However, very little attention has been addressed to the use of signatures to characterize group performance and interactions. Indeed, the spatiotemporal organization of bodily movements (i.e., interpersonal or social motor coordination) can reflect feelings such as connectedness, social rapport or cohesion. In [79], authors proposed an index, namely an individual motor signature (**IMS**), able to capture the subtle differences in the way each of us moves and useful to study sociomotor coordination. IMS captures the main kinematic features of the motion of a person that significantly differs from those of other individuals. This allowed to quantify the dynamic similarity and demonstrated that it facilitates coordination during interaction. In particular, they showed how coordination in a dyadic joint-action task is higher if the motions of the players share similar dynamic features.

In this appendix, we present preliminary results on the definition of a **Group Motor Signature**, useful to describe and study group synchronization dynamics.

A.1 Motor Signatures

The Individual Motor Signature, as defined in [79], is represented by the probability density function of the individual velocity profile and it has been shown that it satisfies two main features:

- time-persistence;
- capability to differentiate among individuals.

Therefore, IMS allows to identify each different participant and is useful to measure the dynamic similarity between players and to study its effects on joint synchronization.

In Chapter 2, we highlighted how the majority of studies on human group coordination focused mainly on dyadic interactions. This preliminary investigation is devoted to the definition of a Group Motor Signature (GMS), able to identify and discriminate different human groups, useful to study the degree of synchronization among the agents and to understand how player plasticity can facilitate a good group performance.

In this Appendix, we aim at investigating:

- if it is possible to define a GMS able to **discriminate and classify groups**;
- whether it is **task-invariant**;
- and if it is **topology-invariant**.

A.2 Experimental setups

The results presented in this appendix are based on the analysis of data collected in three distinct experimental scenarios, each with a different group of participants.

Respectively, in scenario 1, participants interacted through the hardware/software Chronos platform (see Section 4.1). In scenario 2, we collected data in a different context where volunteers were asked to track each other finger's movements. At the end, in scenario 3, human participants were asked to synchronize the movement of pendula.

In the following sections, we detail data collection and experimental setups in each scenario.

Scenario 1- Virtual interaction

For this scenario, we considered the data described in Chapter 6. Specifically, we considered only the first and the second experimental sessions that include the trials dedicated to the kinematic characterization of the players and to the group interaction.

Scenario 2- Social interaction

Seven volunteers took part in the experiment- 4 males and 3 females, 2 out of the 7 participants were left handed. Participants were required to sit in a circle and move their preferred hand back and forth (i.e., away from and towards their bodies, along a straight direction) to produce oscillations, as smoothly as possible, and to synchronize their movement with the others. The motion was required to be performed on a parallel direction to the floor. Four different interaction patterns were implemented among subjects- the Complete graph, the Path graph, the Ring graph and the Star graph.

The group performed the experiments in two different sessions:

1. Eyes-closed condition. Participants were required to oscillate their preferred hand at their own natural rhythm for 30s, trying to maintain a constant oscillation frequency while keeping their eyes closed. 16 trials were performed.
2. Eyes-open condition. Participants were asked to intentionally synchronize the motion of each other's preferred hands during 30s trials, while keeping their eyes open. For each topology, 10 trials were performed.

In order to detect the movements of the participants, circular markers were attached on top of the index finger of their preferred hands, respectively. Eight infrared cameras (Nexus MX13 Vicon System, 350Hz) were appropriately located around the experimental room to record the positions of the markers.

Data were interpolated with a sampling frequency of 100Hz.

Scenario 3: social interaction with pendula

A total of 7 volunteers took part in this experiment: 5 males and 2 females, all right-handed.

Participants were asked to sit comfortably on a chair and to create motion by moving a pendulum (see Fig. 3.1). The group performed 5 trials for each topology (Complete, Path, Ring and Star graphs). During group interaction, each participant was required to perform five trials, lasting 45s, each divided in the following way:

1. 15 s in Eyes-closed condition;
2. 30 s in Eyes-open condition.

The motion was captured by rotary potentiometer sensors connected to a laptop, with sampling frequency equal to 200Hz.

Table A.1: **Details of the three experimental setups.**

Experiment	**Setup**	**Social dimension**	**Interaction**	**Number of players**	**Number of trials**
Scenario 1	Chronos	No	Voluntary synchronization	5	7
Scenario 2	Arm	Yes	Voluntary synchronization	7	10
Scenario 3	Pendulum	Yes	Spontaneous synchronization	7	5

A.2.1 Data processing

The collected data were analysed by means of the software Matlab.

The position timeseries were filtered by means of a Moving Average Filter and used to numerically estimate the corresponding velocity signals with a fourth-order finite difference scheme.

IMS is estimated from the probability density function (pdf) of the player's velocity. Therefore, we defined the probability density function (pdf) of the group's velocity (**GMS**), as the normalized histogram with 101 equally distant bins between the detected extreme values, built on the collection of the velocity timeseries of all the players. It can be easily shown that it is equivalent to the average of the normalized histograms of the velocity timeseries of each player.

A.2.2 Results

From the global inspection of the distributions obtained in different experimental contexts and topologies (see Figures A.1, A.2, and A.3), we derived the observations described in the next sections.

All the estimated group motor signatures are quasi-symmetric, given the oscillatory nature of the task. In particular, the probability distributions completely change across the groups. This aspect could support the GMS power to discriminate interacting groups from their collective dynamics.

Looking at the mean group pdf in Figure A.1 computed during the virtual interaction, it is possible to notice the presence of 3 peaks, whereas the average of the IMS of each individual playing in solo condition has two peaks. The synchronization instruction during the experiment invite people to stop and wait for the others or, at least, stop and think about what to do. This could explain the emergence of a central peak- corresponding to null velocity- during group interaction.

When human players are asked to coordinate involving their bodies, the central peak in the mean GMS is mitigated (Figure A.2). This could be due to the higher inertia involved (arm instead of forearm) and this element does not allow players to stop a lot and wait for the others to synchronize. In addition, differently from the virtual scenario, the players are visually coupled and, therefore, social information could disturb the synchronization process.

Then, if participants are asked to create motion using a pendula (see Figure A.3), the central peak in the mean GMS disappears and this can be explained, again, by the higher inertia involved in the movement (pendula instead of arm). This does not allow players to stop and wait for the others to synchronize.

At the end, the visual inspection of the GMS estimated in each group shows that the signature does not change across the topologies.

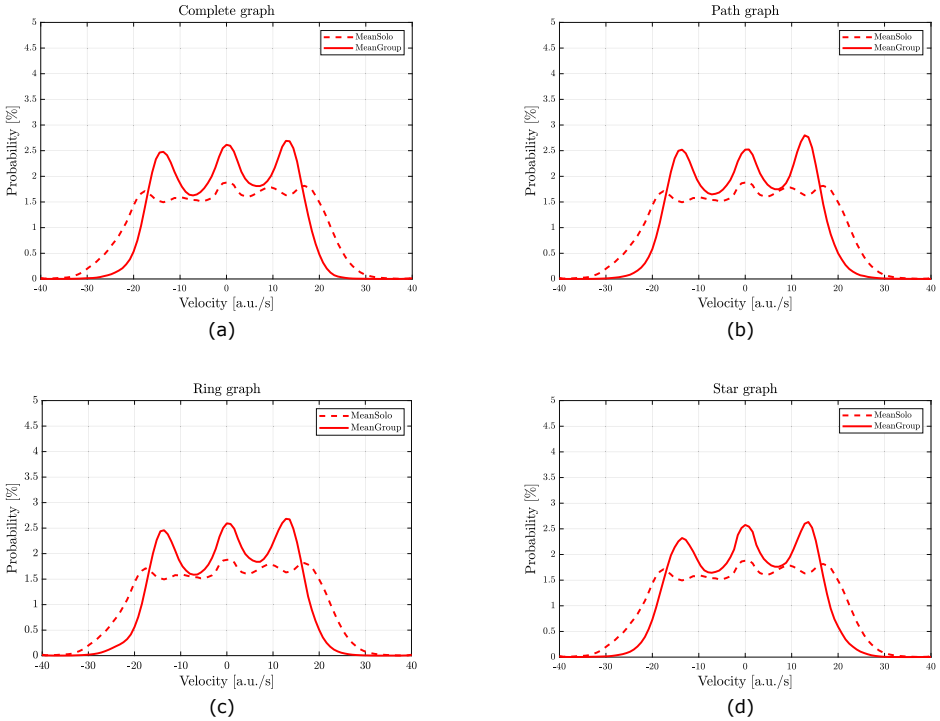

Figure A.1: **Main results of Scenario 1.** In each panel, we represented the average of the individual motor signatures computed in the solo session, and the GMS estimated in (a) the Complete graph; (b) the Path graph; (c) the Ring graph, and in (d) the Star graph. It is worth noting how three peaks in the GMS emerge during the group interaction.

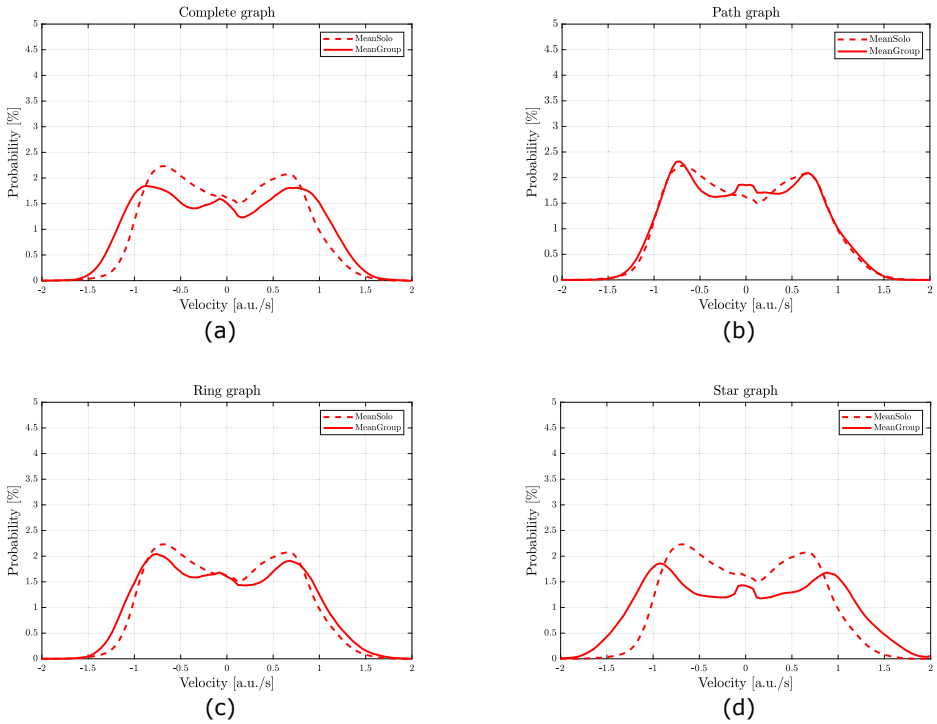

Figure A.2: **Main results of Scenario 2.** In each panel, we represented the average of the individual motor signatures computed in the solo session, and the GMS estimated in (a) the Complete graph; (b) the Path graph; (c) the Ring graph, and in (d) the Star graph. It is worth noting how the central peak appearing in the previous GMS is less prominent in the second context.

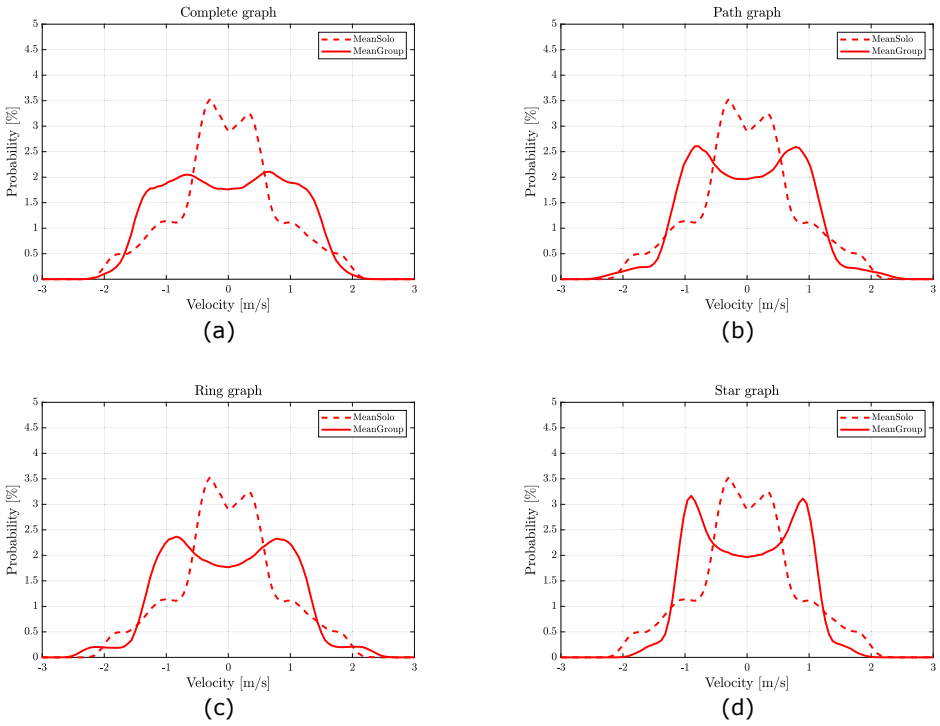

Figure A.3: **Main results of Scenario 3.** In each panel, we represented the average of the individual motor signatures computed in the solo session, and the GMS estimated in (a) the Complete graph; (b) the Path graph; (c) the Ring graph, and in (d) the Star graph. It is interesting to point out that the GMS is completely different from the average of the individual motor signatures. In addition, the central peak in the pdf disapperared with respect to the previous GMS.

A.3 Summary

In this appendix, we briefly showed few interesting observations about the possibility of defining a Group Motor Signature (**GMS**). In our preliminary exploration, we observed that GMS seems to be task-variant. We considered all oscillating behaviours but each of them involved different inertias in the movement that, somehow, reflected in the probability distributions. In addition, GMS seems not changing as function of the configuration implemented among the players during the interaction.

Obviously, we recognize that there are too many factors that can have influenced the three experimental setups to understand the potentiality of GMS for the description of collective behaviour. However, these observations can open future interesting research lines. It could be useful to test if the GMS is able to discriminate among different groups playing the same task or if the GMS associated to a single group changes when the participants are asked to play different tasks to test the task-specifity of the signature. It could be also relevant to test an important aspect that is the time-invariance of the Group Motor Signature, by considering additional experimental sessions over time. In addition, it could be interesting to define or use metrics on the pdf, such as the Earth's movers distance, and check if any correlation with the group synchronization indices exists or if the relation between Individual and Group Motor Signatures could represent a predicting factor of the individual influence on the collective dynamics and, then, represent an additional leadership analysis tool.

B A network model of Italy shows that intermittent regional strategies can alleviate the COVID-19 epidemic

In this appendix, we briefly address a completely distinct topic that, in many ways, is linked to human social interaction but in a fully different and sad way. It could not be ignored, given its worldwide significance.

The beginning of the new decade made history with a challenging event, unbelievable and hard to imagine. A pandemic has upset our lives and we had to learn to face the distance with our dears and to deal with the unavoidable stall of research activities. Epidemics are not unknown in human history but research has shown that they will occur with increasing frequency because of the strongly interconnected reality we live in. In fact, among the factors facilitating virus diffusion, scientists highlight different hygienic and climatic conditions, increasing population density and mobility among people. For this reason, in this context complex science represents the most suitable clue to understand epidemic dynamics. And in this scenario, I decided to give my contribution to a great modelling and controlling effort faced by the Complex Network research unit at the University of Naples Federico II, led by professor Mario di Bernardo.

Network modelling is fundamental to simulate virus spread dynamics and to support the decision-makers of different yet interconnected regions in a country. Italy was among the first countries to be particularly hit by the COVID-19 outbreak and, as many other governments around the world, strict national lockdown rules were adopted to immediately overcome this emergence and to mitigate the epidemic, ignoring the federal structure of the Italian constitution. Each of Italy's twenty administrative regions is independent on Health and oversees its own share of the Italian National Health service. The regional presidents and their councils can independently take their own actions, strengthening or, at times, weakening national containment rules. This heterogeneity between regions plays a key-role to understand the spread of the epidemic and to design effective strategies to control the disease. Previous studies have modelled the spread of the epidemics and its

evolution in the country at the national level by means of aggregate models- originated from the classical SIR model-, and some have looked at the effects of different types of containment and mitigation strategies but limited works have taken into account the spatial dynamics of the epidemic.

In our study [253], we investigated Italy's dynamics, by modelling it as a network whose nodes represent the twenty Italian regions, each parametrized with different values on real data, and the links model both proximity flows and long-distance transportation routes (ferries, trains, and planes). The goal was to analyse the effectiveness of measures taken by the Italian government at both the national and the regional level and to uncover the effects on the epidemic spread of regional heterogeneity and interregional flows of people. For this purpose, I dedicated to the reconstruction and inference of links, given the unavailability of public transports data. Specifically, we considered two types of inter-regional fluxes associated to:

1. daily commuters travelling between neighboring regions;
2. long distance travels covered by high-speed trains, planes, and large ferries.

To estimate commuters' fluxes, we used the latest official country-wide assessment of Italian mobility conducted by the Italian Institute of Statistic (ISTAT) in 2011 whereas for longer distance routes covered by high-speed trains, planes, and large ferries we exploited information found on different web sources. Specifically,

1. for railway connections, we exploited the knowledge of the total number of daily high-speed customers of the main Italian carrier, Trenitalia; the total number of high-speed trains per day; the number of high-speed trains and the total resident population in region;
2. for flight connections, we retrieved the info about all the operating Italian airports and for each pair of connected airports, we looked for the number of weekly direct flights in normal operating conditions (i.e., without any restriction due to the emergency) and for the average capacity of the regional fleet of the main carrier serving the route;
3. for ferry connections, we considered the five regions that act as hubs for long range national maritime travel, that is, the two main insular regions, Sardinia and Sicily, together with three mainland regions, Campania, Lazio, and Liguria. We looked for the average number of maritime passengers and for the total number of maritime connections between regions.

Hence, our model took into account commuters fluxes from one region to the other- the infected of a region contribute to increasing the likelihood of generating new infected in the region they move to (see the manuscript [253] and Supplementary Information for additional details on the model and the link inference process).

At this stage, we used control theoretic tools to propose and assess differentiated, yet coordinated, regional interventions to alleviate the epidemic impact, to reopen the country, and to prevent future national lockdowns while avoiding saturation of the regional health systems and mitigating impact on economic costs.

Our results confirmed that the model showed the right level of granularity and complexity to capture the crucial elements needed to correctly predict and reproduce the available data. In particular, we showed that inter-regional fluxes must be carefully controlled as they can have dramatic effects on recurrent epidemic waves. In addition, we convincingly showed that regional feedback interventions, where each of the twenty regions strengthens or weakens local social distancing or inflow/outflow control as a function of the saturation of their hospital capacity can be beneficial in alleviating possible outbreaks and in avoiding recurrent epidemic waves while reducing the costs of a nationwide lockdown. These kinds of interventions have been actually implemented during the second wave occurrence in autumn 2020 by the Italian government.

Bibliography

[1] David Rock and Jeffrey Schwartz. The neuroscience of leadership. *Reclaiming children and youth*, 16(3):10, 2007.

[2] David A Waldman, Pierre A Balthazard, and Suzanne J Peterson. Social cognitive neuroscience and leadership. *The Leadership Quarterly*, 22(6):1092–1106, 2011.

[3] Mark Van Vugt. Evolutionary origins of leadership and followership. *Personality and Social Psychology Review*, 10(4):354–371, 2006.

[4] Herbert S Lewis. *Leaders and followers: Some anthropological perspectives*. Number 50. Addison-Wesley Reading, MA:, 1974.

[5] Chen Wang, Xiaojie Chen, Guangming Xie, and Ming Cao. Emergence of leadership in a robotic fish group under diverging individual personality traits. *Royal Society open science*, 4(5):161015, 2017.

[6] Stefano Carpin and Lynne E Parker. Cooperative leader following in a distributed multi-robot system. In *Proceedings 2002 IEEE International Conference on Robotics and Automation (Cat. No. 02CH37292)*, volume 3, pages 2994–3001. IEEE, 2002.

[7] Nicola Basilico, Nicola Gatti, and Francesco Amigoni. Leader-follower strategies for robotic patrolling in environments with arbitrary topologies. In *Proceedings of The 8th International Conference on Autonomous Agents and Multiagent Systems-Volume 1*, pages 57–64. International Foundation for Autonomous Agents and Multiagent Systems, 2009.

[8] Benjamin E Hermalin. Toward an economic theory of leadership: Leading by example. *American Economic Review*, pages 1188–1206, 1998.

[9] Stephen J Guastello. Evolutionary game theory and leadership. *American Psychologist*, 64(1):53–54, 2009.

[10] MohammadReza EffatParvar, Nasser Yazdani, Mehdi EffatParvar, Aresh Dadlani, and Ahmad Khonsari. Improved algorithms for leader election in distributed systems. In *2010 2nd International Conference on Computer Engineering and Technology*, volume 2, pages V2–6, 2010.

[11] Aihua Hu, Jinde Cao, and Manfeng Hu. Consensus of leader-following multi-agent systems in time-varying networks via intermittent control. *International Journal of Control, Automation and Systems*, 12(5):969–976, 2014.

[12] Matthew J Silk, Kelly R Finn, Mason A Porter, and Noa Pinter-Wollman. Can multilayer networks advance animal behavior research? *Trends in ecology & evolution*, 33(6):376–378, 2018.

[13] John E Mathieu, Herman Aguinis, Steven A Culpepper, and Gilad Chen. Understanding and estimating the power to detect cross-level interaction effects in multilevel modeling. *Journal of Applied Psychology*, 97(5):951, 2012.

[14] Samantha Finkelstein, Tiffany Barnes, Zachary Wartell, and Evan A Suma. Evaluation of the exertion and motivation factors of a virtual reality exercise game for children with autism. In *2013 1st Workshop on Virtual and Augmented Assistive Technology (VAAT)*, pages 11–16, 2013.

[15] Maarit Virta, Anita Vedenpää, Nina Grönroos, Esa Chydenius, Markku Partinen, Risto Vataja, Markus Kaski, and Matti Iivanainen. Adults with adhd benefit from cognitive—behaviorally oriented group rehabilitation: A study of 29 participants. *Journal of Attention Disorders*, 12(3):218–226, 2008.

[16] Tamara Ownsworth and Ken McFarland. Investigation of psychological and neuropsychological factors associated with clinical outcome following a group rehabilitation programme. *Neuropsychological Rehabilitation*, 14(5):535–562, 2004.

[17] Maurice Lamb, Rachel W Kallen, Steven J Harrison, Mario Di Bernardo, Ali Minai, and Michael J Richardson. To pass or not to pass: Modeling the movement and affordance dynamics of a pick and place task. *Frontiers in psychology*, 8:1061, 2017.

[18] Michael J Richardson, Rachel W Kallen, Patrick Nalepka, Steven J Harrison, Maurice Lamb, Anthony Chemero, Elliot Saltzman, and Richard C Schmidt. Modeling embedded interpersonal and multiagent coordination. In *COMPLEXIS*, pages 155–164, 2016.

[19] Joanne Lumsden, Lynden K Miles, Michael J Richardson, Carlene A Smith, and C Neil Macrae. Who syncs? social motives and interpersonal coordination. *Journal of Experimental Social Psychology*, 48(3):746–751, 2012.

[20] Bruno H Repp and Peter E Keller. Sensorimotor synchronization with adaptively timed sequences. *Human movement science*, 27(3):423–456, 2008.

[21] Kevin W Rio, Gregory C Dachner, and William H Warren. Local interactions underlying collective motion in human crowds. *Proceedings of the Royal Society B: Biological Sciences*, 285(1878):20180611, 2018.

[22] Zoltán Néda, Erzsébet Ravasz, Tamás Vicsek, Yves Brechet, and Albert-Lázló Barabási. Physics of the rhythmic applause. *Physical Review E*, 61(6):6987, 2000.

[23] Ralph Adolphs. Cognitive neuroscience of human social behaviour. *Nature Reviews Neuroscience*, 4(3):165–178, 2003.

[24] Sarah-Jayne Blakemore and Jean Decety. From the perception of action to the understanding of intention. *Nature reviews neuroscience*, 2(8):561–567, 2001.

[25] Francesco Alderisio, Gianfranco Fiore, Robin N Salesse, Benoît G Bardy, and Mario di Bernardo. Interaction patterns and individual dynamics shape the way we move in synchrony. *Scientific reports*, 7(1):1–10, 2017.

[26] Francesco Alderisio, Maria Lombardi, and Mario di Bernardo. Emergence of leadership in complex networks and human groups. In *2018 IEEE International Symposium on Circuits and Systems*, pages 1–5, 2018.

[27] Merle T Fairhurst, Petr Janata, and Peter E Keller. Leading the follower: an fmri investigation of dynamic cooperativity and leader–follower strategies in synchronization with an adaptive virtual partner. *Neuroimage*, 84:688–697, 2014.

[28] RC Schmidt, Nicole Christianson, Claudia Carello, and Reuben Baron. Effects of social and physical variables on between-person visual coordination. *Ecological Psychology*, 6(3):159–183, 1994.

[29] Polemnia G Amazeen, RC Schmidt, and Michael T Turvey. Frequency detuning of the phase entrainment dynamics of visually coupled rhythmic movements. *Biological Cybernetics*, 72(6):511–518, 1995.

[30] Lynden K Miles, Jordan L Griffiths, Michael J Richardson, and C Neil Macrae. Too late to coordinate: Contextual influences on behavioral synchrony. *European Journal of Social Psychology*, 40(1):52–60, 2010.

[31] Michael J Richardson, Kerry L Marsh, Robert W Isenhower, Justin RL Goodman, and Richard C Schmidt. Rocking together: Dynamics of intentional and unintentional interpersonal coordination. *Human Movement Science*, 26(6):867–891, 2007.

[32] John RG Dyer, Anders Johansson, Dirk Helbing, Iain D Couzin, and Jens Krause. Leadership, consensus decision making and collective behaviour in humans. *Philosophical Transactions of the Royal Society B: Biological Sciences*, 364(1518):781–789, 2008.

[33] Lior Noy, Erez Dekel, and Uri Alon. The mirror game as a paradigm for studying the dynamics of two people improvising motion together. *Proceedings of the National Academy of Sciences*, 108(52):20947–20952, 2011.

[34] Francesco Alderisio, Maria Lombardi, Gianfranco Fiore, and Mario di Bernardo. A novel computer-based set-up to study movement coordination in human ensembles. *Frontiers in psychology*, 8:967, 2017.

[35] Piotr Słowiński, Francesco Alderisio, Chao Zhai, Yuan Shen, Peter Tino, Catherine Bortolon, Delphine Capdevielle, Laura Cohen, Mahdi Khoramshahi, Aude Billard, et al. Unravelling socio-motor biomarkers in schizophrenia. *npj Schizophrenia*, 3(1):1–10, 2017.

[36] Lorenzo Desideri, Marco Negrini, Massimiliano Malavasi, Daniela Tanzini, Aziz Rouame, Maria Cristina Cutrone, Paola Bonifacci, and Evert-Jan Hoogerwerf. Using a humanoid robot as a complement to interventions for children with autism spectrum disorder: A pilot study. *Advances in Neurodevelopmental Disorders*, 2(3):273–285, 2018.

[37] Benoît G Bardy, Carmela Calabrese, Pietro De Lellis, Stella Bourgeaud, Clémentine Colomer, Simon Pla, and Mario di Bernardo. Moving in unison after perceptual interruption. *Scientific reports*, 10(1):1–13, 2020.

[38] Yoshiki Kuramoto. *Chemical oscillations, waves, and turbulence*. Courier Corporation, 2003.

[39] Iain D Couzin, Jens Krause, Nigel R Franks, and Simon A Levin. Effective leadership and decision-making in animal groups on the move. *Nature*, 433(7025):513, 2005.

[40] Pietro De Lellis, Giovanni Polverino, Gozde Ustuner, Nicole Abaid, Simone Macrì, Erik M Bollt, and Maurizio Porfiri. Collective behaviour across animal species. *Scientific reports*, 4:3723, 2014.

[41] John T Emlen. Flocking behavior in birds. *The Auk*, 69(2):160–170, 1952.

[42] Jennifer L Harcourt, Tzo Zen Ang, Gemma Sweetman, Rufus A Johnstone, and Andrea Manica. Social feedback and the emergence of leaders and followers. *Current Biology*, 19(3):248–252, 2009.

[43] Eric Bonabeau, Guy Theraulaz, Jean-Louls Deneubourg, Serge Aron, and Scott Camazine. Self-organization in social insects. *Trends in ecology & evolution*, 12(5):188–193, 1997.

[44] Carel P Van Schaik. Why are diurnal primates living in groups? *Behaviour*, 87(1-2):120–144, 1983.

[45] Brian L Partridge. The structure and function of fish schools. *Scientific American*, 246(6):114–123, 1982.

[46] M Lindauer. Communication in swarm-bees searching for a new home. *Nature*, 179(4550):63–66, 1957.

[47] Alison Jolly. The evolution of primate behavior: a survey of the primate order traces the progressive development of intelligence as a way of life. *American Scientist*, 73(3):230–239, 1985.

[48] Dora Biro, David JT Sumpter, Jessica Meade, and Tim Guilford. From compromise to leadership in pigeon homing. *Current biology*, 16(21):2123–2128, 2006.

[49] Richard D Alexander. The evolution of social behavior. *Annual review of ecology and systematics*, 5(1):325–383, 1974.

[50] Eörs Szathmáry and John Maynard Smith. The major evolutionary transitions. *Nature*, 374(6519):227–232, 1995.

[51] Michael Tomasello, Alicia P Melis, Claudio Tennie, Emily Wyman, Esther Herrmann, Ian C Gilby, Kristen Hawkes, Kim Sterelny, Emily Wyman, Michael Tomasello, et al. Two key steps in the evolution of human cooperation: The interdependence hypothesis. *Current Anthropology*, 53(6):000–000, 2012.

[52] Kevin W Rio and William H Warren. 1 interpersonal coordination in biological systems. *Interpersonal Coordination and Performance in Social Systems*, pages 3–16, 2016.

[53] David JT Sumpter. The principles of collective animal behaviour. *Philosophical transactions of the royal society B: Biological Sciences*, 361(1465):5–22, 2006.

[54] Andrew J King and Guy Cowlishaw. Leaders, followers, and group decision-making. *Communicative & integrative biology*, 2(2):147–150, 2009.

[55] Shinnosuke Nakayama, Jennifer L Harcourt, Rufus A Johnstone, and Andrea Manica. Who directs group movement? leader effort versus follower preference in stickleback fish of different personality. *Biology letters*, 12(5):20160207, 2016.

[56] N Orange and N Abaid. A transfer entropy analysis of leader-follower interactions in flying bats. *The European Physical Journal Special Topics*, 224(17-18):3279–3293, 2015.

[57] Warren M Lord, Jie Sun, Nicholas T Ouellette, and Erik M Bollt. Inference of causal information flow in collective animal behavior. *IEEE Transactions on Molecular, Biological and Multi-Scale Communications*, 2(1):107–116, 2016.

[58] Mengsen Zhang, JA Scott Kelso, and Emmanuelle Tognoli. Critical diversity: Divided or united states of social coordination. *PLoS One*, 13(4):e0193843, 2018.

[59] Alan M Wing, Satoshi Endo, Adrian Bradbury, and Dirk Vorberg. Optimal feedback correction in string quartet synchronization. *Journal of The Royal Society Interface*, 11(93):20131125, 2014.

[60] John RG Dyer, Christos C Ioannou, Lesley J Morrell, Darren P Croft, Iain D Couzin, Dean A Waters, and Jens Krause. Consensus decision making in human crowds. *Animal Behaviour*, 75(2):461–470, 2008.

[61] Mark Van Vugt, Robert Hogan, and Robert B Kaiser. Leadership, followership, and evolution: Some lessons from the past. *American Psychologist*, 63(3):182, 2008.

[62] Randall Calvert. Leadership and its basis in problems of social coordination. *International Political Science Review*, 13(1):7–24, 1992.

[63] Nathalie Stroeymeyt, Nigel R Franks, and Martin Giurfa. Knowledgeable individuals lead collective decisions in ants. *Journal of Experimental Biology*, 214(18):3046–3054, 2011.

[64] Shinnosuke Nakayama, Jennifer L Harcourt, Rufus A Johnstone, and Andrea Manica. Initiative, personality and leadership in pairs of foraging fish. *PLoS One*, 7(5):e36606, 2012.

[65] Guy Beauchamp. Individual differences in activity and exploration influence leadership in pairs of foraging zebra finches. *Behaviour*, 137(3):301–314, 2000.

[66] Pablo Michelena, Raphaël Jeanson, Jean-Louis Deneubourg, and Angela M Sibbald. Personality and collective decision-making in foraging herbivores. *Proceedings of the Royal Society B: Biological Sciences*, 277(1684):1093–1099, 2010.

[67] Jennifer E Smith, Sergey Gavrilets, Monique Borgerhoff Mulder, Paul L Hooper, Claire El Mouden, Daniel Nettle, Christoph Hauert, Kim Hill, Susan Perry, Anne E Pusey, et al. Leadership in mammalian societies: Emergence, distribution, power, and payoff. *Trends in ecology & evolution*, 31(1):54–66, 2016.

[68] Peter Behrendt, Sandra Matz, and Anja S Göritz. An integrative model of leadership behavior. *The leadership quarterly*, 28(1):229–244, 2017.

[69] Robert Hogan and Robert B Kaiser. What we know about leadership. *Review of general psychology*, 9(2):169–180, 2005.

[70] Bruce E Winston and Kathleen Patterson. An integrative definition of leadership. *International journal of leadership studies*, 1(2):6–66, 2006.

[71] Victor F Trastek, Neil W Hamilton, and Emily E Niles. Leadership models in health care—a case for servant leadership. In *Mayo Clinic Proceedings*, volume 89, pages 374–381. Elsevier, 2014.

[72] Joris Gillet, Edward Cartwright, and Mark Van Vugt. Selfish or servant leadership? evolutionary predictions on leadership personalities in coordination games. *Personality and Individual Differences*, 51(3):231–236, 2011.

[73] Jeemin Kim, Dimitri Gardant, Grégoire Bosselut, and Mark Eys. Athlete personality characteristics and informal role occupancy in interdependent sport teams. *Psychology of Sport and Exercise*, 39:193–203, 2018.

[74] D Scott DeRue. Adaptive leadership theory: Leading and following as a complex adaptive process. *Research in organizational behavior*, 31:125–150, 2011.

[75] Shinnosuke Nakayama, Manuel Ruiz Marín, Maximo Camacho, and Maurizio Porfiri. Plasticity in leader–follower roles in human teams. *Scientific reports*, 7(1):14562, 2017.

[76] Darja Miscenko, Hannes Guenter, and David V Day. Am i a leader? examining leader identity development over time. *The Leadership Quarterly*, 28(5):605–620, 2017.

[77] Navio Kwok, Samuel Hanig, Douglas J Brown, and Winny Shen. How leader role identity influences the process of leader emergence: A social network analysis. *The leadership quarterly*, 29(6):648–662, 2018.

[78] James K Hazy. Toward a theory of leadership in complex systems: Computational modeling explorations. *Nonlinear Dynamics, Psychology, and Life Sciences*, 12(3):281, 2008.

[79] Piotr Slowinski, Chao Zhai, Francesco Alderisio, Robin Salesse, Mathieu Gueugnon, Ludovic Marin, Benoît G Bardy, Mario Di Bernardo, and Krasimira Tsaneva-Atanasova. Dynamic similarity promotes interpersonal coordination in joint action. *Journal of The Royal Society Interface*, 13(116):20151093, 2016.

[80] Renee Timmers, Satoshi Endo, Adrian Bradbury, and Alan M Wing. Synchronization and leadership in string quartet performance: a case study of auditory and visual cues. *Frontiers in Psychology*, 5:645, 2014.

[81] Andrew Chang, Steven R Livingstone, Dan J Bosnyak, and Laurel J Trainor. Body sway reflects leadership in joint music performance. *Proceedings of the National Academy of Sciences*, 114(21):E4134–E4141, 2017.

[82] Thomas Ducourant, Stéphane Vieilledent, Yves Kerlirzin, and Alain Berthoz. Timing and distance characteristics of interpersonal coordination during locomotion. *Neuroscience letters*, 389(1):6–11, 2005.

[83] Margarete Boos, Johannes Pritz, Simon Lange, and Michael Belz. Leadership in moving human groups. *PLoS computational biology*, 10(4):e1003541, 2014.

[84] Jolyon J Faria, John RG Dyer, Colin R Tosh, and Jens Krause. Leadership and social information use in human crowds. *Animal Behaviour*, 79(4):895–901, 2010.

[85] François Aubé and Robert Shield. Modeling the effect of leadership on crowd flow dynamics. In *International Conference on Cellular Automata*, pages 601–611. Springer, 2004.

[86] Wei Wang and J-JE Slotine. A theoretical study of different leader roles in networks. *IEEE Transactions on Automatic Control*, 51(7):1156–1161, 2006.

[87] Joshua Garland, Andrew M Berdahl, Jie Sun, and Erik M Bollt. Anatomy of leadership in collective behaviour. *Chaos: An Interdisciplinary Journal of Nonlinear Science*, 28(7):075308, 2018.

[88] Andra Serban, Francis J Yammarino, Shelley D Dionne, Surinder S Kahai, Chanyu Hao, Kristie A McHugh, Kristin Lee Sotak, Alexander BR Mushore, Tamara L Friedrich, and David R Peterson. Leadership emergence in face-to-face and virtual

teams: A multi-level model with agent-based simulations, quasi-experimental and experimental tests. *The Leadership Quarterly*, 26(3):402–418, 2015.

[89] Hermann Haken, JA Scott Kelso, and Heinz Bunz. A theoretical model of phase transitions in human hand movements. *Biological Cybernetics*, 51(5):347–356, 1985.

[90] Daniele Avitabile, Piotr Słowiński, Benoit Bardy, and Krasimira Tsaneva-Atanasova. Beyond in-phase and anti-phase coordination in a model of joint action. *Biological Cybernetics*, 110(2-3):201–216, 2016.

[91] Michael J Richardson, Steven J Harrison, Rachel W Kallen, Ashley Walton, Brian A Eiler, Elliot Saltzman, and RC Schmidt. Self-organized complementary joint action: Behavioral dynamics of an interpersonal collision-avoidance task. *Journal of Experimental Psychology: Human Perception and Performance*, 41(3):665, 2015.

[92] JA Scott Kelso, Gonzalo C de Guzman, Colin Reveley, and Emmanuelle Tognoli. Virtual partner interaction (vpi): exploring novel behaviors via coordination dynamics. *PloS One*, 4(6):e5749, 2009.

[93] Francesco Alderisio, Benoît G Bardy, and Mario Di Bernardo. Entrainment and synchronization in networks of rayleigh–van der pol oscillators with diffusive and haken–kelso–bunz couplings. *Biological Cybernetics*, 110(2-3):151–169, 2016.

[94] Shir Shahal, Ateret Wurzberg, Inbar Sibony, Hamootal Duadi, Elad Shniderman, Daniel Weymouth, Nir Davidson, and Moti Fridman. Synchronization of complex human networks. *Nature communications*, 11(1):1–10, 2020.

[95] D Xenides, DS Vlachos, and TE Simos. Synchronization in complex systems following a decision based queuing process: rhythmic applause as a test case. *Journal of Statistical Mechanics: Theory and Experiment*, 2008(07):P07017, 2008.

[96] Jenny Allen, Mason Weinrich, Will Hoppitt, and Luke Rendell. Network-based diffusion analysis reveals cultural transmission of lobtail feeding in humpback whales. *Science*, 340(6131):485–488, 2013.

[97] Lauren A White, James D Forester, and Meggan E Craft. Using contact networks to explore mechanisms of parasite transmission in wildlife. *Biological Reviews*, 92(1):389–409, 2017.

[98] Kelly R Finn, Matthew J Silk, Mason A Porter, and Noa Pinter-Wollman. The use of multilayer network analysis in animal behaviour. *Animal behaviour*, 149:7–22, 2019.

[99] Johann Mourier, Elodie JI Ledee, and David MP Jacoby. A multilayer perspective for inferring spatial and social functioning in animal movement networks. *bioRxiv*, page 749085, 2019.

[100] Sandra E Smith-Aguilar, Filippo Aureli, Laura Busia, Colleen Schaffner, and Gabriel Ramos-Fernández. Using multiplex networks to capture the multidimensional nature of social structure. *Primates*, 60(3):277–295, 2019.

[101] Anirudh Vemula, Katharina Muelling, and Jean Oh. Social attention: Modeling attention in human crowds. In *2018 IEEE international Conference on Robotics and Automation*, pages 1–7, 2018.

[102] JA Scott Kelso, Guillaume Dumas, and Emmanuelle Tognoli. Outline of a general theory of behavior and brain coordination. *Neural Networks*, 37:120–131, 2013.

[103] James J Wright and David TJ Liley. Simulation of electrocortical waves. *Biological Cybernetics*, 72(4):347–356, 1995.

[104] Shun-ichi Amari. Dynamics of pattern formation in lateral-inhibition type neural fields. *Biological Cybernetics*, 27(2):77–87, 1977.

[105] Peter A Robinson, Christopher J Rennie, and James J Wright. Propagation and stability of waves of electrical activity in the cerebral cortex. *Physical Review E*, 56(1):826, 1997.

[106] Souvik Roy, Mario Annunziato, and Alfio Borzì. A fokker–planck feedback control-constrained approach for modelling crowd motion. *Journal of Computational and Theoretical Transport*, 45(6):442–458, 2016.

[107] Aimé Lachapelle and Marie-Therese Wolfram. On a mean field game approach modeling congestion and aversion in pedestrian crowds. *Transportation research part B: methodological*, 45(10):1572–1589, 2011.

[108] Christian Dogbé. Modeling crowd dynamics by the mean-field limit approach. *Mathematical and Computer Modelling*, 52(9-10):1506–1520, 2010.

[109] RC Schmidt, Samantha Morr, Paula Fitzpatrick, and Michael J Richardson. Measuring the dynamics of interactional synchrony. *Journal of Nonverbal Behavior*, 36(4):263–279, 2012.

[110] Adam W Kiefer, Kevin Rio, Stéphane Bonneaud, Ashley Walton, and William H Warren. Quantifying and modeling coordination and coherence in pedestrian groups. *Frontiers in psychology*, 8:949, 2017.

[111] Moreno I Coco and Rick Dale. Cross-recurrence quantification analysis of categorical and continuous time series: an r package. *Frontiers in psychology*, 5:510, 2014.

[112] Henri J Nussbaumer. The fast fourier transform. In *Fast Fourier Transform and Convolution Algorithms*, pages 80–111. Springer, 1981.

[113] Olivier Oullier, Gonzalo C De Guzman, Kelly J Jantzen, Julien Lagarde, and JA Scott Kelso. Social coordination dynamics: Measuring human bonding. *Social Neuroscience*, 3(2):178–192, 2008.

[114] Michael Richardson, Randi L Garcia, Till D Frank, Madison Gregor, and Kerry L Marsh. Measuring group synchrony: a cluster-phase method for analyzing multivariate movement time-series. *Frontiers in physiology*, 3:405, 2012.

[115] R Quian Quiroga, Thoma Kreuz, and Peter Grassberger. Event synchronization: a simple and fast method to measure synchronicity and time delay patterns. *Physical review E*, 66(4):041904, 2002.

[116] Violet Mwaffo, Jishnu Keshavan, Tyson L Hedrick, and Sean Humbert. Detecting intermittent switching leadership in coupled dynamical systems. *Scientific Reports*, 8:10338, 2018.

[117] Badino Leonardo, Volpe Gualtiero, Tokay Serâ, Fadiga Luciano, Camurri Antonio, et al. Multi-layer adaptation of group coordination in musical ensembles. *Scientific reports*, 9(1):1–10, 2019.

[118] Etienne Burdet, Keng Peng Tee, I Mareels, Theodore E Milner, Chee-Meng Chew, David W Franklin, Rieko Osu, and Mitsuo Kawato. Stability and motor adaptation in human arm movements. *Biological cybernetics*, 94(1):20–32, 2006.

[119] Steven L Bressler and Anil K Seth. Wiener–granger causality: a well established methodology. *Neuroimage*, 58(2):323–329, 2011.

[120] Ming Li, Paul Vitányi, et al. *An introduction to Kolmogorov complexity and its applications*, volume 3. Springer, 2008.

[121] Rolf Herken. The universal turing machine. a half-century survey. 1992.

[122] Alvin E Roth. *The Shapley value: essays in honor of Lloyd S. Shapley*. Cambridge University Press, 1988.

[123] Ivan Belik and Kurt Jörnsten. The method of leader's overthrow in networks based on shapley value. *Socio-Economic Planning Sciences*, 56:55–66, 2016.

[124] Daniel Gomez, Enrique González-Arangüena, Conrado Manuel, Guillermo Owen, Monica del Pozo, and Juan Tejada. Centrality and power in social networks: a game theoretic approach. *Mathematical Social Sciences*, 46(1):27–54, 2003.

[125] Francesco Bullo. *Lectures on network systems*. Kindle Direct Publishing, 2019.

[126] Elizabeth B Torres, Maria Brincker, Robert W Isenhower III, Polina Yanovich, Kimberly A Stigler, John I Nurnberger Jr, Dimitri N Metaxas, and Jorge V José. Autism: the micro-movement perspective. *Frontiers in Integrative Neuroscience*, 7:32, 2013.

[127] Elizabeth B Torres. Two classes of movements in motor control. *Experimental Brain Research*, 215(3-4):269–283, 2011.

[128] Svante Wold, Kim Esbensen, and Paul Geladi. Principal component analysis. *Chemometrics and intelligent laboratory systems*, 2(1-3):37–52, 1987.

[129] Norbert Marwan, M Carmen Romano, Marco Thiel, and Jürgen Kurths. Recurrence plots for the analysis of complex systems. *Physics reports*, 438(5-6):237–329, 2007.

[130] Mengsen Zhang, William D Kalies, JA Scott Kelso, and Emmanuelle Tognoli. Topological portraits of multiscale coordination dynamics. *Journal of Neuroscience Methods*, page 108672, 2020.

[131] Sally Robinson, Lorna Goddard, Barbara Dritschel, Mary Wisley, and Pat Howlin. Executive functions in children with autism spectrum disorders. *Brain and cognition*, 71(3):362–368, 2009.

[132] MA Dziuk, JC Gidley Larson, A Apostu, Ernest M Mahone, Martha Bridge Denckla, and Stewart H Mostofsky. Dyspraxia in autism: association with motor, social, and communicative deficits. *Developmental Medicine & Child Neurology*, 49(10):734–739, 2007.

[133] Michael Sachse, Sabine Schlitt, Daniela Hainz, Angela Ciaramidaro, Shella Schirman, Henrik Walter, Fritz Poustka, Sven Bölte, and Christine M Freitag. Executive and visuo-motor function in adolescents and adults with autism spectrum disorder. *Journal of Autism and Developmental Disorders*, 43(5):1222–1235, 2013.

[134] John R Best. Exergaming immediately enhances children's executive function. *Developmental psychology*, 48(5):1501, 2012.

[135] David R Lubans, Philip J Morgan, Dylan P Cliff, Lisa M Barnett, and Anthony D Okely. Fundamental movement skills in children and adolescents. *Sports medicine*, 40(12):1019–1035, 2010.

[136] Cay Anderson-Hanley, Kimberly Tureck, and Robyn L Schneiderman. Autism and exergaming: effects on repetitive behaviors and cognition. *Psychology research and behavior management*, 4:129, 2011.

[137] Nancy Getchell, Dannielle Miccinello, Michelle Blom, Lyssa Morris, and Mark Szaroleta. Comparing energy expenditure in adolescents with and without autism while playing nintendo® wii™ games. *GAMES FOR HEALTH: Research, Development, and Clinical Applications*, 1(1):58–61, 2012.

[138] Russell Lang, Lynn Kern Koegel, Kristen Ashbaugh, April Regester, Whitney Ence, and Whitney Smith. Physical exercise and individuals with autism spectrum disorders: A systematic review. *Research in Autism Spectrum Disorders*, 4(4):565–576, 2010.

[139] Claudia List Hilton, Kristina Cumpata, Cheryl Klohr, Shannon Gaetke, Amanda Artner, Hailey Johnson, and Sarah Dobbs. Effects of exergaming on executive function and motor skills in children with autism spectrum disorder: A pilot study. *American Journal of Occupational Therapy*, 68(1):57–65, 2014.

[140] Niall Maclean, Pandora Pound, Charles Wolfe, and Anthony Rudd. The concept of patient motivation: a qualitative analysis of stroke professionals' attitudes. *Stroke*, 33(2):444–448, 2002.

[141] Samantha L Finkelstein, Andrea Nickel, Tiffany Barnes, and Evan A Suma. Astrojumper: Designing a virtual reality exergame to motivate children with autism to exercise. In *2010 IEEE Virtual Reality Conference (VR)*, pages 267–268. IEEE, 2010.

[142] Adriana Tapus, Andreea Peca, Amir Aly, Cristina Pop, Lavinia Jisa, Sebastian Pintea, Alina S Rusu, and Daniel O David. Children with autism social engagement in interaction with nao, an imitative robot: A series of single case experiments. *Interaction studies*, 13(3):315–347, 2012.

[143] Thomas W Malone. Heuristics for designing enjoyable user interfaces: Lessons from computer games. In *Proceedings of the 1982 conference on Human factors in computing systems*, pages 63–68, 1982.

[144] Cheryl Campanella Bracken, Leo W Jeffres, and Kimberly A Neuendorf. Criticism or praise? the impact of verbal versus text-only computer feedback on social presence, intrinsic motivation, and recall. *Cyberpsychology & behavior*, 7(3):349–357, 2004.

[145] April K Bay-Hinitz, Robert F Peterson, and H Robert Quilitch. Cooperative games: a way to modify aggressive and cooperative behaviors in young children. *Journal of applied behavior analysis*, 27(3):435, 1994.

[146] Tobias Greitemeyer and Christopher Cox. There's no "i" in team: Effects of cooperative video games on cooperative behavior. *European Journal of Social Psychology*, 43(3):224–228, 2013.

[147] Elisabeth M Whyte, Joshua M Smyth, and K Suzanne Scherf. Designing serious game interventions for individuals with autism. *Journal of autism and developmental disorders*, 45(12):3820–3831, 2015.

[148] Hsiu-Ting Hung, Jie Chi Yang, Gwo-Jen Hwang, Hui-Chun Chu, and Chun-Chieh Wang. A scoping review of research on digital game-based language learning. *Computers & Education*, 126:89–104, 2018.

[149] Melissa H Kuo, Gael I Orsmond, Ellen S Cohn, and Wendy J Coster. Friendship characteristics and activity patterns of adolescents with an autism spectrum disorder. *Autism*, 17(4):481–500, 2013.

[150] Taiwoo Park, Uichin Lee, Bupjae Lee, Haechan Lee, Sanghun Son, Seokyoung Song, and Junehwa Song. Exersync: facilitating interpersonal synchrony in social exergames. In *Proceedings of the 2013 conference on Computer supported cooperative work*, pages 409–422, 2013.

[151] Paula Fitzpatrick, Veronica Romero, Joseph L Amaral, Amie Duncan, Holly Barnard, Michael J Richardson, and RC Schmidt. Social motor synchronization: Insights for understanding social behavior in autism. *Journal of autism and developmental disorders*, 47(7):2092–2107, 2017.

[152] JAS Kelso, John P Scholz, and Gregor Schöner. Nonequilibrium phase transitions in coordinated biological motion: critical fluctuations. *Physics Letters A*, 118(6):279–284, 1986.

[153] Steven Strogatz. *Sync: The emerging science of spontaneous order*. Penguin Group, New York NY, USA, 2004.

[154] Arkady Pikovsky, Jurgen Kurths, Michael Rosenblum, and Jürgen Kurths. *Synchronization: a universal concept in nonlinear sciences*, volume 12. Cambridge University Press, Cambridge, UK, 2003.

[155] Zhong Zhao, Robin N Salesse, Mathieu Gueugnon, Richard C Schmidt, Ludovic Marin, and Benoît G Bardy. Moving attractive virtual agent improves interpersonal coordination stability. *Human Movement Science*, 41:240–254, 2015.

[156] Irini Giannopulu, Kazunori Terada, and Tomio Watanabe. Emotional empathy as a mechanism of synchronisation in child-robot interaction. *Frontiers in Psychology*, 9:1852, 2018.

[157] Lynden K Miles, Louise K Nind, and C Neil Macrae. The rhythm of rapport: Interpersonal synchrony and social perception. *Journal of Experimental Social Psychology*, 45(3):585–589, 2009.

[158] Atsushi Takagi, Gowrishankar Ganesh, Toshinori Yoshioka, Mitsuo Kawato, and Etienne Burdet. Physically interacting individuals estimate the partner's goal to enhance their movements. *Nature Human Behaviour*, 1(3):0054, 2017.

[159] Richard C Schmidt, Claudia Carello, and Michael T Turvey. Phase transitions and critical fluctuations in the visual coordination of rhythmic movements between people. *Journal of Experimental Psychology: Human Perception and Performance*, 16(2):227, 1990.

[160] Janeen D Loehr, Edward W Large, and Caroline Palmer. Temporal coordination and adaptation to rate change in music performance. *Journal of Experimental Psychology: Human Perception and Performance*, 37(4):1292, 2011.

[161] Zoltán Néda, Erzsébet Ravasz, Yves Brechet, Tamás Vicsek, and A-L Barabási. Self-organizing processes: The sound of many hands clapping. *Nature*, 403(6772):849, 2000.

[162] Andrew Chang, Haley E Kragness, Steven R Livingstone, Dan J Bosnyak, and Laurel J Trainor. Body sway reflects joint emotional expression in music ensemble performance. *Scientific Reports*, 9(1):205, 2019.

[163] Gualtiero Volpe, Alessandro D'Ausilio, Leonardo Badino, Antonio Camurri, and Luciano Fadiga. Measuring social interaction in music ensembles. *Philosophical Transactions of the Royal Society B: Biological Sciences*, 371(1693):20150377, 2016.

[164] Falisha J Karpati, Chiara Giacosa, Nicholas EV Foster, Virginia B Penhune, and Krista L Hyde. Dance and music share gray matter structural correlates. *Brain Research*, 1657:62–73, 2017.

[165] Bettina Bläsing, Beatriz Calvo-Merino, Emily S Cross, Corinne Jola, Juliane Honisch, and Catherine J Stevens. Neurocognitive control in dance perception and performance. *Acta Psychologica*, 139(2):300–308, 2012.

[166] Janet Karin. Recontextualizing dance skills: overcoming impediments to motor learning and expressivity in ballet dancers. *Frontiers in Psychology*, 7:431, 2016.

[167] Johann Issartel, Ludovic Marin, and Marielle Cadopi. Unintended interpersonal co-ordination:"can we march to the beat of our own drum?". *Neuroscience Letters*, 411(3):174–179, 2007.

[168] Xinhong Jin, Biye Wang, Yuanxin Lv, Yingzhi Lu, Jiacheng Chen, and Chenglin Zhou. Does dance training influence beat sensorimotor synchronization? differences in finger-tapping sensorimotor synchronization between competitive ballroom dancers and nondancers. *Experimental Brain Research*, 237(3):743–753, 2019.

[169] Akito Miura, Shinya Fujii, Masahiro Okano, Kazutoshi Kudo, and Kimitaka Nakazawa. Upper rate limits for one-to-one auditory–motor coordination involving whole-body oscillation: a study of street dancers and non-dancers. *Journal of Experimental Biology*, 221(16):jeb179457, 2018.

[170] Björn Kralemann, Laura Cimponeriu, Michael Rosenblum, Arkady Pikovsky, and Ralf Mrowka. Phase dynamics of coupled oscillators reconstructed from data. *Physical Review E*, 77(6):066205, 2008.

[171] Daniel M Wolpert, Kenji Doya, and Mitsuo Kawato. A unifying computational framework for motor control and social interaction. *Philosophical Transactions of the Royal Society of London. Series B: Biological Sciences*, 358(1431):593–602, 2003.

[172] Vittorio Gallese and Alvin Goldman. Mirror neurons and the simulation theory of mind-reading. *Trends in cognitive sciences*, 2(12):493–501, 1998.

[173] Koenraad Van Braeckel, Phillipa R Butcher, Reint H Geuze, Elisabeth F Stremmelaar, and Anke Bouma. Movement adaptations in 7-to 10-year-old typically developing children: Evidence for a transition in feedback-based motor control. *Human movement science*, 26(6):927–942, 2007.

[174] Natalie Sebanz, Harold Bekkering, and Günther Knoblich. Joint action: bodies and minds moving together. *Trends in Cognitive Sciences*, 10(2):70–76, 2006.

[175] Harold Bekkering, Ellen RA De Bruijn, Raymond H Cuijpers, Roger Newman-Norlund, Hein T Van Schie, and Ruud Meulenbroek. Joint action: Neurocognitive mechanisms supporting human interaction. *Topics in Cognitive Science*, 1(2):340–352, 2009.

[176] Laura S Cuijpers, Ruud JR Den Hartigh, Frank TJM Zaal, and Harjo J de Poel. Rowing together: Interpersonal coordination dynamics with and without mechanical coupling. *Human Movement Science*, 64:38–46, 2019.

[177] Julie Duque, Ian Greenhouse, Ludovica Labruna, and Richard B Ivry. Physiological markers of motor inhibition during human behavior. *Trends in neurosciences*, 40(4):219–236, 2017.

[178] Andrea Cavallo, Caroline Catmur, Sophie Sowden, Francesco Ianì, and Cristina Becchio. Stopping movements: when others slow us down. *European Journal of Neuroscience*, 40(5):2842–2849, 2014.

[179] Charles A Coey, Auriel Washburn, Justin Hassebrock, and Michael J Richardson. Complexity matching effects in bimanual and interpersonal syncopated finger tapping. *Neuroscience letters*, 616:204–210, 2016.

[180] Tamara Lorenz, Alexander Mörtl, Björn Vlaskamp, Anna Schubö, and Sandra Hirche. Synchronization in a goal-directed task: human movement coordination with each other and robotic partners. In *2011 RO-MAN*, pages 198–203. IEEE, 2011.

[181] Jože Guna, Grega Jakus, Matevž Pogačnik, Sašo Tomažič, and Jaka Sodnik. An analysis of the precision and reliability of the leap motion sensor and its suitability for static and dynamic tracking. *Sensors*, 14(2):3702–3720, 2014.

[182] Richard J Jagacinski, Min-Ju Liao, and Elias A Fayyad. Generalized slowing in sinusoidal tracking by older adults. *Psychology and aging*, 10(1):8, 1995.

[183] Liam Cross, Martine Turgeon, and Gray Atherton. How moving together binds us together: The social consequences of interpersonal entrainment and group processes. *Open Psychology*, 1(1):273–302, 2019.

[184] Maria Christine Van Der Steen and Peter E Keller. The adaptation and anticipation model (adam) of sensorimotor synchronization. *Frontiers in human neuroscience*, 7:253, 2013.

[185] Alexander J McC Foulkes and R Chris Miall. Adaptation to visual feedback delays in a human manual tracking task. *Experimental brain research*, 131(1):101–110, 2000.

[186] Robert A Scheidt, David J Reinkensmeyer, Michael A Conditt, W Zev Rymer, and Ferdinando A Mussa-Ivaldi. Persistence of motor adaptation during constrained, multi-joint, arm movements. *Journal of neurophysiology*, 84(2):853–862, 2000.

[187] Gowrishankar Ganesh, Atsushi Takagi, Rieko Osu, Toshinori Yoshioka, Mitsuo Kawato, and Etienne Burdet. Two is better than one: Physical interactions improve motor performance in humans. *Scientific reports*, 4:3824, 2014.

[188] Chiara Maria Portas, Geraint Rees, AM Howseman, Oliver Josephs, Robert Turner, and Christopher D Frith. A specific role for the thalamus in mediating the interaction of attention and arousal in humans. *Journal of Neuroscience*, 18(21):8979–8989, 1998.

[189] Virginia I Douglas. Cognitive control processes in attention deficit/hyperactivity disorder. In *Handbook of disruptive behavior disorders*, pages 105–138. Springer, 1999.

[190] Cynthia L Huang-Pollock, Thomas H Carr, and Joel T Nigg. Development of selective attention: Perceptual load influences early versus late attentional selection in children and adults. *Developmental psychology*, 38(3):363, 2002.

[191] Thilo Womelsdorf and Pascal Fries. The role of neuronal synchronization in selective attention. *Current Opinion in Neurobiology*, 17(2):154–160, 2007.

[192] Francesca Capozzi, Cristina Becchio, Cesco Willemse, and Andrew P Bayliss. Followers are not followed: Observed group interactions modulate subsequent social attention. *Journal of Experimental Psychology: General*, 145(5):531, 2016.

[193] Kerry Kawakami, Amanda Williams, David Sidhu, Becky L Choma, Rosa Rodriguez-Bailón, Elena Cañadas, Derek Chung, and Kurt Hugenberg. An eye for the i: Preferential attention to the eyes of ingroup members. *Journal of Personality and Social Psychology*, 107(1):1, 2014.

[194] Nikolai Bernstein. The co-ordination and regulation of movements. *The co-ordination and regulation of movements*, 1966.

[195] Mark L Latash, John P Scholz, and Gregor Schöner. Motor control strategies revealed in the structure of motor variability. *Exercise and sport sciences reviews*, 30(1):26–31, 2002.

[196] Roger Bartlett, Jon Wheat, and Matthew Robins. Is movement variability important for sports biomechanists? *Sports biomechanics*, 6(2):224–243, 2007.

[197] Richard EA Van Emmerik and Erwin EH Van Wegen. On the functional aspects of variability in postural control. *Exercise and sport sciences reviews*, 30(4):177–183, 2002.

[198] Daniel Hamacher and Astrid Zech. Development of functional variability during the motor learning process of a complex cyclic movement. *Journal of biomechanics*, 77:124–130, 2018.

[199] Cassie Wilson, Scott E Simpson, Richard EA Van Emmerik, and Joseph Hamill. Coordination variability and skill development in expert triple jumpers. *Sports biomechanics*, 7(1):2–9, 2008.

[200] Ludovic Seifert, Leo Wattebled, Romain Hérault, Germain Poizat, David Adé, Nathalie Gal-Petitfaux, and Keith Davids. Neurobiological degeneracy and affordance perception support functional intra-individual variability of inter-limb coordination during ice climbing. *PloS One*, 9(2), 2014.

[201] Genevieve KR Williams, Gareth Irwin, David G Kerwin, Joseph Hamill, Richard EA Van Emmerik, and Karl M Newell. Coordination as a function of skill level in the gymnastics longswing. *Journal of Sports Sciences*, 34(5):429–439, 2016.

[202] JB Dingwell, JP Cusumano, D Sternad, and PR Cavanagh. Slower speeds in patients with diabetic neuropathy lead to improved local dynamic stability of continuous overground walking. *Journal of biomechanics*, 33(10):1269–1277, 2000.

[203] Alessia Longo and Ruud Meulenbroek. Precision-dependent changes in motor variability during sustained bimanual reaching. *Motor control*, 22(1):28–44, 2018.

[204] Karen HE Søndergaard, Christian G Olesen, Eva K Søndergaard, Mark De Zee, and Pascal Madeleine. The variability and complexity of sitting postural control are associated with discomfort. *Journal of biomechanics*, 43(10):1997–2001, 2010.

[205] Nicholas Stergiou and Leslie M Decker. Human movement variability, nonlinear dynamics, and pathology: is there a connection? *Human movement science*, 30(5):869–888, 2011.

[206] Andrew M Colman. Cooperation, psychological game theory, and limitations of rationality in social interaction. *Behavioral and brain sciences*, 26(2):139–153, 2003.

[207] Joachim I Krueger and David C Funder. Towards a balanced social psychology: Causes, consequences, and cures for the problem-seeking approach to social behavior and cognition. *Behavioral and Brain Sciences*, 27(3):313–327, 2004.

[208] Marco K Wittmann, Nils Kolling, Nadira S Faber, Jacqueline Scholl, Natalie Nelissen, and Matthew FS Rushworth. Self-other mergence in the frontal cortex during cooperation and competition. *Neuron*, 91(2):482–493, 2016.

[209] Arpan Banerjee and Viktor K Jirsa. How do neural connectivity and time delays influence bimanual coordination? *Biological Cybernetics*, 96(2):265–278, 2007.

[210] Bhumika Thakur, Abhishek Mukherjee, Abhijit Sen, and Arpan Banerjee. A dynamical framework to relate perceptual variability with multisensory information processing. *Scientific Reports*, 6:31280, 2016.

[211] E Halgren. How can intracranial recordings assist meg source localization? *Neurology & Clinical Neurophysiology*, 2004:86–86, 2004.

[212] JEFFREY M CLARKE and ERAN ZAIDEL. Simple reaction times to lateralized light flashes: Varieties of interhemispheric communication routes. *Brain*, 112(4):849–870, 1989.

[213] Carlo A Marzi, P Bisiacchi, and R Nicoletti. Is interhemispheric transfer of visuomotor information asymmetric? evidence from a meta-analysis. *Neuropsychologia*, 29(12):1163–1177, 1991.

[214] Warren S Brown, Malcolm A Jeeves, Rosalind Dietrich, and Debra S Burnison. Bilateral field advantage and evoked potential interhemispheric transmission in commissurotomy and callosal agenesis. *Neuropsychologia*, 37(10):1165–1180, 1999.

[215] Jeffrey M Clarke, Eric Halgren, and Patrick Chauvel. Intracranial erps in humans during a lateralized visual oddball task: Ii. temporal, parietal, and frontal recordings. *Clinical Neurophysiology*, 110(7):1226–1244, 1999.

[216] Peter A Tass. *Phase resetting in medicine and biology: stochastic modelling and data analysis*. Springer Science & Business Media, 2007.

[217] Simon Thorpe, Denis Fize, and Catherine Marlot. Speed of processing in the human visual system. *Nature*, 381(6582):520–522, 1996.

[218] Piotr Slowinski, Sohaib Al-Ramadhani, and Krasimira Tsaneva-Atanasova. Neurologically motivated coupling functions in models of motor coordination. *SIAM Journal on Applied Dynamical Systems*, 19(1):208–232, 2020.

[219] Spase Petkoski and Viktor K Jirsa. Transmission time delays organize the brain network synchronization. *Philosophical Transactions of the Royal Society A*, 377(2153):20180132, 2019.

[220] Liam Timms and Lars Q English. Synchronization in phase-coupled kuramoto oscillator networks with axonal delay and synaptic plasticity. *Physical Review E*, 89(3):032906, 2014.

[221] Michael I Jordan and Daniel M Wolpert. Computational motor control. In Michael Gazzaniga, editor, *The Cognitive Neurosciences*. MIT Press Cambridge, MA, 1999.

[222] David W Franklin and Daniel M Wolpert. Computational mechanisms of sensorimotor control. *Neuron*, 72(3):425–442, 2011.

[223] R Chris Miall and Daniel M Wolpert. Forward models for physiological motor control. *Neural networks*, 9(8):1265–1279, 1996.

[224] John Milton, Juan Luis Cabrera, Toru Ohira, Shigeru Tajima, Yukinori Tonosaki, Christian W Eurich, and Sue Ann Campbell. The time-delayed inverted pendulum: implications for human balance control. *Chaos: An Interdisciplinary Journal of Nonlinear Science*, 19(2):026110, 2009.

[225] Robert J Peterka. Sensorimotor integration in human postural control. *Journal of Neurophysiology*, 88(3):1097–1118, 2002.

[226] Yao Li, William S Levine, and Gerald E Loeb. A two-joint human posture control model with realistic neural delays. *IEEE Transactions on Neural Systems and Rehabilitation Engineering*, 20(5):738–748, 2012.

[227] Carmela Calabrese, Maria Lombardi, Erik Bollt, Pietro De Lellis, Benoıt G. Bardy, and Mario di Bernardo. Patterns of leadership emergence organize coordinated motion in human groups. under review, 2020.

[228] Jie Sun and Erik M Bollt. Causation entropy identifies indirect influences, dominance of neighbors and anticipatory couplings. *Physica D: Nonlinear Phenomena*, 267:49–57, 2014.

[229] Jie Sun, Dane Taylor, and Erik M Bollt. Causal network inference by optimal causation entropy. *SIAM Journal on Applied Dynamical Systems*, 14(1):73–106, 2015.

[230] Claude E Shannon. A mathematical theory of communication. *Bell system technical journal*, 27(3):379–423, 1948.

[231] Thomas Schreiber. Measuring information transfer. *Physical Review Letters*, 85(2):461, 2000.

[232] Doug P Hanes and Jeffrey D Schall. Neural control of voluntary movement initiation. *Science*, 274(5286):427–430, 1996.

[233] Haline E Schendan and Giorgio Ganis. Top-down modulation of visual processing and knowledge after 250 ms supports object constancy of category decisions. *Frontiers in Psychology*, 6:1289, 2015.

[234] Terrence R Stanford, Swetha Shankar, Dino P Massoglia, M Gabriela Costello, and Emilio Salinas. Perceptual decision making in less than 30 milliseconds. *Nature neuroscience*, 13(3):379, 2010.

[235] Alexander Kraskov, Harald Stögbauer, and Peter Grassberger. Estimating mutual information. *Physical review E*, 69(6):066138, 2004.

[236] Richard O Duda, Peter E Hart, and David G Stork. *Pattern classification*. John Wiley & Sons, 2012.

[237] Corrado Gini. Variabilità e mutabilità reprinted in memorie di metodologica statistica. *Rome: Libreria Eredi Virgilio Veschi*, 1955.

[238] Kerry L Marsh, Robert W Isenhower, Michael J Richardson, Molly Helt, Alyssa D Verbalis, RC Schmidt, and Deborah Fein. Autism and social disconnection in interpersonal rocking. *Frontiers in integrative neuroscience*, 7:4, 2013.

[239] Guillaume Dumas, Gonzalo C de Guzman, Emmanuelle Tognoli, and JA Scott Kelso. The human dynamic clamp as a paradigm for social interaction. *Proceedings of the National Academy of Sciences*, 111(35):E3726–E3734, 2014.

[240] Astrid A Prinz, LF Abbott, and Eve Marder. The dynamic clamp comes of age. *Trends in neurosciences*, 27(4):218–224, 2004.

[241] Hiroka Sabu, Tomoyo Morita, Hideyuki Takahashi, Eiichi Naito, and Minoru Asada. Being a leader in a rhythmic interaction activates reward-related brain regions. *Neuroscience research*, 145:39–45, 2019.

[242] Xiaoyuan Luo, Shaobao Li, and Xinping Guan. Decentralised control for formation reorganisation of multi-agent systems using a virtual leader. *International Journal of Systems Science*, 42(1):171–182, 2011.

[243] H Ronald Pulliam. Living in groups: is there an optimal group size? *Behavioural Ecology: an Evolutionally Approach*, pages 122–147, 1984.

[244] Derek J Hoare, Iain D Couzin, J-GJ Godin, and Jens Krause. Context-dependent group size choice in fish. *Animal Behaviour*, 67(1):155–164, 2004.

[245] Andrew J King and Guy Cowlishaw. When to use social information: the advantage of large group size in individual decision making. *Biology letters*, 3(2):137–139, 2007.

[246] Larry L Cummings, George P Huber, and Eugene Arendt. Effects of size and spatial arrangements on group decision making. *Academy of Management Journal*, 17(3):460–475, 1974.

[247] Bruno Siciliano and Oussama Khatib. *Springer handbook of robotics*. Springer, 2016.

[248] Robin R Murphy. Human-robot interaction in rescue robotics. *IEEE Transactions on Systems, Man, and Cybernetics, Part C (Applications and Reviews)*, 34(2):138–153, 2004.

[249] Anna Anzulewicz, Krzysztof Sobota, and Jonathan T Delafield-Butt. Toward the autism motor signature: Gesture patterns during smart tablet gameplay identify children with autism. *Scientific reports*, 6(1):1–13, 2016.

[250] Gary Bargary, Jenny M Bosten, Patrick T Goodbourn, Adam J Lawrance-Owen, Ruth E Hogg, and JD Mollon. Individual differences in human eye movements: An oculomotor signature? *Vision Research*, 141:157–169, 2017.

[251] Alexandre Coste, Benoît G Bardy, and Ludovic Marin. Towards an embodied signature of improvisation skills. *Frontiers in Psychology*, 10, 2019.

[252] Manuel Varlet, Ludovic Marin, Delphine Capdevielle, Jonathan Del-Monte, Richard Schmidt, Robin Salesse, Jean-Philippe Boulenger, Benoît Gaël Bardy, and Stéphane Raffard. Difficulty leading interpersonal coordination: towards an embodied signature of social anxiety disorder. *Frontiers in Behavioral Neuroscience*, 8:29, 2014.

[253] Fabio Della Rossa, Davide Salzano, Anna Di Meglio, Francesco De Lellis, Marco Coraggio, Carmela Calabrese, Agostino Guarino, Ricardo Cardona-Rivera, Pietro De Lellis, Davide Liuzza, et al. A network model of italy shows that intermittent regional strategies can alleviate the covid-19 epidemic. *Nature communications*, 11(1):1–9, 2020.